ANALYSIS OF A NOVEL HDAC8-H1.3 COMPLEX IN SEVERAL HUMAN CARCINOMA CELL LINES

A DISSERTATION

SUBMITTED IN PARTIAL FULFILLMENT OF THE REQUIREMENTS

FOR THE DEGREE OF DOCTOR OF PHILOSOPHY

IN THE GRADUATE SCHOOL OF THE

TEXAS WOMAN'S UNIVERSITY

DEPARTMENT OF BIOLOGY

COLLEGE OF ARTS AND SCIENCES

BY

RHIANNON WOLD GONZALEZ B.S.

DENTON, TEXAS

MAY 2016

TEXAS WOMAN'S UNIVERSITY
DENTON TEXAS

April 5, 2016

To the Dean of the Graduate School:

I am submitting herewith a dissertation written by Rhiannon Wold Gonzalez, entitled "Analysis of a Novel HDAC8-H1.3 Complex in Several Human Carcinoma Cell Lines". I have examined this dissertation for form and content and recommend that it be accepted in partial fulfillment of the requirements for the degree of Doctor of Philosophy with a major in Molecular Biology.

Michael Bergel, PhD, Major Professor

We have read this dissertation and recommend its acceptance:

Heather Conrad-Webb, PhD

Nathaniel Mills, PhD

Camelia Maier, PhD

Parakat Vijayagopal, PhD

Interim Chair of the Department: DiAnna Hynds, PhD

Accepted:

Dean of the Graduate School

DEDICATION

This dissertation is dedicated to my family. My parents, Gale and Maria Wold; my brother, Timothy Wold; grandparents, Alfredo and Mary Fernandez, Alfred and Adella Wold, and my godmother, LaLa Fernandez. My aunts and uncles Carlos Fernandez, Mina Treick, and Gary Wold. Thank you for always supporting me, believing in me and showing me endless love.

ACKNOWLEDGMENTS

I would like to acknowledge the individuals who have contributed to this dissertation and the research herein. I would like to thank my mentor Dr. Michael Bergel, who spent many hours teaching, guiding, and supporting me throughout the years, and who has patiently edited this dissertation. I would like to thank my committee for their support, input, and critical insights. Thank you, Dr. Heather Conrad-Webb, Dr. Nathaniel Mills, Dr. Camelia Maier, and Dr. Parakat Vijayagopal. I would also like to thank Dr. Shazia Ahmed for her support and guidance in teaching. Thank you Dr. Lynda Uphouse and the MBRS program for you financial and professional support. Thank you also to my lab colleagues and friends: Mangalam Subramanian, Hemangi Patil, LaTondra Lawrence, Carrie Wilks, Maria Raya, and Jessica Feyen. Thank you also to Dr. Joseph Albanesi of UT Southwestern Medical Center at Dallas for the generous gift of the Rab plasmids and antibodies.

ABSTRACT

RHIANNON WOLD GONZALEZ

ANALYSIS OF A NOVEL HDAC8-H1.3
COMPLEX IN SEVERAL HUMAN CARCINOMA CELL LINES

MAY 2016

The compaction level of chromatin regulates DNA accessibility, gene expression, and cell division. Transcription factors and other proteins cannot access the DNA within compacted chromatin. Two types of proteins that contribute to chromatin compaction are histone deacetylases (HDACs) and linker histones (H1s). H1s are chromatin-binding structural proteins required for the formation of the higher order chromatin structure. H1 subtypes also differentially regulate transcription and apoptosis. HDACs cause chromatin compaction by deacetylating lysine residues on core histone tails, causing core histones to closely interact with DNA. HDACs regulate many other cellular processes including: mitosis, intracellular trafficking, microtubule dynamics, and cell cycle events, through deacetylation of non-histone proteins. This work describes a novel HDAC8-H1.3 protein complex found in several human cancerous cell lines. The goal of this research was to gather insight as to the function of the HDAC8-H1.3 complex using co-immunoprecipitation, chromatin-binding electrophoretic mobility shift assays, deacetylation assays, immunocytochemistry, confocal microscopy, and complex

protein mixture identification by LC/MS/MS. The hypothesis was that HDAC8 and H1.3 work synergistically to cause chromatin compaction. Results showed that H1.3, but not HDAC8 binds to nucleosomes. HDAC8 was found to deacetylate H1.3. In MCF-7 cells the complex was found to associate with ER-Golgi associated vesicles and late endosomes during interphase. This is the first report for a non-mitotic cytoplasmic association of a linker histone and HDAC. Also, this is the first reported association of a linker histone with vesicle trafficking.

TABLE OF CONTENTS

LIST OF TABLES

Table Page

LIST OF FIGURES

Figure Page

CHAPTER I

INTRODUCTION

Chromatin Structure

The size range of a human chromosome is approximately 10^7 to 10^8 base pairs of DNA, with the combined length of all chromosomes reaching nearly two meters. In eukaryotes, an extensive amount of DNA must be carefully organized within a nucleus that is about 10 μm in diameter (Cooper, 2004; Hassig and Schreiber, 1997). In the eukaryote cell the DNA associates with histone proteins, which facilitate the ordered compaction of DNA, forming the first level of chromatin, the nucleosome.

Nucleosomes

The nucleosome core particle (NCP) is the most basic unit of chromatin organization. Nucleosomes consist of 146 bp of DNA wrapped 1.65 times around a disk-shaped octamer of four core histones, two of each: H2A, H2B, H3, and H4 (Luger et al., 1997). Core histones bind DNA in a non-sequence-specific manner. An H3-H4 tetramer is deposited first in newly synthesized DNA by chaperone protein CAF-1. Next, chaperone NAP-1 incorporates two dimers of H2A-H2B to form the histone octamer (Bertin et al., 2007; Watson, 2004). The

negatively charged phosphate backbone of DNA interacts with the positively charged histone-fold domain of core histones. A large number of hydrogen bonds are formed between the histones and DNA that further stabilize the structure (Tomasi et al., 2006; Watson et al., 2004). N-terminal tails of the eight core histones and two H2A C-terminal tails protrude from the core particle and interact with the DNA (Figure 1). The tails wrap around the core particle causing a stabilized nucleosome structure. Histone tails are positively charged, containing highly conserved amino acid sequences with many Lys and Arg residues. The N-terminal tails are targets for a variety of posttranslational modifications including: acetylation, methylation, phosphorylation, ubiquitination, sumoylation, and ADP-ribosylation (Marino-Ramirez et al., 2005). Posttranslational modifications on histone tails create recognition signals for nonhistone proteins to modulate a specific chromatin structure and gene activity. Linker DNA of variable lengths connects NCPs thus forming the 10 nm “beads-on-a-string” nucleosomal array (Lodish et al. 2003; Tomasi et al., 2006; 2004).

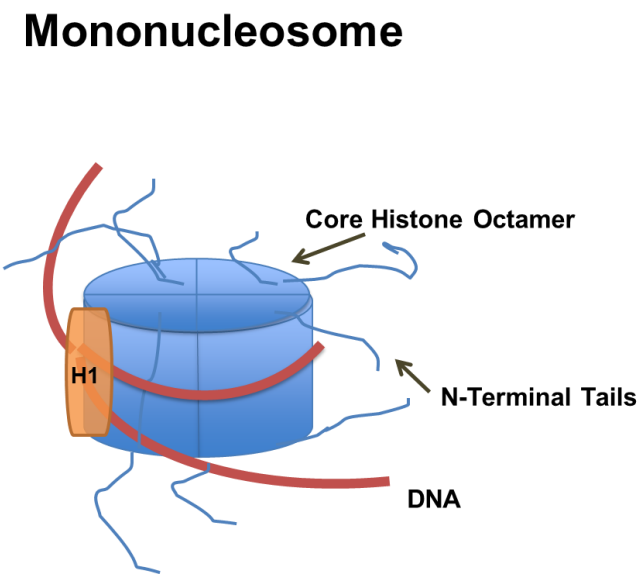

Figure 1. Nucleosome Structure. The first level of chromatin compaction is the nucleosome. A nucleosome consists of a octamer of eight core histones, two of each: H2A, H2B, H3, and H4. DNA is wrapped around the octamer 1.64 times. The negatively charged DNA is held onto the positively charged core histones. Core histone tails are epigenetically modified to regulate chromatin structure and gene expression. Linker histone H1 binds to the DNA entering and exiting the nucleosome dyad axis, further compacting the chromatin, bringing nucleosomes closer together (Watson et al., 2004).

Linker Histone H1 and Higher Order Chromatin Structure

A fifth histone, H1, binds to the linker DNA on one side of the nucleosome and to the dyad axis of the 146 bp DNA around the histone core. H1 has a globular domain and two tails, one which is the positively charged unstructured C-terminal domain. The binding of H1 stabilizes the nucleosomal array and narrows the linker DNA entry and exit angle. Thus, H1 binding triggers the formation of the more compact 30 nm chromatin fiber (Luger et al., 1997; Watson et al., 2004).

The next level of chromatin compaction is the formation of the 300 nm fiber. In this level the 30 nm fiber is folded into long loops that are attached to an X-shaped scaffold of nonhistone proteins. During interphase, the chromatin stays attached to the matrix and each chromosome is organized into a specific domain in the nucleus. The interphase matrix is made up of RNA, ribonucleoproteins, NuMA, actin, Topoisomerase II (Topo II), cohesion, HATs, and DNA and RNA polymerases. In mitosis the chromatin fiber is highly compacted into dense chromosomes. To prepare for mitosis Topo II and condensin function to untangle and organize the DNA. Each sister chromatid must be clearly defined and attached to one another only at the centromere. The 700 nm fiber is the condensed diameter of each individual chromatid and the 1400 nm fiber represents the size of a completely condensed metaphase chromosome including both sister chromatids (Lodish et al., 2003).

Linker Histone H1 Functions and Subtypes

The histone H1 family has 11 different H1 subtypes, 7 somatic subtypes H1.X, H1.0, H1.1-H1.5, and four tissue specific subtypes H1t, H1T2, H1ILS1, H1.oo. Most organisms express multiple subtypes and variable expression of subtypes is seen between cell lines (Medrzycki et al., 2012). While some functional redundancy in H1 subtypes has been observed in knock-out mice studies, there is evidence that the different subtypes have specific roles and different binding affinities for chromatin (Harshman et al., 2013). All H1 subtypes

bind nucleosomes, compact chromatin, and modulate the accessibility of DNA to transcription factors. However, H1 subtypes carry different posttranslational modifications, which modulate their interaction with different partners and pinpoint specific subtypes to regulate specific subsets of genes (Clausell et al., 2009; Jullien et al., 2010; Nguyen et al., 2014a; Zhang et al., 2012). Also, multi-protein complexes containing H1 variants have recently been discovered which are involved in: nucleosome remodeling, modulating epigenetic markers on DNA and chromatin in response to environmental signals, adaptive responses, gene regulation, cell differentiation, and cancer development (Kinoshita and Seki, 2014; Smith and Workman, 2012).

Non-chromatin functions of H1 subtypes have been recently discovered. For example, H1.2 has been described in several works to have cytoplasmic localization and extra-chromosomal functions (Bleher and Martin, 1999; Green et al., 2010). H1.2 was shown to migrate to the cytoplasm in response to x-ray induced double strand breaks, triggering a Bak dependent release of mitochondrial cytochrome C along with caspase-3, caspase-7 activation and cell death (Figure 2) (Ruiz-Vela and Korsmeyer, 2007).

Results from Garg et al. 2014 support these results by showing the involvement of H1.1 and H1.2 in apoptotic signaling where H1.2 a forms cytoplasmic complexes with proapoptotic mitochondrial protein Bak (Figure 2). H1.2 was also shown to have a cytoplasmic response to treatment of lymphocytic

leukemia (Gine et al., 2008). Additionally, cells treated with flavopiridol showed an increase in cytosolic H1 (all subtypes) as a result of decreasing cell viability (Harshman et al., 2013). In normal fibroblast cell lines H1.2 and H1.5 have been observed in the cytoplasm at various times during the cell cycle (Talasz et al., 2009). These data indicate that although there may be some functional overlap between linker histone subtypes, they also have subtype specific functions and activities which are not associated with chromatin (Izzo et al., 2013).

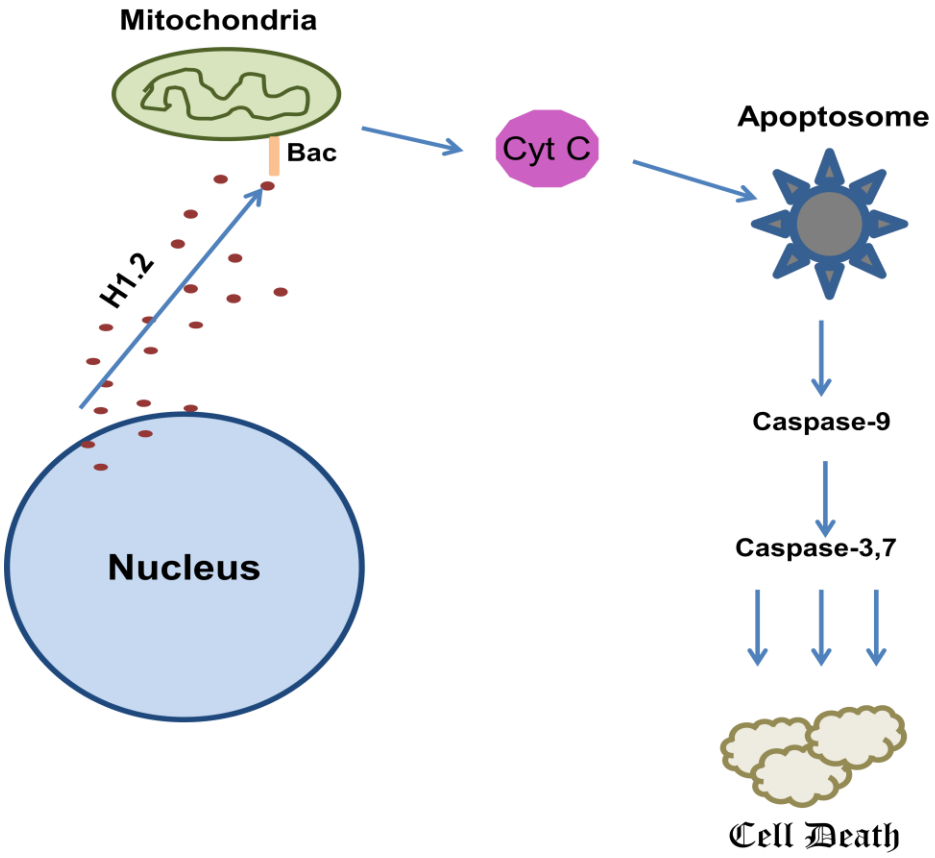

Figure 2. Apoptotic Signaling Through H1.2 Nuclear Release. Upon x-ray induced DNA double strand breaks or treatment with anticancer genotoxic drugs H1.2 is released from the nucleus. Nuclear evacuation of H1.2 followed by interaction with mitochondrial Bac and cytochrome C-dependent caspase activation and cell death (Garg et al., 2014; Gine et al., 2008).

Linker Histone H1.3

This work describes the association of linker histone subtype H1.3 with various cellular processes. The chromatin architectural role of H1.3 has been well documented. Previous works have shown H1.3 to have high affinity to nucleosomes recruitment, intermediate binding strength to chromatin and high

DNA-condensing properties (Garg et al., 2014). H1.3 expression is cell-type and tissue-type specific and is regulated throughout cell differentiation and organismal development. H1.3 traditionally has lower expression in differentiated cells as compared to increased expression in pluripotent cells and many cancers. Furthermore, differential expression of H1.3 is correlated with various cancer processes (Ascenzi and Gantt, 1999; Harshman et al., 2014; Millan-Arino et al., 2014; Scaffidi, 2016). Nuclear distribution of H1.3 differs from that of other linker histones in both plants and human cell lines.

H1.3 expression was shown to be stress induced in tomato plants where the H1-D (H1.3 ortholog) gene was strongly induced by drought and abscisic acid (ABA) (Ascenzi and Gantt, 1999). Rutowicz et al. (2015), show that in *A. thaliana* H1.3 has faster and less stable binding mainly heterochromatin regions, H1.3 is constitutively expressed in guard cells but not in other cells, and reduces it stress response to drought (Rutowicz et al., 2015).

Functions of H1.3 not related to transcription regulation or chromatin structure have been reported by the discovery of an HDAC3-H1.3 complex that is colocalized to polar microtubules and spindle poles in mitotic HeLa cells. This data suggests a potential role for H1.3 in the regulation of polar microtubule dynamics in mitosis (Patil et al., 2016).

Histone Deacetylases

Histone acetyltransferases (HATs) catalyze the transfer of an acetyl moiety from acetyl-CoA to the amino group of lysine residues on the N-terminal tail of core histones. Acetylation neutralizes the positively charged lysines and loosens the interactions between the histone tails and nucleosomal DNA. This relaxed from of chromatin destabilizes the chromatin structure and is necessary to allow nonhistone proteins access to DNA for transcription, replication, and DNA repair. Histone deacetylase enzymes (HDACs) remove posttranslational acetylation on lysine residues, causing chromatin compaction and diminishing the accessibility of the DNA (Di Gennaro et al., 2004; Watson et al., 2004). In addition to regulating the chromatin structure HATs and HDACs also regulate the function of nonhistone proteins through acetylation and deacetylation. Some nonhistone protein targets include: p53, α-tubulin, E2F, MyoD, HMG proteins, and various other transcription factors (Gao et al., 2010; Gregoire et al., 2007; Juan et al., 2000; Kachhap et al., 2010; Vogelauer et al., 2012). Most nuclear localized HDACs function as part of large corepressor complexes, which are recruited to target DNA through DNA binding elements or transcription factors. HDAC proteins play a large role within the cell, participating in critical events such as chromatin organization, gene regulation/silencing, and mitosis. HDAC proteins also play a large role within the cytoplasm of the cell, regulating intracellular trafficking, cell signaling, and apoptosis (de Ruijter et al., 2003;

Ropero and Esteller, 2007; Ververis et al., 2013; Verdin, E., and Ott, M. 2015).

HDAC Classification

There are four classes of HDACs in humans. Class I, homologous to yeast RPD3, includes: HDAC 1, 2, 3, & 8. Class II, homologous to yeast HDA1, can be further broken down into class II a: HDAC 4, 7, & 9, and class II b: HDAC 6 & 10. Class III, sirtuins, are homologous to yeast Sir2 and include SirT1-7. Class IV is HDAC11 (Gregoire et al., 2007; Gregoretti et al., 2004). Class I HDACs are ubiquitously expressed and localized to the nucleus. Class II HDACs have tissue specific expression and can shuttle between the cytoplasm and nucleus. Class I, II and IV require zinc as a cofactor for enzyme activity. Class III HDACs require NAD^+ as a cofactor and are insensitive to the HDAC inhibitor trichostatin A (TSA). The recently discovered nuclear localized HDAC11 resembles both class I and II HDACs. The overall sequence similarity is too low for HDAC11 to be placed in either group, so class IV was proposed by Gregoretti (Gregoretti et al., 2004; Saleem et al., 2015). The fact that all classes of HDACs are found in eukaryotic organisms (except HDAC11 which is not found in fungi) suggests that each class has a non-redundant function in the cell (Gregoretti et al., 2004).

Class I HDACs and Heterochromatin

There are two types of heterochromatin within the nucleus, facultative and constitutive. Facultative heterochromatin is regulated and assembled to silence genes which were previously active or located in euchromatin. Constitutive

heterochromatin is a region of the genome that is always condensed throughout the life of the organism and generally does not contain genes, such as centromeric DNA, pericentric satellites and telomeres (Craig, 2005). During interphase individual chromosomes occupy distinct domains of the nucleus, with heterochromatin found at the nuclear periphery and euchromatin located toward the center of the nucleus (Cooper, 2004; Weierich et al., 2003). Epigenetically, heterochromatin is characterized by heavy CpG methylation, hypoacetylated histones, and tightly condensed chromatin resistant to transcription (Rountree et al., 2000).

As a cell differentiates, spatial reorganization of constitutive and facultative heterochromatin occurs; this process is dependent on HDAC activity (Terranova et al., 2005). In some cells, differentiation triggers centromere clustering and increased tri-methylation of histone H3 Lys9 and H4 Lys20. HDACi treatment at the onset of differentiation inhibits cellular differentiation, while HDACi treatment under conditions allowing for differentiation prevents the reorganization of constitutive heterochromatin (Terranova et al., 2005).

Condensation of mitotic chromosomes is another event when the cell utilizes histone deacetylases to facilitate chromatin compaction. Acetylation levels of core histones begin to decrease in early mitosis, are absent in metaphase and anaphase, and increase again in late mitosis near G1. While there has been extensive research investigating the role of HDAC proteins in

gene regulation, the role of HDACs in the condensation of mitotic metaphase chromosomes has received little attention. However, recent publications show evidence of HDAC participation in regulating mitotic proteins as well as chromatin structure (George and Walworth, 2015; Li et al., 2006; Li et al., 2015; Zullo et al., 2015).

Class I HDACs Involvement with Mitotic Chromosomes

Initial studies to investigate HDAC involvement in mitosis utilized the HDACi TSA, which targets class I and II HDACs. Treatment of cells with TSA resulted in chromosomal instability, chromosome breaks, and impaired segregation of sister chromosomes during mitosis. These data indicated that HDACi treatment can target cellular processes not linked with transcription (Chatterjee et al., 2013; Habold et al., 2008; Kimata et al., 2008; Ma et al., 2008).

The TSA treatment phenotype resembles the deficiency in chromosome segregation observed in cells with defective mitotic spindle assembly checkpoint (Lodish et al., 2003; Magnaghi-Jaulin et al., 2007). There is substantial evidence that HDAC inhibition may cause the spindle assembly checkpoint to be ineffective, causing premature sister chromatid separation (Dowling et al., 2005; Magnaghi-Jaulin et al., 2007). The disruption of the spindle assembly checkpoint is due to altered acetylation levels in involved proteins due to the HDACi activity. Recently, it has been demonstrated that HDACs regulate a subunits of APC/C and adherin (Kimata et al., 2008). Anaphase promoting complex (APC) is a multi-

subunit ubiquitin ligase that promotes degradation of securin, sister chromatid cross-linking proteins and in late anaphase, mitotic cyclins. APC activation by Cdc20 leads to sister chromatid separation and the onset of anaphase (Lodish et al., 2003). It has also been proposed that HDAC inhibition induces down regulation of the mitosis-promoting cyclin B1. Premature mitosis exit along with spindle assembly checkpoint inactivation caused partial decondensation of chromosomes upon TSA treatment (Dowling et al., 2005).

The breakage of chromosomes observed during mitosis after HDACi treatment is likely due to impaired topological organization of the chromatin. DNA topoisomerase II (Topo II) plays a role in mitosis to facilitate the untangling of sister chromatids to prevent segregation errors during anaphase (Navarro and Bachant, 2008). Topo II is found to be associated with chromosomes throughout mitosis and during interphase it is part of the nuclear scaffold. HDAC1 and HDAC2 have been found to interact directly with Topo II through the NuRD and mSin3a complexes (He et al., 2015; Zhang et al., 2013). This interaction seems to be destabilized after HDACi treatment, possibly resulting in Topo II's inability to correctly untangle the DNA between sister chromatids. In mitotic HeLa cells HDAC1-HDAC2 dimers within corepressor complexes disassociate from each other but not the corepressor complex. This is caused by increased phosphorylation of HDAC2 by CK2. HDAC2 does remain enzymatically active

with the increased phosphorylation do to HDAC2 homodimer formation in the corepressor complex (Khan et al., 2013).

Recently, HDAC3 has been implicated in a novel mitotic pathway involving Aurora B kinase and kinase anchor proteins AKAP95 and HA95 (Li et al., 2006). AKAP95 and HA95 are recruited to mitotic chromosomes and are involved in mitotic progression. HDAC3 forms a complex with AKAP95 and HA95; this association has been shown to be required for global histone deacetylation during mitosis, mitotic phosphorylation of H3 Ser10 and normal mitotic progression (Li et al., 2006). Phosphorylation of H3 Ser10 is a well-established and conserved mitotic event. The serine/threonine kinase Aurora B is responsible for phosphorylating H3 Ser10 during early mitosis, triggering the disassociation of HP1 from methylated Lys9 on H3. Aurora B kinase activity is dependent upon hypoacetylation of histone tails. Inhibition of Aurora B leads to impaired chromosome condensation, and segregation during cell division (Wang et al., 2015; Zullo et al., 2015, Li et al., 2006) shows that the AKAp-HDAC3 complex works upstream from the Aurora B-HP1 “meth-phos switch” to deacetylate histone tails and recruit Aurora B (Li et al., 2006).

Also, disassociation of HP1 and phosphorylation of H3 Ser10 leads to chromatin compaction and mitotic progression. Treatment of prostrate carcinoma PC3-PCa with HDACi Probinostat (LBH589) resulted in HDAC6 inhibition and dissociation of HDAC6 from PP1α, increased 14-3-3 acetylation, G2/M arrest

through aurora A/B kinase down regulation and apoptosis. Treatment normal cells with Probinostat resulted in cell cycle arrest in G2, as well as altered acetylation levels of α-tubulin and HSP90 (Chuang et al., 2013).

HDAC3 has recently been implicated in the formation of functional mitotic spindles and kinetochore microtubule attachment (Fadri-Moskwik et al., 2012; Ishii et al., 2008). HDAC3, through the complex N-CoR –TBL1-TBLR1, has been seen to localize to mitotic spindles. Ishii et al. (2008) reports that knock down of HDAC3 or N-CoR results in collapsed mitotic spindles and dome shaped chromosomes. HDAC3 or N-CoR knock down cells showed intact kinetochores and spindle assembly checkpoint, but impaired kinetochore-microtubule attachment. Enzymatically active HDAC3 reverted the collapsed mitotic spindles and changed the distorted shape chromosomes back to wild type. These results demonstrate that the enzymatic activity of HDAC3 is important for spindle function, possibly through deacetylation of mitotic spindle components (Ishii et al., 2008).

Class I HDACs and Transcription Regulation

Higher eukaryotes regulate gene expression at the level of transcription. Local chromatin structure strongly influences the transcriptional potential of genes. Posttranslational modifications such as acetylation and methylation trigger epigenetic events that change chromatin structure. Hyperacetylation is associated with active transcription and euchromatin, while hypoacetylation is

seen in heterochromatin and is associated with transcriptional repression. The first step to gene silencing is the binding of a transcriptional repressor directly to a specific DNA regulatory sequence. After the recruitment of a corepressor-HDAC complex, modification of the chromatin structure occurs. (Clark et al., 2015; Kim et al., 2015; Meier and Brehm, 2014; Saez et al., 2015). Silenced genes are assembled into condensed chromatin, where transcription factors and RNA Pol II are unable to access the DNA. HDACs 1 and 2 are known to function in corepressor complexes: mSin3, Mi-2/NuRD and CoREST. HDAC3 is part of the corepressors SMRT and N-CoR. HDAC8 is not known to be a part of any corepressor complexes (Saez et al., 2015).

HDAC Involvement with ER/Golgi Vesicle Trafficking and Regulation

Microtubules are made up of α-tubulin and β-tubulin dimers assembled into tubular filaments. Each filament has a (+) and (-) end. Filaments emerge from the microtubule-organizing center (MTOC) with the (-) ends anchored onto the MTOC and extension of the (+) end toward the cell periphery. MTOCs are made up of a pair of centrioles and pericetriolar material, located near the nucleus and the Golgi apparatus. MTOC are also involved with mitotic and meiotic spindle fiber organization during cell division. Vesicle trafficking on microtubule tracks is regulated through acetylation of tubulin. Tubulin acetylation is modulated through regulation of HAT and HDAC activity on microtubules.

Acetylation of tubulin leads to stabilization of the microtubule and enhanced vesicle transport (GM, 2000; Gnanambal and Lakshmipathy, 2016).

Vesicles are transported on microtubules via kinesin and dynein, which utilize energy from ATP hydrolysis to power their movement. Vesicles are coated with effector proteins that identify the starting point, direction, and target of vesicles to their final destination. One such protein family is the Rab proteins. Rabs associate with organelles and also with transport vesicles to regulate vesicle formation, transport, tethering and fusion to the desired cellular location. For example, Rab4 is involved in targeting vesicles to Rab11 positive recycling endosomes. Rab5 positive early endosomes mature to Rab7 positive late endosomes targeted to lysosomes for degradation. Rab7 is also involved with transport of late endosomes towards centrosomes. Rab6 regulates retrograde traffic between endosomes, Golgi, ER, and exocytic trafficking to the plasma membrane. Rab6 is involved indirectly in the positive vesicles and the dynein-dynactin kinesin motor complexes and Rab7 links lysosomal protein RILP and dynein-dynactin motors (Figure 3) (Inoshita and Imai, 2015; Stenmark, 2009).

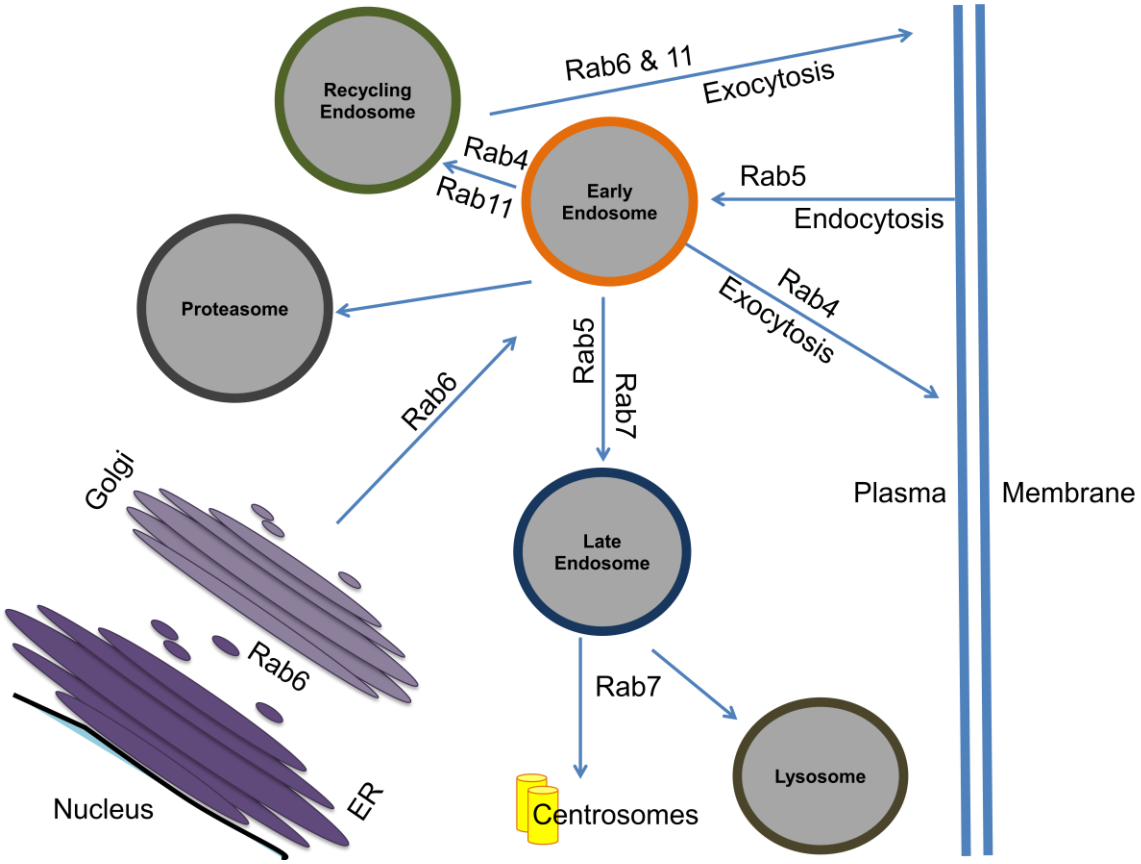

Figure 3. Rab Mediated Intracellular Trafficking. Rab proteins are members of the Ras superfamily of monomeric G proteins. They aid in the recruitment and targeting of vesicles to their destinations. Rab4 is involved in targeting vesicles to Rab11 positive recycling endosomes. Rab5 positive early endosomes mature to Rab7 positive late endosomes targeted to lysosomes for degradation. Rab7 is also involved with transport of late endosomes towards centrosomes. Rab6 regulates trafficking between endosomes, Golgi, ER, and exocytic trafficking to the plasma membrane.

Recent data have shown that HDACs participate in regulating vesicle trafficking via microtubule tracks. Class IIb HDAC6 was shown to deacetylate α-tubulin. Lee et al. show that sodium influx in to the cell induces tubulin acetylation by suppression of HDAC6, resulting in EGR-EGFR vesicle trafficking. Inhibition of HDAC6 accelerates the trafficking of EGFR from early endosomes to late endosomes along the microtubules (Figure 4) (Gao et al., 2010; Kovacs et al., 2004; Lee et al., 2015).

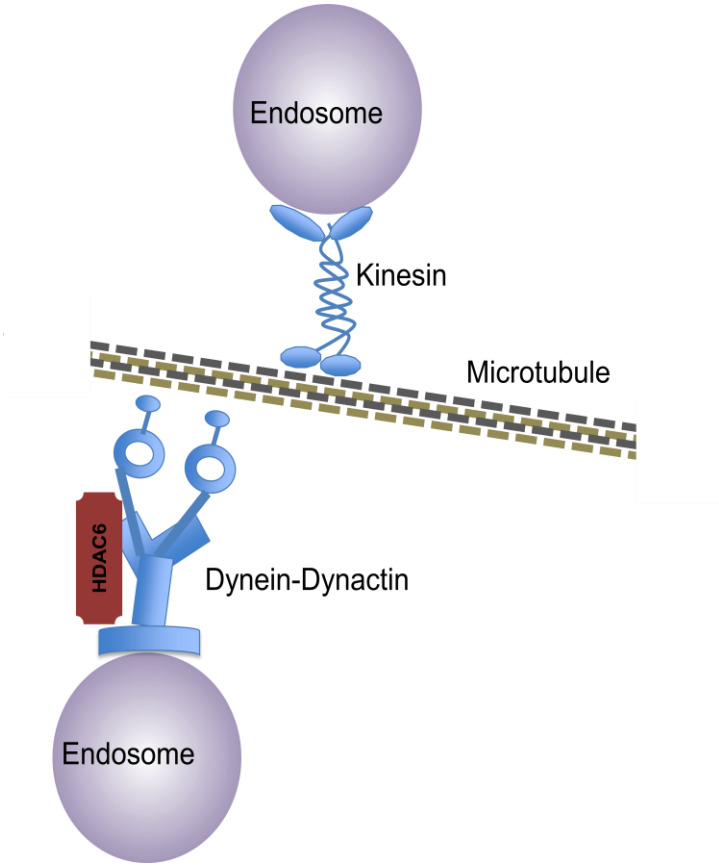

Figure 4. HDAC6 Deacetylation of Microtubules. HDAC6 deacetylates α-tubulin and binds to dynein motors. HDAC6 knockdown accelerated trafficking of endocytosed EGFR to lysosomes of (Gao et al., 2010; Lee et al., 2015).

HDAC8 Specific Cellular Functions

The exact cellular functions of HDAC8 are not clear despite the fact that its structure has been extensively characterized (Decroos et al., 2015a; Decroos et al., 2015b; Galletti et al., 2009). HDAC8 appears to be involved in many cellular processes from regulating gene expression, mitotic progression, cellular trafficking, and microtubule dynamics. HDAC8 is the most unique of the class I HDACs with the closest sequence homology to HDAC1 with a consensus of 37%. HDAC8 is only expressed in vertebrates, with levels varying by tissue type (Hu et al., 2000). The highest levels of HDAC8 are seen in cells showing smooth muscle differentiation (Waltregny et al., 2005). In many cancers there is increased expression of HDAC8, or activated expression when normal tissues do not express HDAC8 (Hsieh et al., 2016; Kang et al., 2014; Niegisch et al., 2013; Park et al., 2011). Recombinant HDAC8 is active when purified from *E. coli*, indicating that its functionality does not require posttranslational modifications for co-activators (Hu et al., 2000). HDAC8 can catalyze deacetylation *in vivo* in the absence of a protein complex. HDAC8 is localized in both the nucleus and the cytoplasm (Lee et al., 2004). While there is evidence that HDAC8 is involved in transcription regulation it has also been implicated in cellular functions within the cytoplasm. HDAC8 is phosphorylated by protein kinase A (PKA) on Ser^{39}, which leads to inactivation of its deacetylase capabilities (Lee et al., 2004; Lee et al.,

2006). Phosphorylated HDAC8 functions to protect human ever-shorter telomeres 1B (hEST1B) from ubiquitin-mediated degradation, thus regulating telomerase activity (Lee et al., 2006). HDAC8 catalyzes deacetylation of the C-terminal end of p53 and Estrogen-Related Receptor alpha (ERRα). Deacetylation of these transcription factors enhances their affinity for DNA binding (Qi et al., 2015; Wilson et al., 2010; Yan et al., 2013). Co-IP studies by Gao et al. show that HDAC8 associates with CREB when both proteins are overexpressed in HEK293 cells (Gao et al., 2009).

Recent data from studies of patients with Cornelia de Lange syndrome (CdLS) show mutations in HDAC8 can cause the CdLS phenotype, including: growth and mental retardation, and limb and facial dysmorphism. Most CdLS patients have mutations in genes related to the cohesion complex but investigation into the association of HDAC8 and cohesion revealed that HDAC8 deacetylates cohesion subunit SMC3 and is involved in cohesion localization to chromosomes (Decroos et al., 2014; Decroos et al., 2015a; Mannini et al., 2015; Parenti et al., 2015).

HDAC8 has also been implicated in the regulation of cytoskeleton dynamics in smooth muscle cells. Recent experiments have shown HDAC8 to associate with α-actin *in vivo,* in a manner essential for muscle contractility (Waltregny et al., 2005). Additionally, HDAC8 was shown to colocalize and IP with smooth muscle myosin heavy chain (de Leval et al., 2006) Additionally, Pull

down data show HDAC8 to associate with myosin heavy chain, and the actin filament regulating protein cofilin. Acetylation levels of α-tubulin increase after addition of HDAC8i or HDAC8 siRNA, which destabilizes microtubules (Li et al., 2014b; Yamauchi et al., 2011). Evidence of HDAC8 involvement in actin binding, cell contractility, and interactions with cytoskeletal components, demonstrates the importance of HDAC8 in modulating microtubule dynamics and possibly cellular transport. This evidence strongly demonstrate HDAC8's role in regulating cell motility and microtubule dynamics. Interestingly, Patil et al. (2016), also demonstrated that linker histone subtype H1.3 associated with both HDAC3 and HDAC8.

Concluding Remarks

HDACs have been shown to regulate chromatin structure, gene expression, and protein function. HDAC 1, 2, and 3 have long been known to act as part of corepressors complexes for transcription. In recent studies, some advancement has been made towards the elucidation of HDACs function in mitosis and regulation of cellular trafficking. Connections have been found between the deacetylation of spindle components (by HDAC3) and correct chromatid segregation. Studies of HDACi targeting class I HDACs show aberrant mitotic progression due to: G2/M arrest, microtubule instability, chromosomal instability, and breaks. Further study is needed to determine how each Class I HDAC specifically contributes to mitosis and cellular differentiation. As science

begins to clearly understand the various activities of HDACs more effective HDACi cancer therapies can be developed that can target specific cellular functions such as growth inhibition and apoptosis. Also, altered expression levels of HDACs and other cellular proteins such as H1s could be used as diagnostic biomarkers in tumor profiling. Thus anti-cancer therapies can be carefully selected per tumor-type for the best patient outcomes.

Current Research and Hypothesis

This research describes a novel HDAC8-H1.3 complex. Previous studies demonstrated that HDAC3 interacts with linker histone H1 (Patil et al., 2016). Results I have obtained (through co-immunoprecipitation and Western blot) show an interaction between HDAC8 and H1. Further analysis of H1 by variant-specific antibodies (H1.1-H1.3 and H1.5) demonstrated an association between HDAC8 and linker histone variant H1.3. We postulated that linker histone H1 and HDAC proteins could function together in a complex to promote formation of higher order chromatin structures and gene silencing. Experiments were designed to characterize the function of the HDAC8-H1.3 complex in order to determine if it function was nuclear or cytoplasmic, and whether it was cell cycle dependent.

CHAPTER II

MATERIALS AND METHODS

Cell Culture Methods

Cell lines MCF-7 (breast carcinoma), MDA-MB-231 (breast carcinoma), DU 145 (prostate carcinoma), HFL-α (lung epidermoid carcinoma), and HeLa (cervical carcinoma) were grown and maintained in Dubelco's Modified Eagle's Medium (DMEM, from Gibco #10566, Carlsbad, CA, USA). SK-OV-3 (ovarian carcinoma) and HCT-116 (colorectal carcinoma) were grown in McCoy's 5A media (ATCC, Manassas, VA, USA). All media was supplemented with heat-inactivated 10% fetal bovine serum (FBS) (Gemini, Bench Mark FBS #100-106, West Sacramento, CA), 1% penicillin and 1% streptomycin (Gibco #15140-122, Carlsbad, CA, USA). Cells were maintained at 37°C, 100% humidity and 5% CO_2 in 75 cm^2, 185 cm^2, or spinner flasks with 200-500 ml total volume. Cell populations used for all experiments were harvested during the exponential stage of cell growth as determined by cell growth curve and cell counts.

Cell Synchronization

Synchronization of cells to various stages of the cell cycle was accomplished using a double thymidine block followed by nocodazole treatment

for mitotic synchronization. Cells were given 2 mM thymidine (Sigma #T1895) for 12 hours followed by an 8-hour release in thymidine free media. A second 2 mM. Thymidine block was given for 12 hours. Cells were synchronized to G1/S checkpoint of the cell cycle after the second thymidine block. Collection and lysis of G1/S synchronized cells was performed after the second thymidine block. To obtain cells synchronized at the G2 stage of the cell cycle, cells were released into thymidine free media for six hours after the second block to allow for progression through S-phase and entry into G2. Cells were then collected and lysed after the six-hour release. For mitotic synchronization, cells were treated with 125 ng/ml nocodazole (Sigma #M1404) for 20 hours following three-hour release after the second thymidine block. Cells were collected and lysed following nocodazole treatment. Synchronization for the various stages of the cell cycle was verified by Florescent Activated Cell Sorting (FACS) analysis, as described below.

Flow Cytometry Analysis

To confirm cell synchronization, flow cytometric analysis (FCM) was performed using the BD Bioscience FACSCalibur system. Synchronized cells were fixed with 4% para-formaldehyde, permeablized with 0.25% Triton X-100 (Fisher #BP151), and blocked with 1% BSA (Bovine Serum Albumin, Sigma #B4287) for 30 minutes at room temperature. DNA from 3 X 10^6 cells was stained with 1 ml propidium iodide (PI) plus RNAse solution

(BD Bioscience #550825) for 15 minutes at room temperature. Cells were then passed through a mesh of 37 microns to separate clumps. Cells were analyzed for PI staining by FCM at 585/42 nm. To distinguish G2 from mitotic cells, cells were stained with PI and the florescent antibody against mitotic marker pospho-H3S10-FITC, 1.5 µg in 500 µl 1% BSA), antibody (Millipore #16-222). Non-synchronized cells were also stained with PI and anti-pospho-H3S10-FITC antibody (Millipore #12-487) as a synchronization control, distinguishing G2 from mitotic cells. As a control for anti-pospho-H3S10-FITC antibody staining, a fraction of the G2/M synchronized cells were stained with non-immune-IgG-FITC antibody as a binding control for the mitotic marker. Cells were then analyzed at 530/30 nm for detection of pospho-H3S10-FITC. Dot plots generated show the percentage of cells positive for pospho-H3S10-FITC.

SDS-PAGE and Immunoblot Protein Detection

Whole cell extracts from synchronized and non-synchronized cells were made by lysing exponentially growing cells with 1 X SDS Laemmli buffer (62.5 mM Tris pH 6.8, 2% SDS, 10% glycerol, 0.1 M DTT, 0.01% bromophenol blue). All 1 X SDS cell extracts were analyzed for protein concentration using Peirce 560 nm protein estimation kit (Peirce # 23235). Equal loading of protein onto SDS-PAGE gels was verified by Coomassie blue RX-250 (Bio-Rad #161-0400) staining of the gel and densitometric analysis of core histone proteins. Volume

adjustments of each extract were made until equal densitometric values (±10%) were seen across all extracts under analysis.

Proteins from cell extracts and Co-IP experiments were resolved on the basis of molecular weight using electrophoresis on either 10% or 15% SDS-polyacrylamide gels and tris-glycine SDS running buffer (0.025 M Tris pH 8.3, 192 mM glycine, 0.1% SDS). Proteins were transferred from the gel to a PVDF membrane (Millipore #IPVH20200) using the semi-dry transblot transfer method (Bio-Rad) at 28 mA (~ 3 mA/cm^2) for two hours. Membranes were blocked for 45 minutes at room temperature using 5% nonfat milk (Nestle-Carnation) in PBS with 0.1% Tween-20 (Fisher #BP337). Membranes were probed overnight for the protein of interest with a primary detection antibody in 2.5% milk-PBS. Following overnight incubation, membranes were washed consecutively with PBS for ten, five, and five minutes, and then probed with a secondary antibody that detects the primary antibody, for one hour at room temperature. All secondary antibodies were conjugated to horseradish peroxidase (HRP). HRP was activated with ECL prime detection reagent (GE Healthcare #RPN2232). Visualization of antibody-bound protein bands were detected by x-ray film exposure and development (GE Healthcare Hyperfilm #28906835) (Kodak X-Omat fixer and developer (#1249259, #8868804 respectively). Image acquisition and densitometric analysis of bands were carried out using the

Alpha Innotech imager and Fluorchem HD2 software (Alpha Innotech, San Leandro CA). Densitometric band determination was carried out by band selection, measuring the integrated density value (IDV) for each band. Bands from the same gel were all selected using the same sized selection tool. A portion of the background was also selected and subtracted from each band's intensity to get the net IDV for each band. Background subtracted IDV values were used for statistical analysis and diagram generation.

Co-immunoprecipitation

Cells in log phase of growth were lysed using Radio Immunoprecipitation Assay (RIPA) buffer (1X PBS, 0.5% NP40, 0.5 M NaF, 100 mM Na-Orthovanodate, one complete mini protease inhibitor tablet (mini complete # 04693159001, Roche Diagnostics, San Francisco, CA, USA). Cell lysates were kept on ice while passed through a 21-gauge needle 10 times. Lysates were incubated on ice for 30 minutes then centrifuged at 10,000 g for 20 min at 4°C. After centrifugation the supernatant was collected and protein concentration of the lysate was determined using the Pierce Micro BCA Protein Estimation kit (Pierce Biotechnology #23235, Rockford, IL, USA). For immunoprecipitation (IP) lysate volume was adjusted to 500-2000 µg/ml total protein in one ml final volume. IP tubes were precleared with 1 µg non-immune IgG and 20 µl

protein A/G or L agarose beads for one hour at 4°C. Nonimmune IgG and agarose beads were removed from the lysates by centrifugation at 1000 X g for 5 minutes. Proteins of interest were precipitated from precleared lysates using 2-4 µg of antibody (Santa Cruz Biotechnology #2027, #2025, or #2028) and 20 µl protein A/G or L agarose beads (Santa Cruz Biotechnology #2003, #2336) rocking overnight at 4°C. For each IP against a specific protein of interest there was a corresponding negative control IP using a non-immune IgG antibody of the same species as the specific antibody (Table 2) (Santa Cruz Biotechnology #2027, #2025, or #2028). Immunoprecipitated complexes attached to the beads were collected the next day by centrifugation at 1000 X g for 5 min. After washing the immunoprecipitated beads twice with 1X RIPA buffer, complexes were disassociated into individual polypeptides using 30 µl 1X SDS Laemmli buffer and incubated at 95°C for 5 minutes. Samples were run on SDS-PAGE gels and analyzed by Immunoblot analysis. Positive control inputs were cell lysates equal to ~1.5-10% protein used in IP. Antibodies used in immunoblot detection were from a different species from those used in immunoprecipitation.

In vitro **Pull-down Assay**

Recombinant human HDAC8 (R&D Systems #4359-DA) and recombinant human H1.3 (Alexis Biochem #ALX-201-157, San Diego CA

USA) were incubated together in equal molar ratios, of protein in each reaction in 1 ml total volume RIPA buffer. Two µg of precipitating antibody was used for each reaction (Table 2) (Santa Cruz Biotechnology #SC17778, #SC11544, #SC11405, and #SC8030). Immune complexes were formed overnight at 4°C, collected the next morning with A/G agarose bead precipitation. Immune complexes were dissociated with 1 X SDS and resolved via SDS-PAGE on 12% or 10% gels (using the same protocol as IP) for H1.3 and HDAC8 immunoblot detection respectively. Antibodies used in immunoblot detection were from a different species than those used for protein precipitation.

Immunocytochemistry (ICC)

Cells were plated at $2X10^4$ - $4X10^4$ cells/well (number of cells plated is based on cell size, which is cell line dependent). Cells were grown for two days on coverslips placed in wells of a 24-well plate, until 80% confluency is reached. Cells were fixed with 2% paraformaldehyde (Fisher #T353) in PBS for ten minutes at room temperature. After fixation, cells were blocked and permeabilized with 0.1% Triton X-100, 1% Donkey Serum, 0.1% NaN_3 in 1X PBS (TNBS buffer) for 20 minutes at room temperature. Cells were then incubated overnight at 4°C with the primary antibodies targeting the proteins of interest. The antibodies used were rabbit anti-H1.3 (Abcam #ab24174) at 10 µg/well and mouse anti-HDAC8 (Santa Cruz Biotechnology #SC17778)

at 2 µg/well, rabbit anti-Rab6 1:50 dilution, concentration not specified (Cell Signaling #4879S), rabbit anti-Rab7 1:50 dilution, concentration not specified (Cell Signaling #9367S), was used for ICC. After overnight incubation with antibody and washes the cells were probed with secondary antibodies, donkey α-rabbit-Texas Red ® (Santa Cruz Biotechnology #SC2784) and donkey α-mouse-FITC (fluorescein isothiocyanate) (Santa Cruz Biotechnology #SC2099) for one hour at room temperature. Next, cells were washed to remove nonspecific binding of antibodies, and then the DNA was stained with 1 µg/ml Hoechst (Invitrogen #H3570) for five minutes room temperature. After Hoechst staining cells were washed three times for five minutes in 1X PBS. Coverslips were removed from the wells after the final wash and were air dried at room temperature and mounted onto slides using Prolong Antifade Mounting Medium (Invitrogen #P7481). As a negative control cells were stained with the FITC-conjugated and Texas Red-conjugated secondary antibodies only, without primary antibodies (Table 2) (Santa Cruz Biotechnology #SC2784, #SC2099).

MCF-7 Transfection with Plasmids Expressing Fluorescent Tagged Proteins

Cells were plated on coverslips, 6 X 10^4 in 48 well plates containing 1 ml DMEM supplemented with 10% inactivated FBS and 1% penicillin and streptomycin. Cells were grown for 48 hours until 75% confluency was

reached. Media was removed form cells and cells were washed twice with 1X PBS. For each transfection reaction two tubes were made. One containing 0.25 µg plasmid DNA combined with DMEM for a total volume of 50 µl. and a second tube with 2µl transfection reagent, Liopfectamine LTX (Life Technologies # 153338-100) and 48 µl DMEM. All DMEM used in transfections was free of antibiotics and FBS. Tubes 1 and 2 were combined and incubated for 20 minutes at room temperature with gentle rocking to form transfection complexes. After incubation, transfection complexes were added to cells along with 400 µl DMEM (free of antibiotics and FBS). Cells were then incubated for 24 hours at 37°C to allow for transfection and tagged protein expression to take place. After the 24 hour incubation, cells were washed twice with 1 X PBS, fixed with 2% paraformaldehyde, washed once with 1X PBS + Hoechst, then washed twice more with 1X PBS. Cells that were transfected and then stained with antibodies following the antibody staining procedure for ICC after formaldehyde fixation. Plasmids used for transfection (Table 1):

Table 1.

Plasmids Used for ICC Experiments

Plasmid	**Protein**	**pDNA/well**	**Company**
pCMV-Rab5-GFP	Rab5-GFP	250 µg	Gift Dr. Albanesi
pCMV6-HDAC8-AC-GFP	HDAC8-GFP	125 µg	OriGene
pCMV6-H1.3-AC-RFP	H1.3-RFP	125 µg	OriGene

Confocal Imaging

. Cells were imaged at 600X total magnification, using the Nikon Eclipse Ti microscope with confocal attachment, and analyzed with the Nikon NIS Elements imaging software. Cell images were taken of a single section of the cell at 1 unit confocal.

Core Histone and H1.3 Acetylation/Deacetylation Assay

Recombinant human H1.3 (Alexis Biochem #ALX-201-157), at 0.5 µg was acetylated by recombinant GCN5 that was expressed in and crudely extracted from *E. coli* (Dr. Bergel's lab TWU, Denton, TX). Acetylation reactions of the H1 subtypes were carried out with GCN5 and 100 µg Acetyl-CoA (Sigma #A2181) in 1X HDAC buffer (25 mM Tris-Cl pH 8.0, 137 mM NaCl, 2.7 mM KCl, 1 mM $MgCl_2$, 1 mM BSA) for one hour at 37°C. GCN5 then be inhibited by 1 mM anacardic acid (Sigma #A7236). One µg human recombinant HDAC8 (R&D Systems #4359-DA) was added to the reaction mixture and deacetylation of H1.3 was carried out for one hour at 37°C. As a negative control H1.3 was acetylated by GCN5, anacardic acid was added but HDAC8 was excluded from the one hour deacetylation incubation. Acetylation levels of H1.3 were determined by immunoblot using an antibody against general acetylated-lysine residues (Millipore #16-222). The concentration and location of H1.3 was verified by Western blot against

H1.3 (Abcam #ab183736). The ratio of acetylated H1.3 to total H1.3 was used to determine the percent of deacetylation of H1.3 by HDAC8.

Acetylated mononucleosomes (equivalent to 3.75 µg DNA) were incubated with 1 µg recombinant human HDAC8 or both 0.5 µg H1.3 and 1 µg HDAC8. All reactions were carried out in 1 X HDAC buffer at 37°C for one hour. Acetylation levels of core histones after incubation with HDAC8 were detected by general anti-acetylated lysine antibody.

Electrophoretic Mobility Shift Assay (EMSA)

Mononucleosomes were used as a binding substrate for H1.3 both alone and in the presence of HDAC8. All EMSA binding reactions were carried out in 1X HDAC buffer at 4°C with H1.3, HDAC8 and mononucleosomes in equal molar ratios 1:1:1. Blue Juice lading buffer (6.5% sucrose, 1 mM Tris pH 7.5 and 0,03% Bromophenol Blue) was used. Resolution of nucleosomes and H1.3-bound nucleosome complexes were carried out on 2% agarose gel in 0.5 X TBE buffer (45 mM Tris-Borate, 1 mM EDTA). Electrophoresis was carried out for two hours at 100 V. Gels were stained with 0.2 µg/ml ethidium bromide (Life Technologies #15585011) for 45 minutes in ultra-pure water. Imaging and densitometric analysis of bands was carried out using the Alpha Innotech imager and Fluorchem HD2 software.

Mononucleosome Preparations

The protocols used to prepare mononucleosomes followed established procedures as reported in Methods in Enzymology and Chromatin Protocols (Bellard et al., 1989; Cirillo and Zaret, 2003; Kornberg et al., 1989; Noll and Noll, 1989). Nuclei were isolated from HeLa cells in the log-phase of growth. Nuclei were digested with nuclease S7 (micrococcal nuclease, 1.6 units/µg DNA, Roche #10107921001) for one hour on ice at room temperature to obtain fragmented chromatin. Digestion was in habited by the addition of EDTA to the final concentration of 10 mM. Nuclei were then lysed and chromatin fragments released. Chromatin bound proteins, including all linker histone H1 subtypes, were removed from the chromatin by increasing the concentration of NaCl to 0.45 M and washing the chromatin through a slurry of CM Sephadex C-25 beads three times (Sigma #C25120). Removal of H1 was verified by Western blot analysis. The salt concentration of the stripped chromatin samples was lowered to 25 mM NaCl by gradual dialysis. Chromatin fragments were separated from one another on the basis of molecular weight by ultracentrifugation (Beckman L8-55M, rotor SW28) through a 12%-50% sucrose gradient in NTE buffer (10 mM NaCl, 10 mM Tris-Cl pH 7.5, 1 mM EDTA), centrifugation was carried out at 131,000 g, for 20 hours at 4°C. After centrifugation, 1 ml fractions of the gradient were collected. Each fraction contained a different

percentage of sucrose and distinct fragments of chromatin corresponding to the number of nucleosomes present on the fragment. Typically, mononucleosomes are expected to be found in fractions containing 15.5 - 17% sucrose. Each fraction was analyzed by agarose gel electrophoresis to identify the chromatin fragments present in each fraction. Fractions containing only mononucleosomes are pooled together and used for EMSAs.

Complex Protein Identification by LC/MS/MS

Proteins from MCF-7 RIPA cell lysates were precipitated with non-immune IgG, α-H1 and α-HDAC8 antibodies (Santa Cruz Biotechnology #SC2025, #SC8030, #SC17778) (Table 2). Immune complexes from immunoprecipitations were run 10 mm into the resolving gel of a pre-cast 10% SDS-PAGE gel (Bio-Rad #456-1033). Gels were stained with Coomassie Blue. The stained area was cut out. Each lane is a separate sample and cut into one mm cubes and submitted for mass spec analysis in an Eppendorf 1.5 ml tube, which has been rinsed with 50% organic ethanol and millipure water. Samples were run on a Thermo Scientific™ Orbitrap Elite™ Hybrid Ion Trap-Orbitrap Mass Spectrometer, using short reverse-phase LC-MS/MS. Samples and results were analyzed at the UT Southwestern proteomic core facility using their in-house data analysis pipeline, with quantitation performed using the Normalized Spectral Index

method (SINQ). The data table lists the proteins identified in both α-H1 and α-HDAC8 immunoprecipitations. The table provides spectral counts and spectral index values and ratios to compare between samples. The mass-spectrometer collects MS/MS fragment spectra, which are generated from peptides. Multiple spectra can be acquired for the same peptide, and different variants of the same peptide may be seen. Protein identifications are inferred from the identified peptides. Protein inference are performed across samples, use the spectral counts or spectral index / ratio column to locate proteins specific to a certain sample. Table guide: Protein accession numbers and descriptions from UniProtKB are listed. Peptide Spectrum Matches (PSM) represents the number of spectra assigned to peptides that contributed to the inference of the protein. Peptide Sequences is the number of different unique peptide sequences, or modified variants of sequences that were identified for the protein. Spectral Counts, for each sample there is a separate spectral counts column, this measures the weighted count of peptide spectrum matches assigned to each protein for the particular sample. MIC Sin is the normalized Spectral Index statistic for the protein for the specified group (quantitative, approximate) and is calculated from the intensity of fragment ions in each spectrum assigned to a particular protein. Ratios are the quantitative ratio for the protein between groups derived from the MIC Sin value. A demonstration of the accuracy of

the method can be found in: Comparative evaluation of label-free SINQ normalized spectral index quantitation in the central proteomics facilities pipeline (Trudgian et al., 2011).

Table 2.

Antibodies Used for ICC, IP, and Immunoblot Experiments

Antibody target	**Manufacture**	**Catalogue Number**	**Immunoblot Dilution**	**[ICC]**	**[IP]**
α-mouse-FITC	Santa Cruz Biotechnology	SC2099			
H1	Santa Cruz Biotechnology	SC8030	1:800-1:1000	10 µg/well	2 µg/ml
H1.1	Abcam	ab17584	1:1000		
H1.2	Abcam	ab17677	1:1000		
H1.3	Abcam	ab24174	1:1000-1:2000	10 µg/ml	
H1.4	Abcam	ab105522	1:1000		
H1.5	Abcam	ab24175	1:1000		
HDAC8	Santa Cruz Biotechnology	SC17778	1:1000	2 µg/well	2 µg/ml
HDAC8	Santa Cruz Biotechnology	SC11544	1:1000	2 µg/well	2 µg/ml
HDAC8	Santa Cruz Biotechnology	SC11405	1:1000	2 µg/well	2 µg/ml
nonimmune-IgG-FITC	Millipore	12-487			
normal goat IgG	Santa Cruz Biotechnology	2028		2 µg/well	2 µg/ml
normal mouse IgG	Santa Cruz Biotechnology	2025		2 µg/well	2 µg/ml
normal rabbit IgG	Santa Cruz Biotechnology	2027		2 µg/well	2 µg/ml
pospho-H3S10-FITC	Millipore	16-222			
Rab6	Cell Signaling	4879S	1:1000	5 µg/well	
Rab7	Cell Signaling	9367S	1:1000	5 µg/well	

(continued)

α-rabbit-Texas Red ®	Santa Cruz Biotechnology	SC2784			
α-mouse-FITC	Santa Cruz Biotechnology	SC358949			

.

CHAPTER III

RESULTS

HDAC8 Associates with Linker Histone H1

This dissertation explored a previously discovered complex between HDAC8 and linker histone H1 (Patil et al., 2016). The interaction between HDAC8 and H1 was verified by immunoprecipitation of HDAC8 from HeLa cell lysates and immunoblot against H1. The results corroborated that H1 association with HDAC8 (Figure 5). The reciprocal experiment was performed where H1 was immunoprecipitated from HeLa cell lysate, complexes were resolved by SDS-PAGE and HDAC8 was detected by immunoblot analysis (Patil et al., 2016). Results from the reciprocal IP also showed an association between H1 and HDAC8. As a negative control for all co-immunoprecipitations, cell lysates were precipitated with nonimmune IgG antibodies derived from the same species as the experimental IP antibody. IgG precipitations when blotted with anti-HDAC8 or anti-H1 antibodies showed no interaction between the nonimmune IgGs and HDAC8 or H1 (Figure 5). These results indicated that HDAC8 and H1 are found together in a stable complex that can be co-immunoprecipitated.

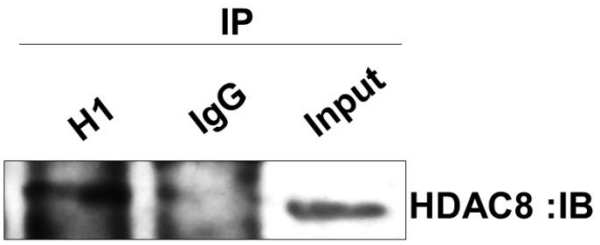

Figure 5. HDAC8 Associates with Linker Histone H1. HeLa cell lysates were immunoprecipitated with an anti-H1 antibody. Precipitated H1 and co-precipitated proteins were resolved by 10% SDS-PAGE and the presence of HDAC8 was detected by immunoblot analysis. A reciprocal co-immunoprecipitation experiment was performed where HDAC8 was immunoprecipitated form HeLa cell lysates, proteins were resolved by 12% SDS-PAGE and H1 was detected by immunoblot analysis, results shown in: (Patil et al., 2016).

HDAC8 Associates with Linker Histone Subtype H1.3.

Since there are several linker histone subtypes, to determine which H1 subtype HDAC8 specifically associates with co-immunoprecipitation of HDAC8 from HeLa cell lysate was performed followed by immunoblot analysis of the somatic linker histone subtypes H1.1, H1.2, H1.3, H1.4, and H1.5. Results showed that HDAC8 specifically associated with linker histone H1.3 and did not associate with subtypes H1.1, H1.2, H1.4 and H1.5 (Figure 6). In the control experiments cell lysates were probed with nonimmune IgG antibodies, and no precipitation of linker histone subtypes was found in the respective immunoblots (Figure 6). The reciprocal of this experiment was attempted; however the available antibodies targeting the tested H1 subtypes were not functional for immunoprecipitation and were not recommended for use in IP (results not shown).

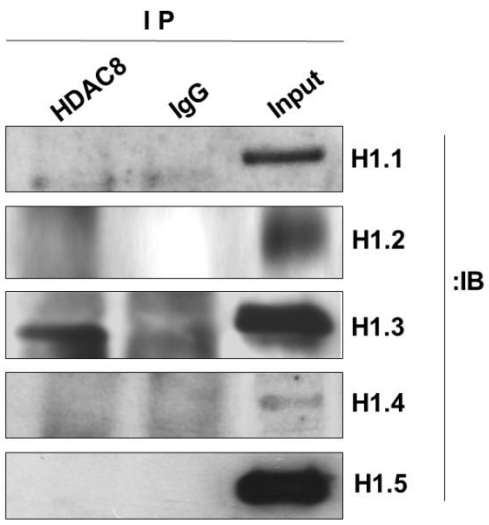

Figure 6. HDAC8 Specifically Associates with Linker Histone Subtype H1.3. HDAC8 from HeLa cell lysates was immunoprecipitated and precipitates were resolved by 15% SDS-PAGE. Association of HDAC8 with the liker histone subtypes H1.1, H1.2, H1.3, H1.4 and H1.5 was determined by immunoblot analysis using the corresponding antibodies. Only linker histone subtype H1.3 showed an association with HDAC8 by immunoblot analysis. Ten percent of the lysate volume used for immunoprecipitation was used as a positive control input. Non-immune IgG antibody was used as a negative control for the immunoprecipitations.

HDAC8 Binds Directly to Linker Histone H1.3

In vitro pull-down assays were used to determine whether the interaction between HDAC8 and H1.3 is a result of direct binding between the two proteins, or an indirect interaction as part of a multi-protein complex. Recombinant human HDAC8 and recombinant human H1.3 were incubated overnight at 4°C in HDAC binding buffer in the presence of an anti-HDAC8 antibody. HDAC8 immune complexes were precipitated and immunoblot analysis was performed with anti-

H1.3 antibody (Figure 7 lane 1 & 6). Control tubes included: anti-HDAC8 antibody with beads and buffer only (Figure 3 lane. 2&5), and anti-HDAC8 antibody with beads, buffer, and H1.3 (Figure 7 lane. 3&4). Immunoblot analysis of the HDAC8 immune complexes showed precipitation of H1.3 in the tube containing HDAC8, H1.3 and the anti-HDAC8 antibody. No precipitation of H1.3 was detected in negative control tubes (Figure 7). Recombinant human H1.3 was used as a positive input control for immunoblot detection. Co-immunoprecipitation of H1.3 with HDAC8 was detected using both anti-HDAC8 mouse or rabbit antibodies. The experiment was performed using two different anti-HDAC8 antibodies to overcome possible interferences between antibody binding and complex formation. No precipitation of H1.3 was seen in the negative control tubes (Figure 7).

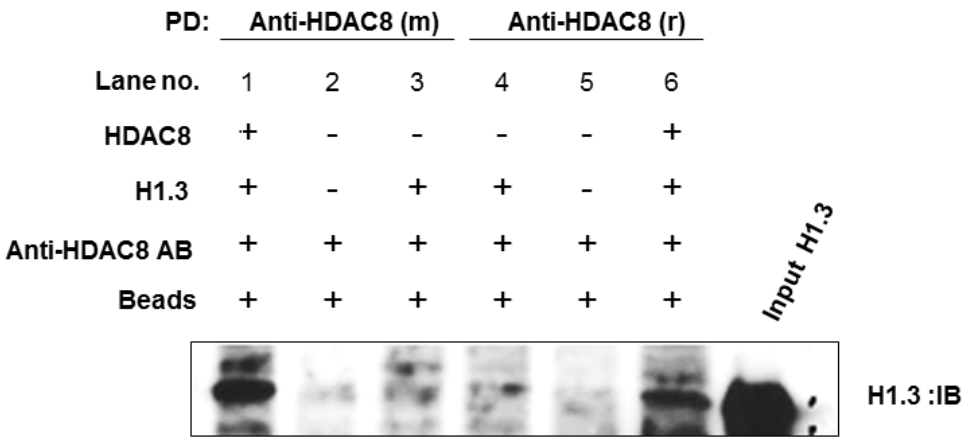

Figure 7. HDAC8 Binds Directly to H1.3. Pull–down assays were used to determine if HDAC8 directly binds to H1.3. Recombinant human HDAC8 and recombinant human H1.3 were incubated together, or individually, with an anti-HDAC8 antibody and AG-agarose conjugated beads overnight in HDAC buffer at 4°C. Both rabbit-anti-HDAC8 and mouse-anti-HDAC8 antibodies were used in separate pull-down reactions, shown above. Precipitated HDAC8 was collected, associated proteins were resolved by 15% SDS-PAGE and immunoblot detection was used to determine H1.3 association to HDAC8.

The reciprocal experiment was performed where H1.3 was pulled down using an anti-H1 antibody and HDAC8 was probed for using immunoblot analysis. As a control HDAC8, H1.3, and actin were incubated together with anti-H1 antibody. Actin is a known HDAC8 binding protein (Li et al., 2014b; Waltregny et al., 2004; Waltregny et al., 2005) and was used as a competitive binding partner for HDAC8. In the absence of the actin there is a strong H1.3-HDAC8 association, but in the presence of actin the association of H1.3 with HDAC8 is reduced. This reduced affinity of HDAC8 for H1.3 is explained by HDAC8s greater affinity for actin than H1.3. Results show that even in the presence of

actin, HDAC8 and H1.3 form a complex (Figure 8). From these results we determined that the interaction between HDAC8 and H1.3 is a direct interaction and no other proteins are required for this interaction to occur. Furthermore, actin can interfere with the H1.3-HDAC8 association either by allosteric changes in HDAC8 after binding actin or through overlapping binding sites between H1.3 and actin.

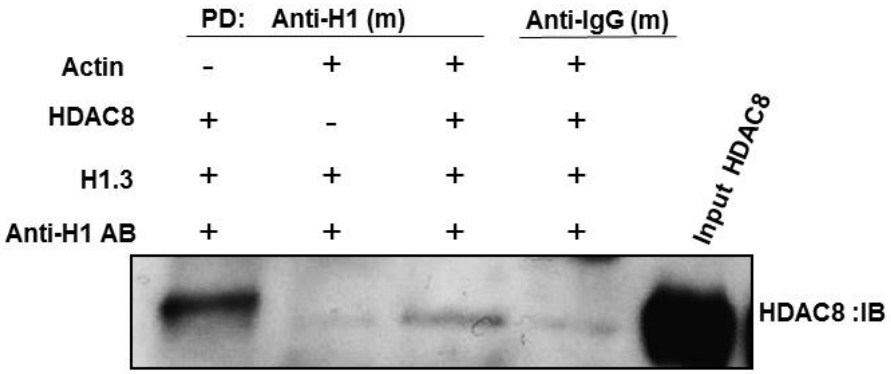

Figure 8. H1.3 Binds Directly to HDAC8. Recombinant human HDAC8 and H1.3 were incubated together, or individually with anti-H1 antibody and AG-agarose conjugated beads, overnight in HDAC buffer at 4°C. Precipitated H1 was collected, protein complexes were resolved by 10% SDS-PAGE and immunoblot detection against HDAC8 was used to determine H1.3 and HDAC8 associations. Purified bovine actin was used to test the competitive binding of the HDAC8 and actin versus the affinity of HDAC8 to H1.3.

H1.3 Has a Higher Binding Affinity to Nucleosomes than it has for HDAC8

Class I HDACs (including HDAC8) and H1.3 are both known to associate with chromatin. Electrophoretic mobility shift assays (EMSAs) were used to test the hypothesis that HDAC8 is recruited by H1.3 to chromatin and to determine if

HDAC8 changes H1.3's ability to bind mononucleosome (Monos). The migration distance of mononucleosomes alone, mononucleosomes in the presence of HDAC8, mononucleosomes with H1.3, and mononucleosomes with both H1.3 and HDAC8 was tested to determine interaction between HDAC8, H1.3 and mononucleosomes under various conditions. All components, HDAC8, H1.3 and mononucleosomes, were incubated in 1:1:1 molar ratio in HDAC buffer at 4°C for various periods of time. To determine if the order of protein incubation had any effect on H1.3 binding to mononucleosomes, differing addition times and order of protein added to the reaction mixture were evaluated. The various experimental conditions are listed in the table below (Table 3). Mononucleosome position within the gel was visualized by ethidium bromide staining.

Results from the EMSA showed that mononucleosomes with HDAC8 alone migrated at the same location as mononucleosomes incubated without any additional proteins at 300 bp (Figure 9, Lane 14). This indicated that HDAC8 does not stably bind mononucleosomes. Mononucleosomes incubated with H1.3 show approximately 50% of the mononucleosome population shifted from 300 bp to 450 bp indicating H1.3 binding to nucleosomes. Mononucleosomes incubated with both H1.3 and HDAC8 migrated at the same location as mononucleosomes incubated with H1.3 alone under all experimental conditions. No super-shift in mononucleosome position was seen with the addition of HDAC8 to H1.3 containing mononucleosomes. This observation suggests that HDAC8 does not

stably bind mononucleosomes in either the presence or absence of H1.3. These results indicate that the H1.3 - HDAC8 complex detected in previous experiments may not occur on the chromatin itself. Additionally, the H1.3-HDAC8 complex was not formed preferentially over H1.3 binding to mononucleosomes as evidenced by unchanging proportion of H1.3 bound mononucleosomes in the presence of HDAC8. When incubation times and order of protein additions were changed no difference in mononucleosome shift patterns between groups were observed (Figures 9 & 11), These observations suggests that H1.3 has a higher affinity to nucleosomes than to HDAC8.

The same EMSA experimental conditions were repeated with nucleosomes containing highly acetylated core histones tails (hyperacetylated mononucleosomes, Ac-Monos). Hyper-acetylated monos were made using the protocol mononucleosomes preparation from cells that were treated with the class I & II HDAC inhibitor Trichostatin A (TSA). The rationale was that HDAC8 may have a higher affinity for hyperacetylated mononucleosomes and that HDAC8 may only be recruited to nucleosomes after H1.3 binding to acetylated mononucleosomes. We demonstrated that using hyperacetylated mononucleosomes we obtained the same results (Figure 12). Thus, mononucleosomes incubated with only HDAC8 migrated at the same molecular weight as hyperacetylated mononucleosomes not incubated with any other proteins. Hyperacetylated mononucleosomes incubated with both H1.3 and

HDAC8 migrated at the same molecular weight as hyperacetylated mononucleosomes incubated with H1.3 alone. Also, the proportion of H1.3-bound hyperacetylated mononucleosomes did not decrease in the presence of HDAC8. Altering the order of protein incubation and binding times had no differing effect when performed on hyperacetylated mononucleosomes as compared to nucleosomes with basal-levels of acetylation. The conclusions are that hyperacetylation of mononucleosome core histone tails does not change the binding affinity of H1.3 or HDAC8 to nucleosome core particles.

Table 3.

Experimental conditions for H1.3, HDAC8 and mononucleosome complex formation for EMSA evaluation.

Lane	**Initial Binding Reaction**	**1st Incubation Time**	**Next Binding Partner Added**	**2nd Incubation Time**	**Total incubation Time**
2	Monos	20 Min	N/A	20 Min	40 Min
3	Monos + H1.3	20 Min	N/A	20 Min	40 Min
4	Monos + H1.3	20 Min	HDAC8	20 Min	40 Min
5	Monos + HDAC8	20 Min	H1.3	20 Min	40 Min
6	H1.3 + HDAC8	20 Min	Monos	20 Min	40 Min
7	Monos + H1.3	20 Min	HDAC8	60 Min	80 Min
8	Monos + HDAC8	20 Min	H1.3	60 Min	80 Min
9	H1.3 + HDAC8	20 Min	Monos	60 Min	80 Min
10	Monos + H1.3	20 Min	N/A	24 Hours	24.33 Hours
11	Monos + H1.3	20 Min	HDAC8	24 Hours	24.33 Hours
12	Monos + HDAC8	20 Min	H1.3	24 Hours	24.33 Hours
13	H1.3 + HDAC8	20 Min	Monos	24 Hours	24.33 Hours
14	Monos + HDAC8	20 Min	N/A	24 Hours	24.33 Hours

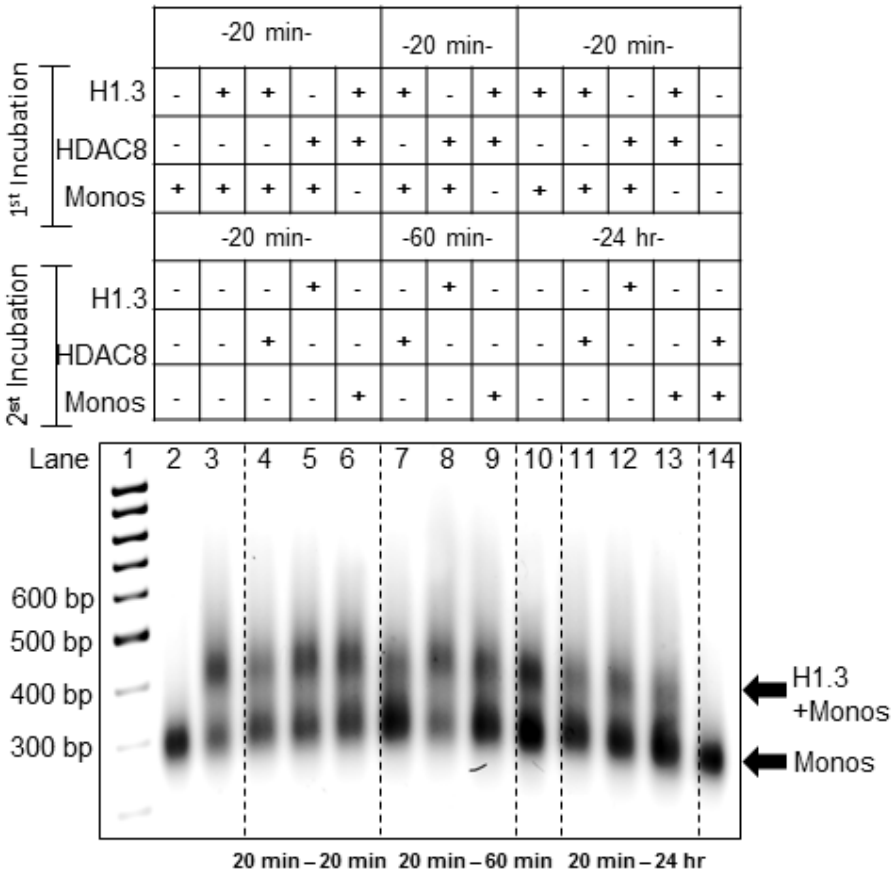

Figure 9. H1.3 Nucleosomal Association in the Presence of HDAC8, Determined by Electrophoretic Mobility Shift Assay (EMSA). Mononucleosome core particles with basal level acetylation (hyperacetylated monos showed the same results on EMSA as monos with basal level acetylation, data not shown) were incubated with HDAC8 and H1.3 in a 1:1:1 molar ratio for various times to determine the binding affinity of H1.3 to mononucleosomes in the presence of HDAC8. Samples were run on 2% agarose gels, stained with ethidium bromide, and mononucleosome position was visualized under UV illumination. Unbound mononucleosome migrated at 300 bp and H1.3 bound monos migrate at 450 bp.

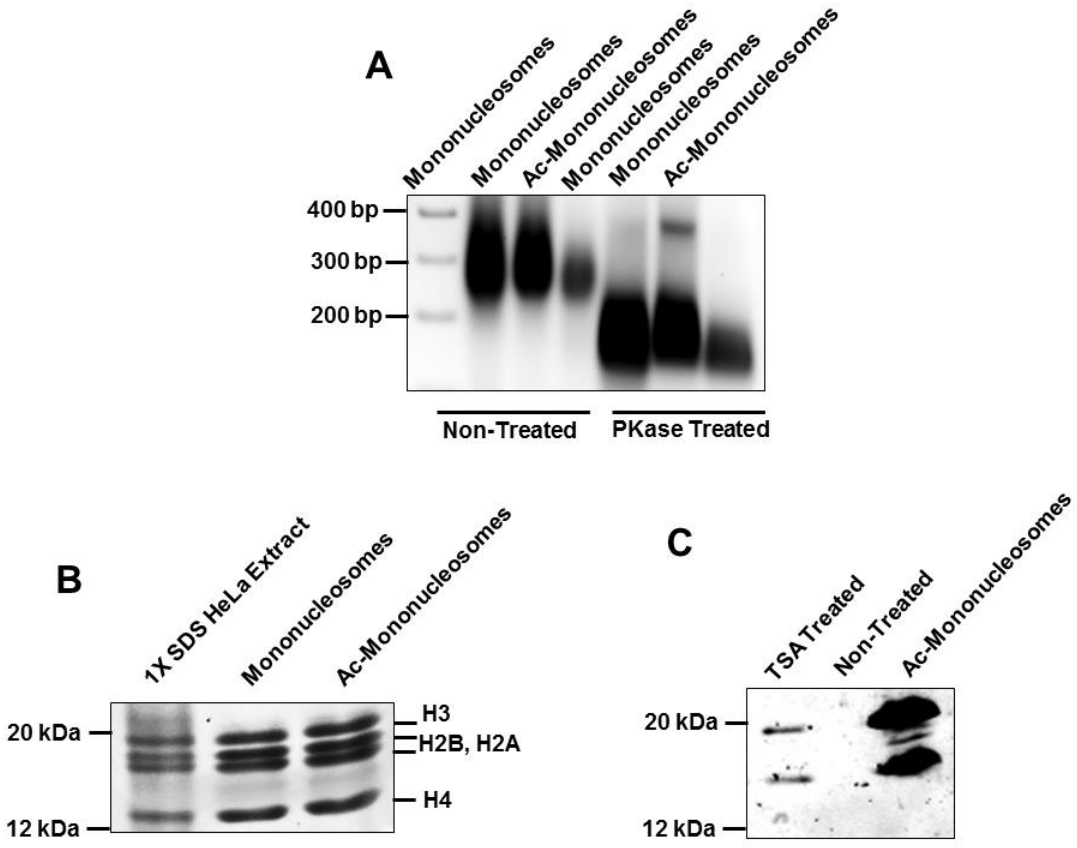

Figure 10. Nucleosome Integrity Verification. (A) Mononucleosomes were treated with proteinase K (PKase) to verify nucleosome structure. Intact nucleosomes with all core histones present run at 300 bp. PKase treated monos with digested core histones run lower than 200 bp. (B) SDS-PAGE of mononucleosomes demonstrate integrity of core histones, all four core histones are present in equal concentrations in intact mononucleosomes. (C) Acetylation levels of core histones on mononucleosomes (TSA treated cell extract, basal level acetylated monos from non-TSA treated cells, hyper-acetylated mononucleosomes from TSA treated cells).

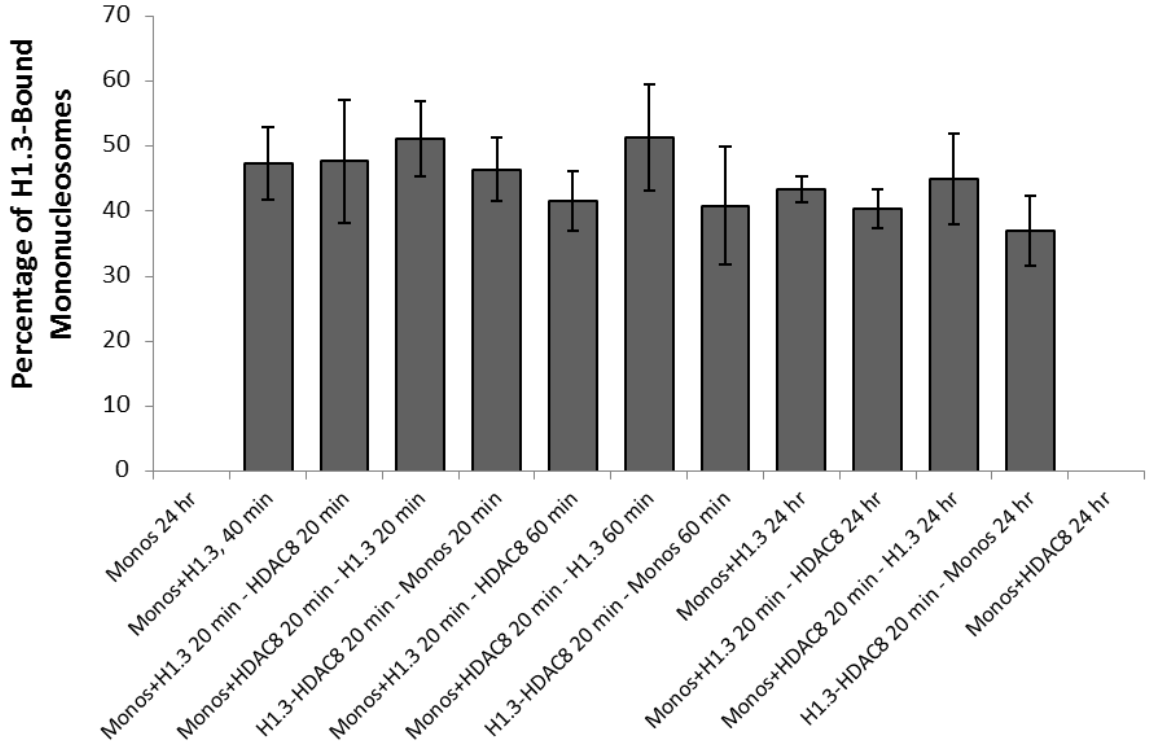

Figure 11. Mononucleosomes With Basal Level Acetylation Bind H1.3 but not HDAC8 or H1.3 and HDAC8 Together. Mononucleosomes were incubated with H1.3 and HDAC8 at a 1:1:1 molar ratio for various incubation times and in varying orders, as indicated. Controls were mononucleosomes alone, monos with only H1.3, and monos with only HDAC8. The average band intensity of monos bound by H1.3 in three independent EMSA experiments showed no significant difference in the affinity for H1.3 to mononucleosomes in the presence of HDAC8. Bars indicate ± standard deviation. One way ANOVA with Holm-Sidak's multiple comparison test, $p \geq 0.05$.

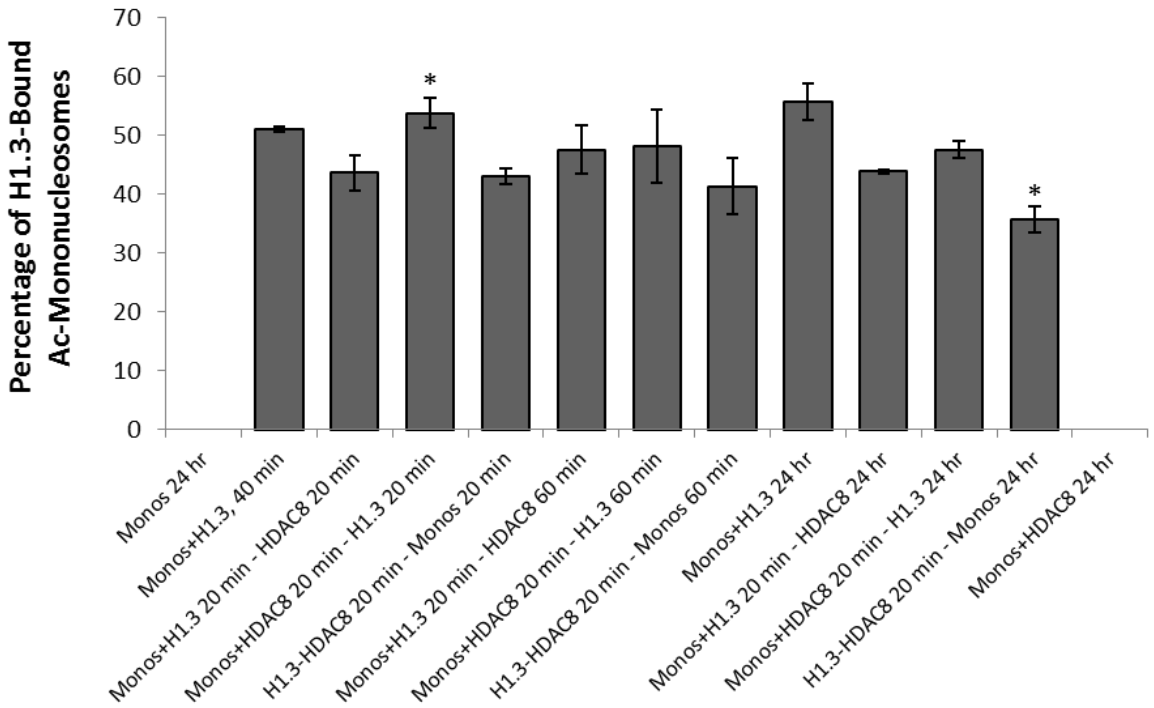

Figure 12. Hyperacetylated Mononucleosomes Bind H1.3 but not HDAC8 or H1.3 and HDAC8 Together. Hyperacetylated mononucleosomes were incubated with H1.3 and HDAC8 in a molar ratio of 1:1:1 were incubated together at various times and in varying orders as indicated. Controls were hyperacetylated mononucleosomes alone, hyperacetylated monos with only H1.3, and hyperacetylated monos with only HDAC8. The average of band intensity of hyperacetylated monos bound by H1.3 in three independent EMSA experiments was plotted. Bars indicate ± the standard deviation. * One way ANOVA with Holm-Sidak's multiple comparison test, $p \leq 0.05$ showed the only significant difference was between indicated groups (*).

HDAC8 Deacetylates H1.3 but not Hyperacetylated Core Histones in Mononucleosomes

Because HDAC8 did not stably bind mononucleosomes or H1.3-containing mononucleosomes and because an HDAC8-H1.3 complex was shown

to form, a deacetylation assay was performed to determine if HDAC8 deacetylates H1.3 or nucleosomes. The rationale for this assay was also supported by the results obtained that demonstrate that H1.3 is a substrate for HDAC3, (Carrie Wilks, personal communications). H1.3 was first acetylated by treatment with recombinant human GCN5, a known histone acetyltransferase (HAT). GCN5 was incubated with H1.3 in HDAC buffer and acetyl-coA for one hour at 37°C. Next, GCN5's enzymatic activity was inhibited with the addition of Garcinol. After GCN5 inhibition, HDAC8 was added to the reaction mixture for one hour at 37°C. Levels of H1.3 acetylation was determined by densitometric analysis of immunoblots using an anti-general acetylated lysine antibody. H1.3 acetylation after incubation with GCN5 was set as one hundred percent acetylation. The relative levels of acetylation before GCN5 treatment and after GCN5 inhibition and HDAC8 treatment were compared to GCN5 treated H1.3. Results showed that H1.3 before GCN5 treatment had low acetylation levels, around 20% acetylation, relative to GCN5 treated H1.3. Acetylation levels of H1.3 after GCN5 treatment, GCN5 inhibition and then HDAC8 addition, returned to that of untreated H1.3, approximately 25% acetylation, one-way ANOVA with Tukey's multiple comparison test $P \leq 0.05$ (Figure 13).

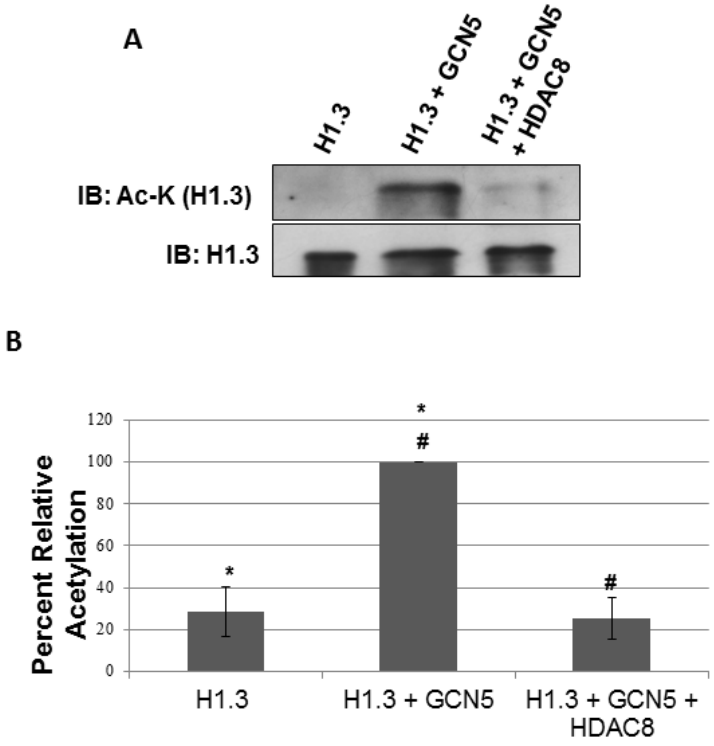

Figure 13. HDAC8 Deacetylates H1.3. Recombinant human H1.3 was acetylated using recombinant human GCN5. After acetylation was achieved, GCN5 was inhibited by Garcinol, after which recombinant human HDAC8 was added to the reaction mixture. This experiment was carried out in triplicate. Graphs are the H1.3 acetylation levels after each incubation. Aliquots of the reaction were taken before addition of GCN5 (H1.3), after GCN5 incubation (H1.3 + GCN5), and after incubation with HDAC8 (H1.3 + GCN5 + HDAC8). Aliquots were used for immunoblot detection of acetylation levels of H1.3 using an anti-acetylated-lysine antibody. Relative acetylation levels of H1.3 in each experimental condition were standardized to H1.3 + GCN5 as 100% and then plotted. Bars indicate standard deviation of three experiments. HDAC8 successfully deacetylated H1.3 and brought the acetylation level of H1.3 back to a level equal to non-treated H1.3. *# One-Way ANOVA with Tukey's multiple comparison test ($p \leq 0.05$).

An HDAC8 deacetylation assay was also used to determine if HDAC8 deacetylates hyperacetylated core histones incorporated into mononucleosomes. Human recombinant HDAC8 was incubated with hyperacetylated mononucleosomes (isolated from TSA treated HeLa cells), with and without H1.3, in HDAC buffer, for one hour, at 37°C. SDS 1X dye was added to the reaction mixture to stop the reaction. Proteins were resolved by SDS-PAGE followed by immunoblot analysis using an antibody against general acetylated lysine residues. Since only 6 proteins of known molecular weight (HDAC8 48 kDa, H1.3 22 kDa, H3 16 kDa, H2A 15 kDa, H2B 14 kDa, and H4 12 kDa) were present, each protein was easily distinguishable on the blot. Results showed that core histones in hyperacetylated mononucleosomes incubated with HDAC8 showed equal acetylation levels to core histones from untreated hyperacetylated mononucleosomes. Hyperacetylated mononucleosomes incubated with both HDAC8 and H1.3 also showed the same level of acetylation on core histones as core histones from untreated hyperacetylated mononucleosomes. There was no change in the level of core histone acetylation in reactions containing HDAC8 as compared with control reactions containing untreated hyperacetylated mononucleosomes alone. Results of three independent repetitions demonstrated that HDAC8 did not deacetylate hyperacetylated core histones of mononucleosomes neither in the presence or absence of H1.3 (Figure 14A & 14B). These results collectively demonstrate that HDAC8 deacetylates acetylated

H1.3 but it does not deacetylate acetylated mononucleosome core histones. These results however cannot rule out the possibility that HDAC8 can deacetylate core histones when it is associated with other subunits in a complex.

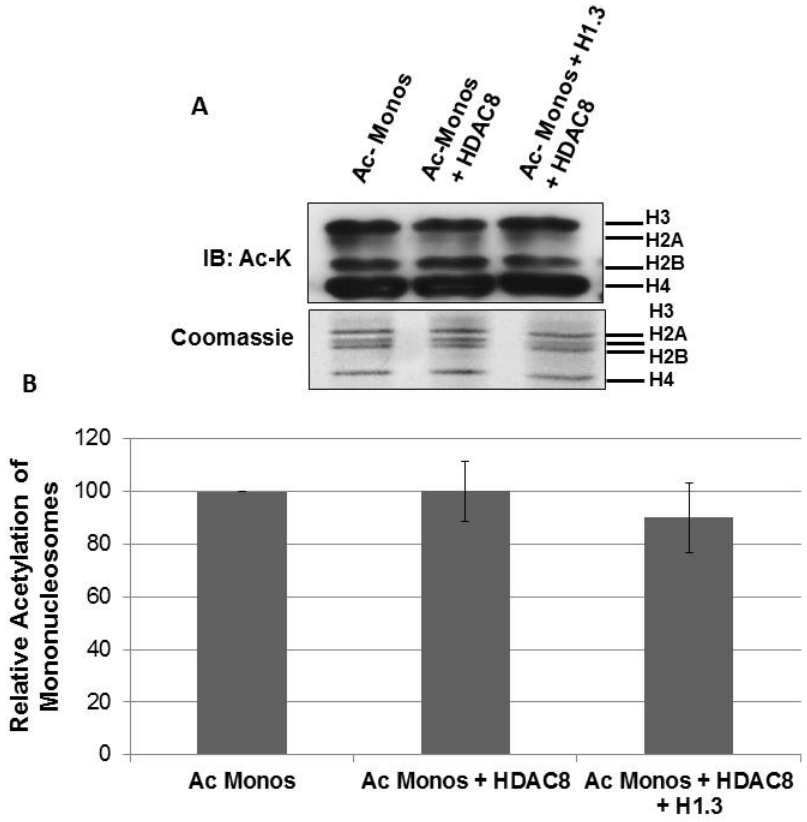

Figure 14. HDAC8 Does not Deacetylate Hyperacetylated Mononucleosomes Regardless of the Presence of H1.3. (A) HDAC8 was incubated with acetylated mononucleosomes in HDAC buffer for one hour at 37°C both with and without H1.3 present (Ac-Monos + HDAC8 + H1.3. and Ac-Monos + HDAC8, respectively). Immunoblot detection of core histone acetylation was carried out with a general anti-acetylated-lysine antibody. Experiments were repeated in triplicate. (B) Plots of the general acetylation levels were standardized to untreated acetylated mononucleosomes as 100% acetylation. Bars indicate standard deviation of the three experiments. No significant difference in acetylation levels between experimental groups was seen. One way ANOVA, with Tukey's multiple comparison test $p \geq 0.05$.

HDAC8 Overexpression is Seen Across Various Cell Lines

Literature has shown that HDAC8 is overexpressed in many types of cancer cells. Also, expression of H1.3 varies by cell line depending on age of the cells and type of tissue. Since there are variable expression levels of both HDAC8 and H1.3 across cell lines we sought to determine which cell lines highly express both proteins and to further explore the formation of the complex in these cells. Cell lines expressing high levels of both HDAC8 and H1.3 were used for further experimental studies. The human cell lines that were chosen for evaluation were: DU145 prostrate carcinoma, MDA-MB-231 breast carcinoma, MCF-7 breast carcinoma, HCT-116 colon carcinoma, HeLa cervical carcinoma, HFL-α lung carcinoma, and SK-OV-3 ovarian carcinoma. Whole cell 1X SDS lysates were prepared for each of the above cell lines. Total protein of each lysate was determined and each sample was standardized for equal loading by Coomassie staining and densitometric evaluation of core histones after SDS-PAGE resolution of lysates. Each cell line expression level of HDAC8 and H1.3 was standardized as a percentage of the highest expressing cell line. Immunoblot detection of H1.3 showed that the cell lines MCF-7, HFL-α, and SK-OV-3 highly expressed H1.3, while DU145, MDA-MB-231, HeLa, and HFL-α showed low expression of H1.3 (Figure 15 & 17).

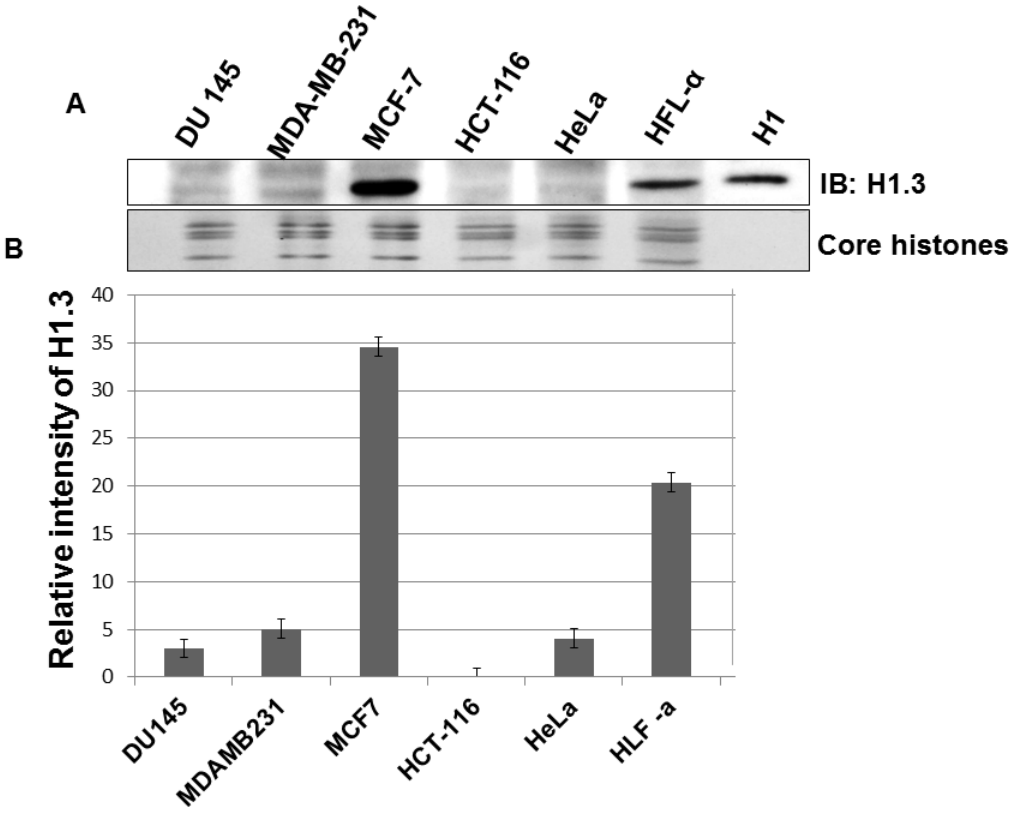

Figure 15. Expression of H1.3 in Various Cancer Cell Lines. (A) Human carcinoma cell lines used to test for H1.3 protein expression levels were: DU145, MDA-MB-231, MCF-7, HCT-116, HeLa, and HFL-α. MCF-7 and HFL-α showed high levels of H1.3 protein expression. The expression level of H1.3 was determined by immunoblot analysis of whole cell lysates. Protein concentration of each lysate was standardized for equal loading by Coomassie staining and densitometric analysis of core histones. (B) The relative intensity of bands was determined by the average of three immunoblots standardizing all cell lines to the highest intensity band. Error bars represent the standard deviation of the average of three experiments.

Immunoblot detection of HDAC8 showed that all cell lines except HFL-α highly expressed HDAC8 (Figure 16 & 17). Since MCF-7 and SK-OV-3 both showed high expression levels of HDAC8 and H1.3, these cell lines were chosen for further study of the HDAC8-H1.3 complex. HFL-α was not chosen for further studies because expression of HDAC8 was low in this cell line. When comparing MCF-7 and SK-OV-3 to each other, it was determined that MCF-7 has higher levels of H1.3 than SK-OV-3 and that SK-OV-3 expresses higher levels of HDAC8 than MCF-7 (Figure 17).

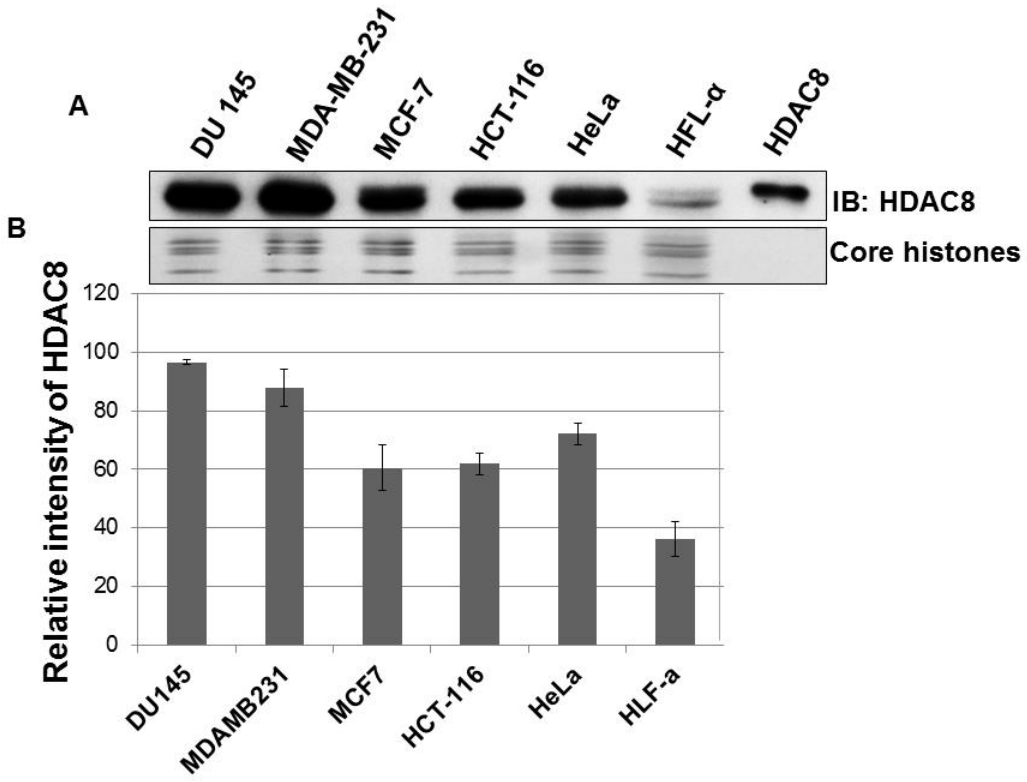

Figure 16. Expression of HDAC8 In Various Cancer Cell Lines. (A) Cell lines tested for the expression HDAC8 expression were: DU145, MDA-MB-231, MCF-7, HCT-116, HeLa, and HFL-α. The expression of HDAC8 was seen in al cell lines tested. Protein concentration of each whole cell lysate was standardized for equal loading by Coomassie staining and densitometric analysis of core histones. (B) The relative intensity of the bands was determined by the average of three immunoblots, standardizing the intensity to a percentage of the highest intensity band. Error bars represent the standard deviation of the average of three experiments.

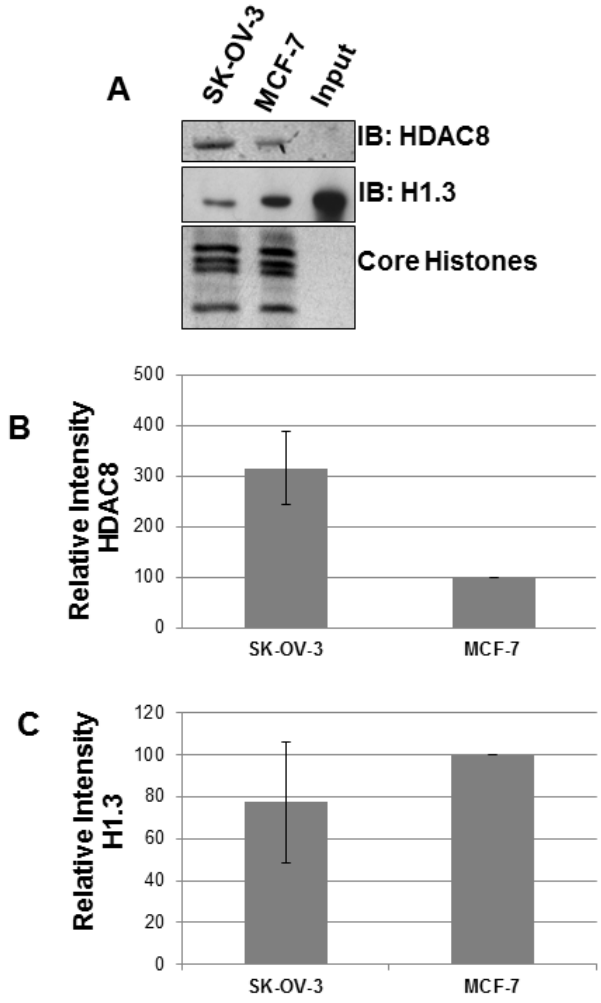

Figure 17. Expression of HDAC8 and H1.3 in Ovarian and Breast Carcinoma Cell Lines. (A) Immunoblot analysis of whole cell lysates of SK-OV-3 and MCF-7 was used to determine the protein expression levels of HDAC8 and H1.3. Protein concentration of each lysate was standardized for equal loading by Coomassie staining and densitometric analysis of core histones. (B&C) The relative intensity of the bands was determined by the average density of three immunoblots, standardizing the intensity to a percentage of the level protein expressed in MCF-7. Error bars represent the standard deviation of the average of three experiments.

The HDAC8-H1.3 Complex Is Detected in both MCF-7 and SK-OV-3 Cell Lines

Cell synchronization followed by co-IP of the HDAC8-H1.3 complex was used to determine if complex formation is cell cycle dependent. MCF-7 and SK-OV-3 were synchronized to mitosis using double thymidine block followed by nocodazole treatment. The synchronization was corroborated by FACS analysis using a double staining of propidium iodide (PI) and α-P-H3S10-FITC (anti-phospho-H3-serine-10, FITC conjugated antibody). These analyses showed mitotic synchronized populations stained with propidium iodide were primarily in G2/M phases (FL2-A axis, intensity 400) of the cell cycle with only a very small portion of the population in G1 and S phase (Figure 18B). Propidium iodide counter stained with FITC-histone H3 phospho-serine 10, a known mitotic marker, was used to verify mitotic synchronization (Figure 18C). Results showed an increase in H3 Ser10 phosphorylation in mitotic synchronized cells (UR quadrant) as compared to non-synchronized cells. FITC-histone H3 phospho-serine 10 staining was seen at approximately 60% of the mitotic population and only approximately 3% in the non-synchronized populations.

Cell lysates were prepared from mitotic and non-synchronized cell populations of MCF-7 and SK-OV-3 cells. Immunoprecipitaed HDAC8 was carried out for each cell lysate, then H1.3 was detected using immunoblot analysis. Co-IP of HDAC8 from mitotic lysates versus non-synchronized lysates

showed varying results dependent on the cell line being tested. In SK-OV-3, the HDAC8-H1.3 complex formation is seen in both non-synchronized and mitotic synchronized cell populations at roughly equal amounts for both cell populations. In MCF-7, HDAC8-H1.3 complex formation is detected primarily in mitotic synchronized populations and to a lesser extent in non-synchronized MCF-7 cells (Figure 18A).

Collectively these results indicate that the HDAC8-H1.3 complex occurs during both mitosis and interphase in both SK-OV-3 and MCF-7 cell lines. Some cell cycle dependent differences are seen in the abundance of the HDAC8-H1.3 complex that appears to be dependent on the different cell types.

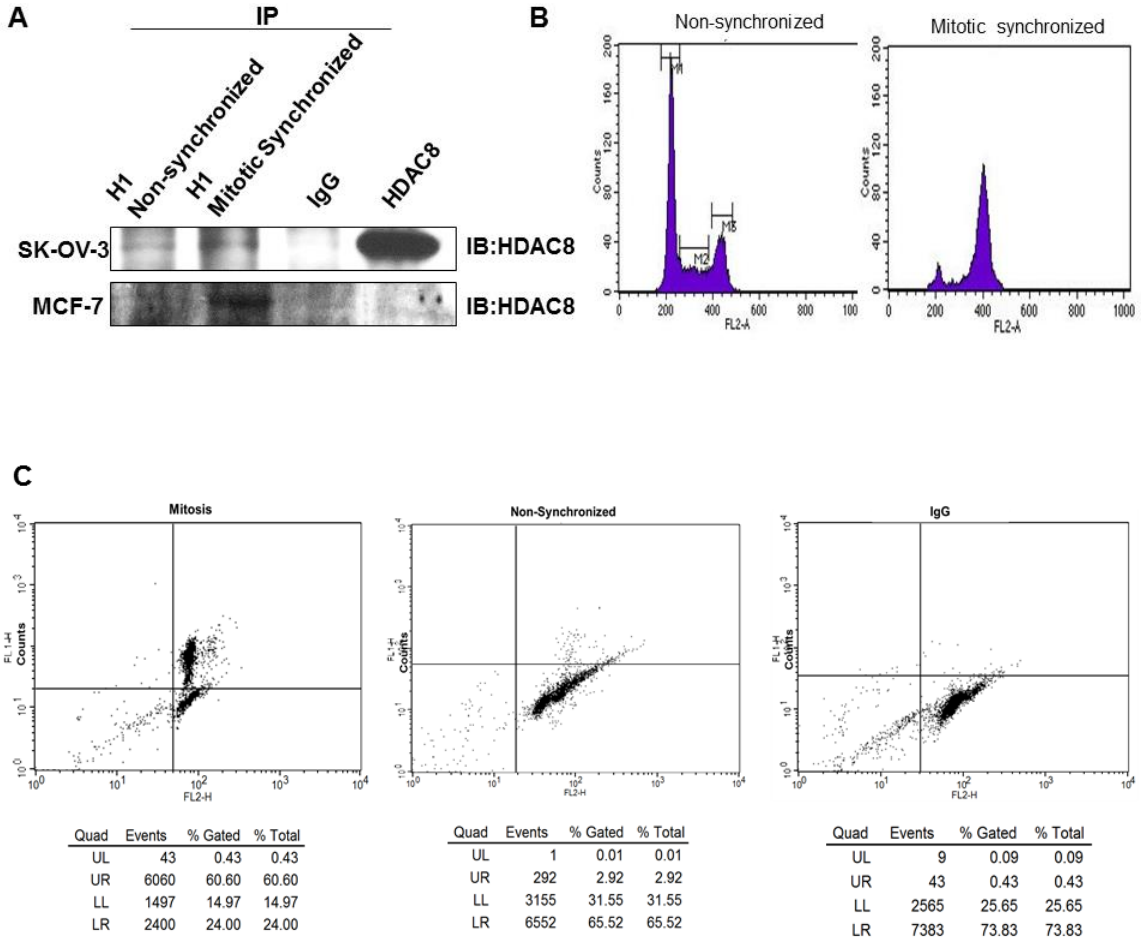

Quad	Events	% Gated	% Total
UL	43	0.43	0.43
UR	6060	60.60	60.60
LL	1497	14.97	14.97
LR	2400	24.00	24.00

Quad	Events	% Gated	% Total
UL	1	0.01	0.01
UR	292	2.92	2.92
LL	3155	31.55	31.55
LR	6552	65.52	65.52

Quad	Events	% Gated	% Total
UL	9	0.09	0.09
UR	43	0.43	0.43
LL	2565	25.65	25.65
LR	7383	73.83	73.83

Figure 18. HDAC8-H1.3 Complex Formation in MCF-7 and SK-OV-3 Mitotic and Unsynchronized Lysates Demonstrated by IP. SK-OV- 3 and MCF-7 cell populations were synchronized to mitosis using a double thymidine block followed by nocodazole treatment. Approximately 60% mitotic synchronization (upper right quadrant, UR). Both non-synchronized and mitotic synchronized SK-OV-3 and MCF-7 cell populations were used for co-IP of linker histone H1 followed by immunoblot of HDAC8. Non-immune IgG was used as a negative control for immunoprecipitation. Mitotic synchronization was verified by propidium iodide and mitotic marker H3 phospho-Ser 10 staining followed by FACS analysis.

HDAC8 and H1.3 are Colocalized to Chromatin in SK-OV-3 and in MCF-7; HDAC8 and H1.3 has Cell Cycle Dependent Colocalization

Indirect immunofluorescence coupled with confocal microscopy was used to visualize the cellular localization of HDAC8 and H1.3 in MCF-7 and SK-OV-3 cells. HDAC8 was visualized with mouse α-HDAC8-FITC and H1.3 was detected with rabbit α-H1.3-Texas Red. In MCF-7 cells HDAC8 showed cytoplasmic localization in both interphase and mitosis. H1.3 in MCF-7 shows nuclear localization during interphase and cytoplasmic localization in mitosis (Figure 19 and table 4).

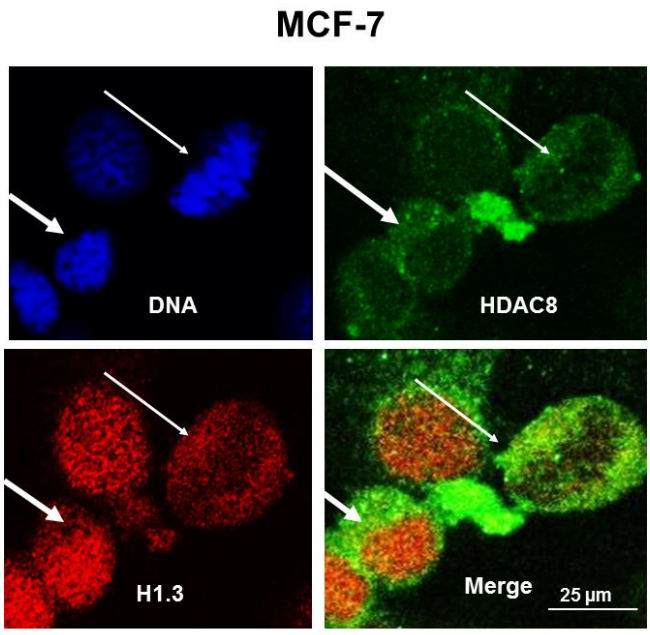

Figure 19. Cellular Colocalization of HDAC8 and H1.3 in Human Breast Carcinoma MCF-7 Cells. HDAC8 and H1.3 were visualized using indirect immunostaining and confocal microscopy. HDAC8 was detected with mouse α-HDAC8 and goat α-mouse-FITC antibodies, and H1.3 was detected using rabbit α-H1.3 and goat α-rabbit-Texas Red antibodies. The DNA was counter stained with Hoechst. Wide arrows indicate interphase cells, narrow arrows indicate mitotic cells. MCF-7 cells showed cytoplasmic localization of HDAC8 in both interphase and mitosis, while H1.3 localization is mainly nuclear during interphase with cytoplasmic localization during mitosis.

In SK-OV-3 HDAC8 was observed to have nuclear localization during interphase and cytoplasmic localization during mitosis. H1.3 in SK-OV-3 is seen to have nuclear localization in interphase and chromosomal localization in mitosis (Figure 20, Table 4).

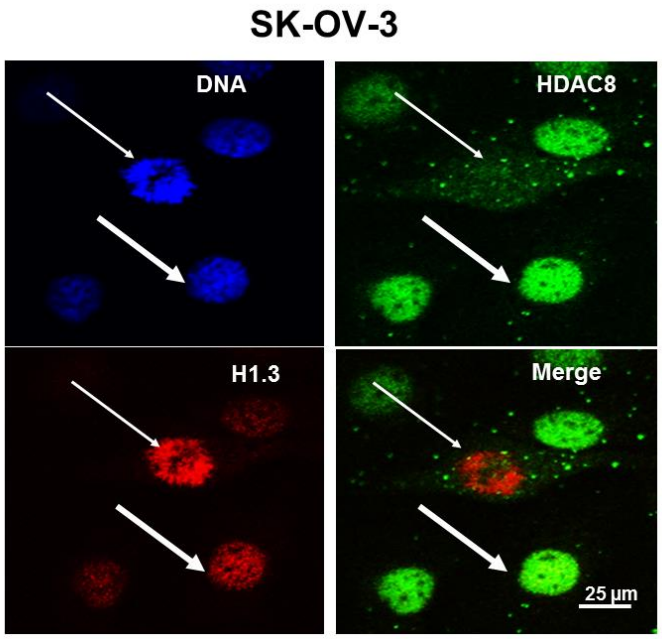

Figure 20. Cellular Colocalization of HDAC8 and H1.3 in Human Ovarian Carcinoma SK-OV-3 Cells. HDAC8 and H1.3 were visualized using indirect immunostaining and confocal microscopy. HDAC8 was detected with mouse α-HDAC8 and goat α-mouse-FITC antibodies and H1.3 was detected using rabbit α-H1.3 and goat α-rabbit-Texas Red antibodies. The DNA was counter stained with Hoechst. HDAC8 has nuclear localization during interphase and cytoplasmic localization during mitosis in SK-OV-3. H1.3 localized to chromosomes during both interphase and mitosis SK-OV-3. Wide arrows indicate interphase cells, narrow arrows indicate mitotic cells.

Table 4.

Summary of HDAC8 and H1.3 cellular localization in MCF-7 and SK-OV-3 cells during interphase and mitosis, visualized by fluorescence confocal microscopy.

	INTERPHASE		**MITOSIS**	
	Cytoplasm	**Nuclear**	**Cytoplasm**	**Chromosomes**
MCF-7	HDAC8 some H1.3	H1.3,	HDAC8, H1.3	-
SK-OV-3	-	HDAC8, H1.3	HDAC8	H1.3

HDAC8 and H1.3 are Colocalized in Vesicles in MCF-7 Cells

HDAC8 and H1.3 were seen localized to the cytoplasm during interphase in MCF-7, leading to further investigation into HDAC8-H1.3 complex formation in MCF-7. Indirect florescent immunostaining of MCF-7 with anti-HDAC8 and goat anti-mouse-FITC antibodies showed a unique cytoplasmic pattern that resembled vesicular staining. H1.3 staining using rabbit anti-H1.3-Texas Red, also revealed nuclear localization of H1.3 and a similar cytoplasmic vesicular staining pattern (Figure 21).

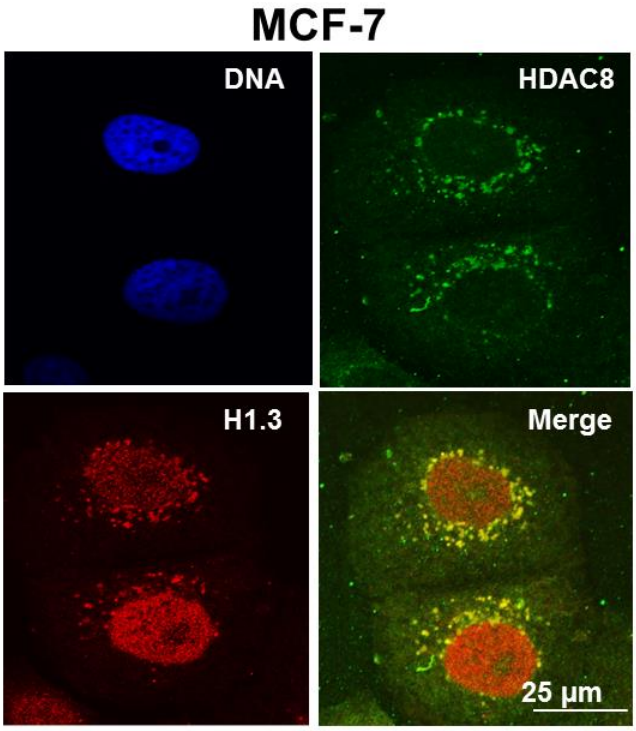

Figure 21. HDAC8 and H1.3 Demonstrate a Cytoplasmic Vesicular Colocalization in MCF-7 cells. Indirect immunostaining of MCF-7 cells with mouse α-HDAC8 and goat α-mouse-FITC show a cytoplasmic vesicular staining pattern. H1.3 was stained using rabbit α-H1.3 and goat α-rabbit-Texas Red, showing a nuclear localization and a cytoplasmic vesicular staining pattern. Hoechst staining was used to counterstain the nucleus.

To corroborate the vesicular colocalization of HDAC8 and H1.3, MCF-7 cells were transfected with plasmids expressing recombinant human HDAC8 tagged to GFP (green fluorescent protein) and/or recombinant human H1.3 tagged to RFP (red fluorescent protein). Cells that were transfected for only one of the proteins of interest were immunostained for the other protein of interest. HDAC8-GFP-transfected MCF-7 cells were stained with anti-H1.3 and goat anti-

rabbit-Texas Red antibodies. H1.3-RFP-transfected MCF-7 cells were stained with anti–HDAC8 and goat anti-mouse-FITC antibodies. Co-transfected cells contained plasmids expressing human recombinant HDAC8 tagged with GFP and human recombinant H1.3 tagged with RFP. Co-transfections and transfections coupled with antibody staining showed HDAC8 and H1.3 colocalization and staining to be vesicular (Figure 22).

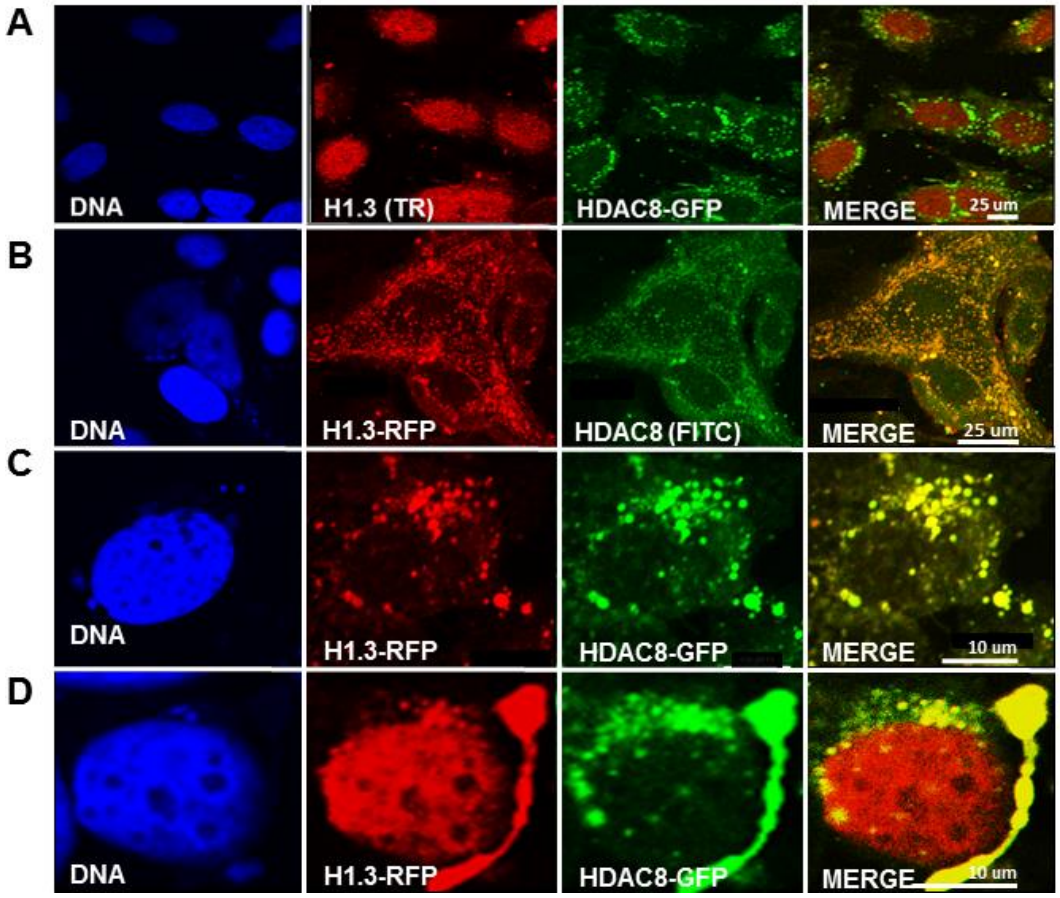

Figure 22. MCF-7 Cells Transfected with HDAC8-GFP and H1.3-RFP Show Colocalization of HDAC8 and H1.3 to Vesicles. (A) HDAC8-GFP-transfected MCF-7 cells were stained with anti–H1.3 antibody and Hoechst. (B) H1.3-RFP-transfected MCF-7 cells were stained with anti–HDAC8 antibody and Hoechst. (C&D) MCF-7 cells were co-transfected with plasmids expressing human recombinant HDAC8 tagged with GFP and human recombinant H1.3 tagged with RFP. Co-transfections and antibody staining of transfected cells showed HDAC8 and H1.3 localization to vesicles. All cells were stained with Hoechst for visualization of the nucleus.

MCF-7 Cells Transfected with RFP-Tagged-H1.3 Show Nuclear, Vesicular, or Localization to both Locations, when Visualizing H1.3

Since H1.3 was detected both in the nucleus and vesicles, localization to each compartment was quantified. Red-Fluorescent-Protein tagged H1.3 was primarily localized to vesicles throughout the cell population, (73%, n=300). Nuclear localization was observed in approximately 30% of the cells and simultaneous localization to vesicles and the nucleus was observed in approximately 13% of cells. The indirect florescence staining of H1.3 by antibodies showed a higher percentage of MCF-7 cells with nuclear staining, which was likely due to cross reaction of the H1.3 antibody with other H1 subtypes (Figure 22 & 23).

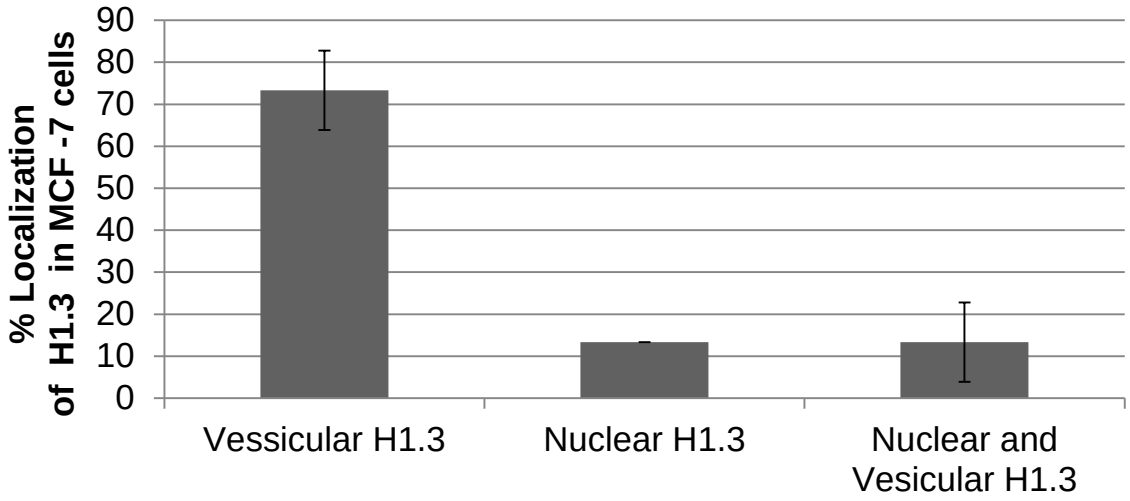

Figure 23. The Percentage of MCF-7 Cells with Vesicular H1.3, Nuclear H1.3, or both Nuclear and Vesicular H1.3. Results from three experiments, scoring one hundred cells from each experiment. Three categories: vesicular H1.3, vesicular and nuclear H1.3, and nuclear only H1.3. Error bars = SD.

HDAC8 is Colocalized to Rab6 Positive Vesicles

MCF-7 cells were transfected with a plasmid expressing recombinant human early endosomal binding protein Rab5 tagged with GFP (gift from Dr. Albanesi from UT Southwestern). The same cells were also stained with mouse anti-HDAC8-Texas Red. Results show both proteins to be localized to the cytoplasm. Rab5 staining showed distinct vesicular staining while HDAC8 showed a spotty pattern of staining around the nucleus but in a differing pattern to that of Rab5. No distinct colocalization of Rab5 and HDAC8 was seen (Figure 24).

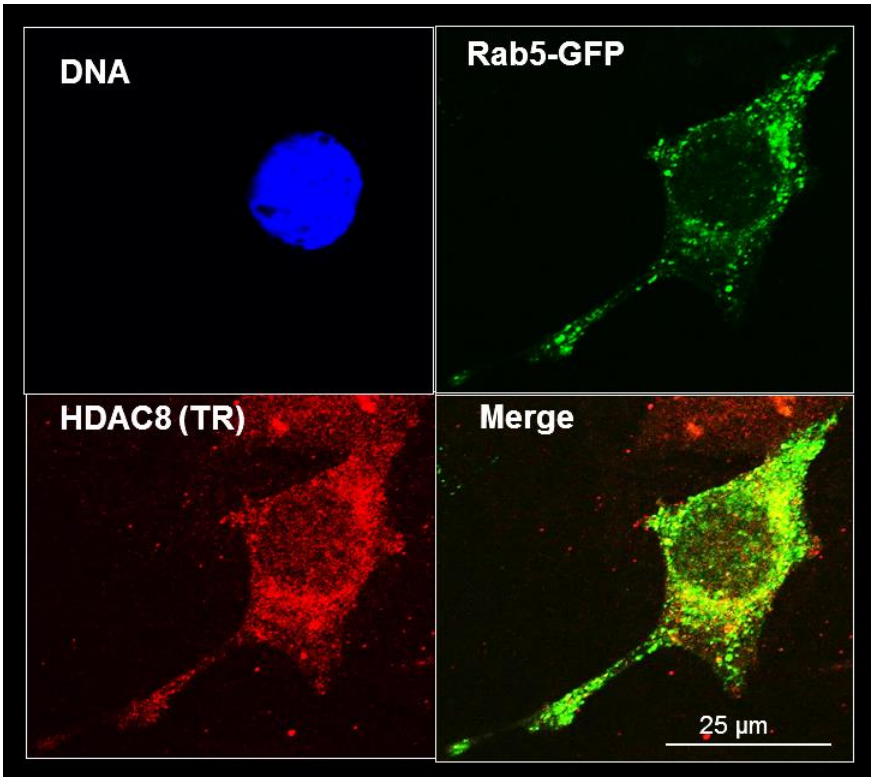

Figure 24. Cellular Localization of HDAC8 and Rab5 in MCF-7 Cells. MCF-7 cells were transfected with a plasmid expressing human recombinant early endosomal binding protein Rab5 tagged with GFP. Cells were also stained with anti–HDAC8 antibody and Hoechst.

Localization of HDAC8 and Rab6, a known marker for trans-Golgi and Golgi-related trafficking vesicles, was determined. MCF-7 cells were co-transfected with plasmids expressing human recombinant HDAC8 tagged with GFP and recombinant human Rab6 tagged with RFP (gift from Dr. Albanesi, UT Southwestern). Co-transfections showed HDAC8-GFP proteins to be co-localized to vesicles positive for Rab6-RFP. Both HDAC8 and Rab6 showed a distinctly

similar vesicular staining pattern with small distinct localizations surrounding the nucleus (Figure 25).

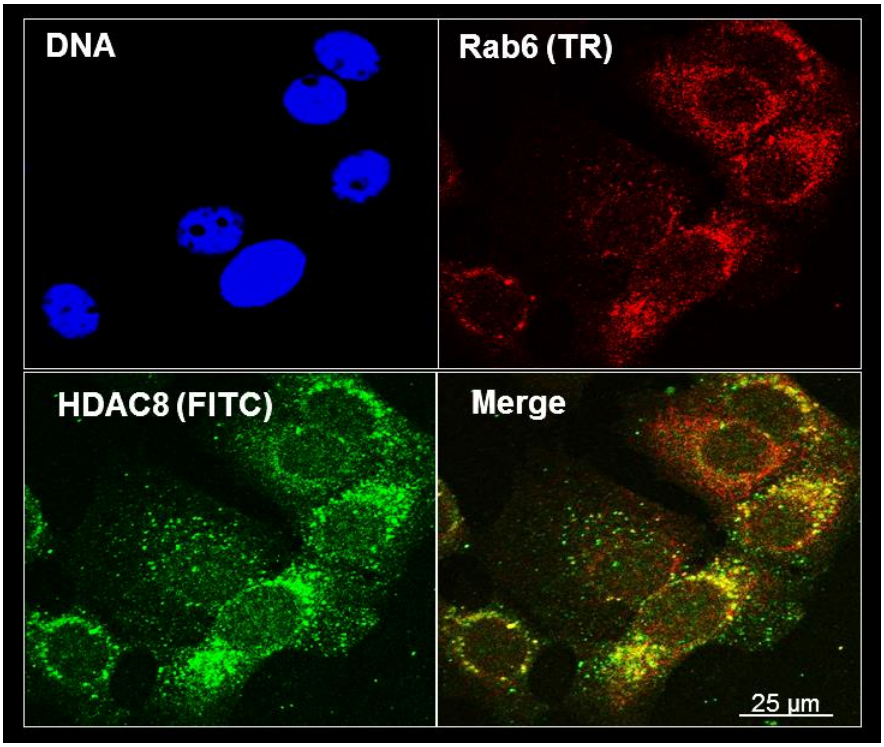

Figure 25. Colocalization of HDAC8 and Rab6 in MCF-7 Cells. MCF-7 cells were co-transfected with plasmids expressing human recombinant HDAC8 tagged with GFP and human recombinant Rab6 tagged with RFP. Co-transfections showed HDAC8-GFP proteins in vesicles positive for Rab6-RFP. In addition cells were counterstained with Hoechst for visualization of the nucleus.

Interaction between HDAC8 and late endosomal binding protein Rab7 was also investigated. MCF-7 cells were co-transfected with plasmids expressing recombinant human HDAC8 tagged with GFP and recombinant human Rab7 tagged with RFP. Co-transfections showed HDAC8-GFP proteins in vesicles surrounding the nucleus and Rab7 localization to Rab7 positive endosomes. Some colocalization was observed between HDAC8 and Rab7 positive vesicles but many vesicles did not show colocalization of the two proteins (Figure 26).

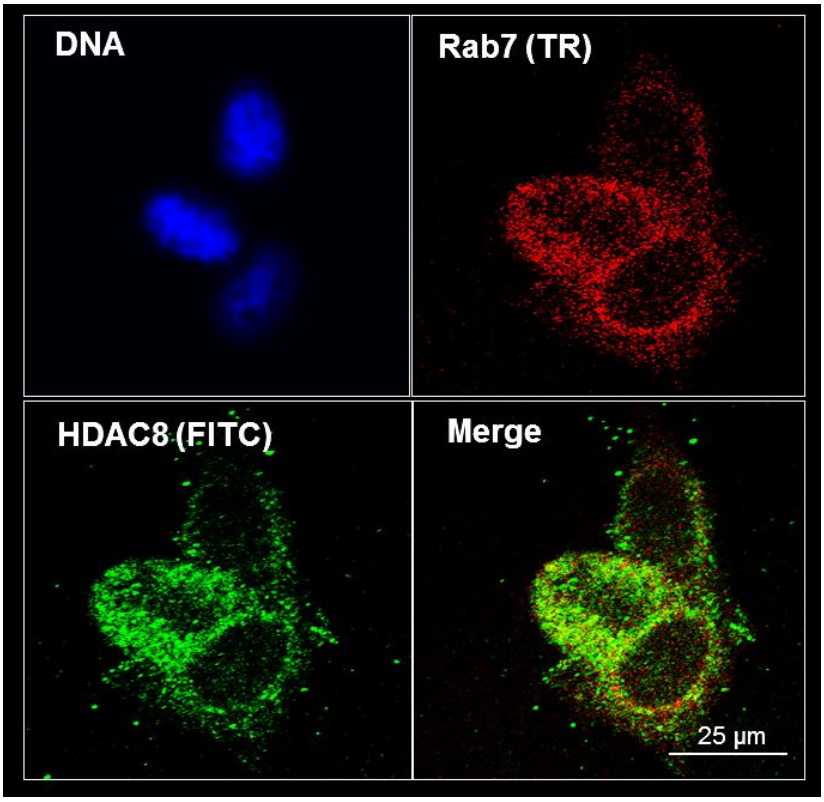

Figure 26. Colocalization of HDAC8 and Rab7 in MCF-7 cells. MCF-7 cells were co-transfected with plasmids expressing human recombinant HDAC8 tagged with GFP and human recombinant Rab7 tagged with RFP. Co-transfections showed a lack of colocalization of HDAC8-GFP proteins in vesicles positive for Rab7-RFP. In addition, cells were stained with Hoechst for visualization of the nucleus.

Complex Mixture Analysis After Co-immunoprecipitation of the HDAC8-H1.3 Complex Reveals Interactions with Vesicle Related Proteins

To verify possible HDAC8 and H1.3 interaction with Rab proteins or Rab-associated proteins, immunoprecipitated HADC8 and H1.3 complexes were submitted to the UT Southwestern proteomic core facility for complex mixture protein identification via Orbitrap LC/MS/MS tandem mass spectroscopy (Table

3). MCF-7 cell lysates were immunoprecipitated with anti-HDAC8, anti-H1 or anti-non-immune IgG antibodies. Each IP was run in a separate lane on 12% SDS-PAGE for a distance of 1 CM. After 1 CM of protein migration through the gel, the gel was Coomassie stained. Lanes were then individually cut from the gel with a clean scalpel for each lane to avoid contamination from one lane to the next. Only the 1 CM lane fragment containing the immunoprecipitated proteins was retained and cubed in to 1 mm X 1 mm pieces. Cubed lanes were submitted for complex mixture protein identification. Common proteins seen with both HDAC8 and H1 IPs, but not IgG precipitation will be evaluated as possible proteins that interact with the HDAC8-H1.3 complex. Comparative analysis *via* SINQ normalized spectral index quantitation, found common proteins in both HDAC8 and H1 IP mixtures. SINQ quantifies proteins based on the number of peptides observed after trypsinization, the fragmentation spectra generated from each peptide, and the intensity of the ions generated from the fragmentation of each peptide (Trudgian et al., 2011). Results from complex mixture identification and SINQ analysis showed several vesicle related proteins that interact with both HDAC8 and H1. Vesicle and or microtubule associate proteins identified in both co-IPs include: COPA coatomer subunit alpha, Sec22B, Sec23A, Sec23B, SEC24, ER-Golgi intermediate compartment protein ERGIC1, peroxisomal membrane protein 11B PEX11B, Ras GTPase-activating-like protein IQGAP1, and clatherin heavy chain 10s protein (Table 5).

Table 5.
Vesicle associated proteins co-immunoprecipitated with H1 and HDAC8 based on mass spec analysis.

							SPECTRAL COUNTS			SPECTRAL INDEX (MIC SIn)			RATIOS	
Protein	Description	Length (AA)	mw (KDa)	PSMs	Peptide Seqs	% Coverage	a-H1	a-HDAC8	a-IgG (neg ctrl)	a-H1	a-HDAC8	a-IgG (neg ctrl)	a-H1/a-IgG (neg ctrl)	a-HDAC8/a-IgG (neg ctrl)
P53621	COPA_HUMAN Coatomer subunit alpha OS=Homo sapiens GN=COPA PE=1 SV=2	1224	139.60	37	25	25.70	20.00	17.00	-	3.21E-06	2.40E-06	-	a-H1 Only	a-HDAC8 Only
E7EP00	E7EP00_HUMAN Protein transport protein Sec24C OS=Homo sapiens GN=SEC24C PE=2 SV=2	975	118.57	29	12	14.80	11.88	12.87	3.96	1.55E-06	1.44E-06	9.06E-07	1.71	1.58
P46940	IQGA1_HUMAN Ras GTPase-activating-like protein IQGAP1 OS=Homo sapiens GN=IQGAP1 PE=1 SV=1	1657	189.62	21	17	13.90	14.99	5.99	-	1.37E-06	4.06E-07	-	a-H1 Only	a-HDAC8 Only
Q00610	CLH1_HUMAN Clathrin heavy chain 1 OS=Homo sapiens GN=CLTC PE=1 SV=5	1675	188.26	21	12	13.10	8.99	10.00	2.00	6.89E-07	7.83E-07	5.51E-07	1.25	1.42
F5H365	F5H365_HUMAN Protein transport protein Sec23A OS=Homo sapiens GN=SEC23A PE=2 SV=1	736	86.32	13	8	15.20	5.92	5.93	0.99	8.58E-07	1.20E-06	4.33E-07	1.98	2.76
Q15437	SC23B_HUMAN Protein transport protein Sec23B OS=Homo sapiens GN=SEC23B PE=1 SV=2	767	86.64	11	8	15.80	6.00	3.00	2.00	1.10E-06	6.35E-07	2.61E-07	4.23	2.44
O75396	SC22B_HUMAN Vesicle-trafficking protein SEC22b OS=Homo sapiens GN=SEC22B PE=1 SV=4	215	24.63	7	4	21.40	4.00	2.00	1.00	2.91E-06	1.34E-06	5.09E-07	5.71	2.64
Q969X5	ERGI1_HUMAN Endoplasmic reticulum-Golgi intermediate compartment protein 1 OS=Homo sapiens GN=ERGIC1 PE=1 SV=1	290	32.20	5	2	19.20	1.98	2.98	-	7.18E-06	1.13E-06	-	a-H1 Only	a-HDAC8 Only
O96011	PX11B_HUMAN Peroxisomal membrane protein 11B OS=Homo sapiens GN=PEX11B PE=1 SV=1	259	26.78	15	10	51.40	7.00	8.00	2.96	2.87E-06	2.51E-06	4.40E-07	6.53	5.70

Note. Cell extracts of mitotic synchronized MCF-7 were immunoprecipitated with either: anti-HDAC8, anti-H1, or anti-nonimmune IgG antibodies. Complexes were resolved by SDS-PAGE through one cm into the resolving gel, lanes were cut from the gel and diced into 1 mm cubes then each lane was individually submitted to complex protein identification mass spectrometry LC/MS/MS. Proteins were identified that have common interaction with both HDAC8, H1 and vesicles using the Normalized Spectral Index (SINQ) method. Spectral counts measures the weighted count of peptide spectrum matches assigned to each protein for the particular sample. MIC SIn represents the normalized Spectral Index statistic for the protein group. This is calculated from the intensity of the fragment ions in each spectrum assigned the protein. The ratios between HDAC8 or H1 and IgG, which are greater than one and present in both IPs, indicate a protein found to co-precipitate with the IP'ed protein. Peptide Spectrum Matches (PSM) represents the number of spectra assigned to peptides that contributed to the inference of the protein. Peptide Sequences is the number of different unique peptide sequences, or modified variants of sequences that were identified for the protein. (Trudgian et al., 2011)

CHAPTER IV

DISCUSSION

HDAC8 Associates with Linker Histone H1.3 to Form a Complex

This body of work identifies a novel HDAC8-H1.3 complex. Evidence from co-Immunoprecipitation (Co-IP) experiments detected the association of HDAC8 with linker histone subtype H1.3. Further analysis of this complex by *in vitro* pull-down assays showed that H1.3 directly binds HDAC8 (Figure 7 & 8). Cumulatively, these results demonstrate the existence of an HDAC8-H1.3 complex in which HDAC8 binds directly to H1.3. Previously published works that lend supporting evidence to HDAC-linker histone interactions include a HDAC3 and H1.3 complex, which is activated by CK2 phosphorylation. Also documented is an interaction between the HDAC SIR-2 and linker histone H1 subtype HIS-24, which was shown to be involved in heterochromatin regulation at subtelomeric regions in *C. elegans* (Patil et al., 2016; Wirth and Jedrusik-Bode, 2009).

HDAC8 Deacetylates Linker Histone H1.3 but Does not Deacetylate or Bind to Mononucleosomes

It was hypothesized that the function of the HDAC8-H1.3 interaction maybe cooperatively inducing the formation of the 30 nm chromatin fiber through

synergistic deacetylation of core histones and H1.3 binding nucleosomes. Previous studies have shown peptide sequences corresponding to acetylated core histones: H3K14, H4K16, and H4K20 to be substrates for HDAC8 deacetylation (Buggy et al., 2000; Smith and Denu, 2007; Van den Wyngaert et al., 2000). Additionally, subsequent studies showed non-specifically hyperacetylated, nucleosome-free core histones to be *in vitro* substrates for HDAC8 deacetylation (Buggy et al., 2000; Hu et al., 2000). While these combined data demonstrate that HDAC8 deacetylates core histones *in vitro* they did not show deacetylation of core histones in the context of chromatin but only free histone proteins or peptides. *In vivo*, the structures of nucleosome-incorporated core histones that interact with DNA contain posttranslational modifications, which alter the affinity of HDAC8 for core histone substrates (Gurard-Levin et al., 2010; Gurard-Levin and Mrksich, 2008).

Based on these data we performed deacetylation assays on both nucleosomes with acetylated core histones (Ac-monos) as well as acetylated linker histone H1.3. Deacetylation assays showed that HDAC8 deacetylates free H1.3 but does not deacetylate acetylated core histones that are nucleosome bound. Currently, there is little evidence definitively demonstrating which lysine residues of core histones undergo deacetylation by HDAC8 *in vivo*. Studies investigating deacetylation levels of core histones after treatment with HDAC inhibitors showed that Trichostatin A (TSA) caused a increase in H4 acetylation

and treatment with Suberoylanilide Hydroxamic Acid (SAHA) caused increased acetylation levels of H3 (Krennhrubec et al., 2007; Olson et al., 2013). However, SAHA and TSA are both pan-HDAC inhibitors and the increase in H3 and H4 acetylation after treatment cannot be attributed solely to inhibition of one particular HDAC. When HeLa cells were treated with the HDAC8/HDAC6 specific inhibitor PCI-34051 no significant changes in acetylation levels of H3 were seen, as compared to SAHA treated cells (Balasubramanian et al., 2008). Based on this current evidence the extent to which HDAC8 participates in the deacetylation of core histones *in vivo* is unknown.

EMSA assays lend supporting evidence as to why HDAC8 may not participate in core histone deacetylation. EMSAs revealed that HDAC8 did not bind to nucleosomes, not even in the presence of H1.3. Reactions with HDAC8, H1.3 and mononucleosomes showed that H1.3 binds to nucleosomes but not HDAC8. Nucleosomes bound with both H1.3 and HDAC8 were not detected under any experimental conditions, such as change in incubation time or change in order of protein introduction into the reaction. HDAC8 in all EMSA experiments was verified to be enzymatically active. Acetylation levels of mononucleosomal core histones had no effect on the above EMSA results. Both hyper-acetylated and basal-level acetylated mononucleosomes yielded the same results. We can conclude from this evidence that H1.3 does not recruit HDAC8 to nucleosomes and that HDAC8 does not enhance H1.3 binding to nucleosomes. HDAC8 may

indeed be recruited to nucleosomes *in vivo* by other protein complexes or miro-RNAs. Evidence from deacetylation assays and EMSAs does not support the hypothesis of synergistic chromatin regulation by the HDAC8-H1.3 complex but that possibly the complex functions on chromatin targets. H1 is rich in lysines, which are positively charged. This could lead to a strong interaction with negatively charged DNA. Acetylation neutralizes the positive charge and reduces the affinity of H1 to DNA. Deacetylation by HDAC8 keeps H1 in its normal positively charged state, and thus maintains its ability to interact with nucleosomes with unaltered affinity.

Cell Cycle Dependent Association of the HDAC8-H1.3 Complex

Mitotically synchronized and non-synchronized MCF-7 and SK-OV-3 cell lysates were co-immunoprecipitated for the HDAC8-H1.3 complex. These immunoprecipitations revealed that the HDAC8-H1.3 complex is present in both interphase and mitosis in MCF-7 and SK-OV-3 cell lines. In SK-OV-3, HDAC8-H1.3 complex formation is seen in both non-synchronized and mitotic synchronized cell populations at roughly equal amounts for both cell populations. In MCF-7, HDAC8-H1.3 complex formation is detected primarily in the mitotic populations and to a lesser extent in non-synchronized cells (Figure 18A).

Evidence for the mitotic formation of the HDAC8-H1.3 complex lead to further investigations into a cell cycle dependent relationship between HDAC8 and H1.3. Additionally, since previous experimentation showed that HDAC8 was

not binding to chromatin or deacetylating mononucleosomes, we hypothesized that the function of the HDAC8-H1.3 complex may be outside the context of chromatin and maybe even non-nuclear.

Co-immunoprecipitation (IP), immunocytochemistry and confocal imaging was used to determine the localization of the HDAC8-H1.3 complex during different cell cycle stages and to gather insight to a possible mechanism of action. The cell lines chosen for further experimentation highly expressed for both HDAC8 and H1.3. Cell lines chosen were breast carcinoma MCF-7 and ovarian carcinoma SK-OV-3 (Figure 15 & 17).

Immunocytochemistry of SK-OV-3 cells revealed that H1.3 remains on the chromosomes during mitosis while HDAC8 is cytoplasmic. In interphase, HDAC8 and H1.3 are both localized within the nucleus. IP however revealed that the complex could be detected in both mitosis and interphase. This indicates that the HDAC8-H1.3 complex potentially forms on the chromatin during mitosis in SK-OV-3 and the complex may have a nuclear function during interphase.

HDAC8-H1.3 Complex is Associated with ER-Golgi Related Vesicles and Late Endosomes

Immunocytochemistry revealed a possible mitotic role for the complex in MCF-7 cells, where H1.3 is seen off the chromatin and localized throughout the cytoplasm during mitosis. HDAC8 was also localized throughout the cytoplasm in a similar pattern to H1.3 (Figure 19). Cytoplasmic colocalization of HDAC8 and

H1.3 during mitosis could indicate HDAC8's involvement in H1.3 trafficking to specific areas during different cell cycle stages. Additionally, regulation of H1.3 acetylation levels could be one mechanism in which cells control the localization of H1.3. During interphase in MCF-7 cells, HDAC8 and H1.3 are localized to the area surrounding the nucleus in a pattern resembling vesicles (Figure 21). To confirm possible vesicular localization in MCF-7 cells, the cells were transfected with plasmids expressing GFP-tagged human HDAC8 and RFP-tagged human H1.3. Confocal microscopy revealed H1.3-RFP localization to both vesicles and the nucleus. HDAC8-GFP localization was primarily vesicular (Figure 22 & 23). After targeting of MCF-7 cells with vesicular markers Rab5, Rab6, and Rab7, the localization of the HDAC8-H1.3 complex was determined to be associated with trans-Golgi vesicles, and late endosomes (Figure 3). It was observed that HDAC8 localized with Rab6 and partially localized with Rab7 positive vesicles (Figure 24-27). LC/MS/MS analysis of co-immunoprecipitations from MCF-7 cell extracts was used to determine additional components of the HDAC8-H1.3 complex, specifically vesicle associated proteins. Results revealed that both HDAC8 and H1.3 were associated with several vesicular proteins: COPA, Sec22B, Sec23A, Sec23B, PX11B, and clathrin heavy chain (CLH1) (Table 5). These results support a cytoplasmic and vesicular role for the HDAC8-H1.3 complex. Specifically, association with COPA, Sec22B, Sec23A, Sec23B, and CLH1 point to the association of HDAC8 and H1.3 with the endoplasmic

reticulum (ER) and Golgi trafficking vesicles. Vesicular interactions of the HDAC8-H1.3 complex are the first evidence for H1.3 involvement with vesicles and ER-Golgi protein trafficking.

Cell-specific differences are seen between MCF-7 and SK-OV-3. In SK-OV-3 the localization of complex is difficult to determine during mitosis, but is detectable though IP. During interphase in SK-OV-3 the complex is detected in the nucleus by both ICC and IP. In MCF-7 cells, the complex is seen in the cytoplasm during mitosis and on vesicles during interphase. These data indicate cell specific roles for the HDAC8-H1.3 complex. Experimental evidence supports the previously reported role for HDAC8 in the cytoplasm (de Leval et al., 2006; Li et al., 2014b; Yamauchi et al., 2011) as demonstrated by colocalization of HDAC8 and H1.3 in vesicles in the cytoplasm and not within the nucleus of interphase MCF-7 cells. The nuclear role for the complex in SK-OV-3 as evidenced by colocalization of HDAC8 and H1.3 to the nucleus during interphase is also supported by previous works (Kang et al., 2014; Yan et al., 2013). It was interesting to see that there are different colocalization patterns of HDAC8 and H1.3 in different cell lines. This is likely related to the fact that each cell line originated from different tissue types and acquired different mutations during malignant transformation. Breast mammary epithelial (MCF-7) and ovarian epithelial (SK-OV-3) have some similarities but vastly different intracellular signaling process and gene expression profiles. For example, MCF-7 and SK-

OV-3 are both estrogen receptor (ER) positive cell lines, however SK-OV-3 has no proliferative response to estrogen while MCF-7 does (Chan et al., 2014; Lattrich et al., 2008; Rochefort et al., 1998). Growth inhibition of MCF-7 occurs in response to anti-estrogen treatment, Tamoxifen, and TNFα. SK-OV-3 growth is not inhibited by anti-estrogen treatment, Tamoxifen, or TNFα. These difference in growth response are due to mutations that lead to altered intracellular signaling pathways between the two cell lines. The differences in these signaling pathways could also be responsible for the difference in the vesicular colocalization and thus different utilization of the HDAC8-H1.3 complex seen in MCF-7 and SK-OV-3 cells (Ahn et al., 2004; Lattrich et al., 2008).

The Role of H1.3 in the HDAC8-H1.3 Complex

Linker histone subtypes H1.0, H1.1-H1.5, and the tissue specific subtypes H1.X, H1t, H1T2, H1ILS1, H1.oo, vary in their expression throughout cell lines and have different binding affinities for chromatin (Harshman et al., 2013). All H1 subtypes modulate the accessibility of DNA to transcription factors (Geeven et al., 2015; Jullien et al., 2010; Pan and Fan, 2016; Siriaco and Tamkun, 2013; Zhang et al., 2012). H1s are well known for their nucleosomal binding and chromatin compacting capabilities. Multi-protein complexes containing H1 variants have recently been discovered and are involved in nucleosome remodeling and the epigenetic modifications of DNA and histones in response to environmental signals, adaptive responses, cell differentiation, cancer

development and gene regulation (Kinoshita and Seki, 2014; Sekeri-Pataryas and Sourlingas, 2007; Smith and Workman, 2012). Likewise, the structural role of H1.3 in modulating chromatin structure has been well documented. Previous works have shown H1.3 to have high affinity to nucleosomes, (Flanagan et al., 2016; Izzo et al., 2013; Izzo and Schneider, 2016; Terme et al., 2011) have intermediate binding strength to chromatin and high DNA-condensing properties (Garg et al., 2014). Subtype H1.3 is also cell type and tissue-specific and its expression is regulated throughout cell differentiation and organismal development (Terme et al., 2011). H1.3 traditionally has lower expression in differentiated cells as compared to increased expression in pluripotent cells and many cancers (Medrzycki et al., 2014; Nguyen et al., 2014b). Furthermore, differential expression of H1.3 is correlated with various cancer processes (Li et al., 2014a; Medrzycki et al., 2014). In our work we found that high expression of H1.3 was seen in several cell lines evaluated, specifically lung (HFL-α), breast (MCF-7), ovarian (SK-OV-3), and cervical (HeLa) carcinomas. Nuclear distribution of H1.3 differs from that of other linker histones in both plants and human cell lines. H1.3 expression was shown to be stress induced in plants where the H1-D gene was induced by drought and abscisic acid (ABA) (Ascenzi and Gantt, 1999; Wei and O'Connell, 1996). Rutowicz et al. 2015b, show that in *A. thaliana* H1.3 has faster and less stable binding to mainly heterochromatic regions in chromatin, is constitutively expressed in guard cells but not in other

cells, and reduces plant stress in response to drought (Rutowicz et al., 2015b). This EMSA data support H1.3's role as a structural protein involved in chromatin formation but ICC and LC/MS/MS data shed light on a potential role for H1.3 in cancer and intracellular vesicular trafficking.

Evidence of linker histone variants, including H1.3, having non-chromatin functions is newly emerging. H1.2 has been demonstrated in multiple works to have extra-chromosomal functions and cytoplasmic localization (Kim et al., 2012; Kim et al., 2013; Millan-Arino et al., 2014; Peng et al., 2015). For example, H1.2 cytoplasmic migration in response to x-ray induced double strand breaks triggers a Bak dependent release of mitochondrial cytochrome C along with caspase-3/caspase-7 activation and cell death (Garg et al., 2014; Okamura et al., 2008; Ruiz-Vela and Korsmeyer, 2007). Results from Garg et al. support these findings by showing the involvement of H1.1 and H1.2 in apoptotic signaling where H1.2 a forms cytoplasmic complexes with the pro-apoptotic mitochondrial protein Bak (Figure 2) (Garg et al., 2014; Okamura et al., 2008; Ruiz-Vela and Korsmeyer, 2007). H1.2 was also shown to have a cytoplasmic response to treatment of lymphocytic leukemia (Gine et al., 2008). Additionally, cells treated with flavopiridol showed an increase in cytosolic H1 (all subtypes) as a result of decreasing cell viability (Harshman et al., 2013). In normal fibroblast cell lines H1.2 and H1.5 have been observed in the cytoplasm at specific times during the cell cycle (Green et al., 2010). Patil et al. have recently demonstrated that

HDAC3 and H1.3 are colocalized to polar microtubules and spindle poles in mitotic HeLa cells suggesting a potential role for H1.3 in the regulation of polar microtubule dynamics in mitosis (Patil et al., 2016). This work is the first published research that suggests involvement of H1.3 with vesicular trafficking. It is possible that if H1.3 is involved with apoptosis or signaling through vesicular trafficking. This could explain the difference in the complex's cellular distribution between MCF-7 and SK-OV-3 cell lines that highly express H1.3.

The Role of HDAC8 in the HDAC8-H1.3 Complex

Class I HDACs are ubiquitously expressed nuclear enzymes. HDAC8 is the best mechanistically and structurally characterized HDAC but its function remains largely uncharacterized due to its multiple roles within different intracellular locations and in different cell types. HDAC8 expression is cell type specific with overexpression of HDAC8 being a common characteristic of tumors, specifically gastric and hepatocellular carcinomas (Balasubramanian et al., 2008; Chakrabarti et al., 2015; Qi et al., 2015). As these results showed, a variety of cancerous cell lines that express HDAC8 at high levels. Cellular localization of HDAC8 in normal and cancerous tissues is both nuclear and cytoplasmic and has been demonstrated in embryonic fibroblasts, smooth muscle, skin fibroblasts, NIH3T3, liver and epithelial cells (de Leval et al., 2006; Parenti et al., 2015; Waltregny et al., 2005). Knockdown or inhibition of HDAC8 leads to apoptosis through activation of either caspase 3 and caspase 6 or p53 (Song et

al., 2015). Previous works, as well as this work, have demonstrated a cytoplasmic role for HDAC8. Current known cytoplasmic functions of HDAC8 include: SMC3 deacetylation resulting in release of the cohesin complex from mitotic chromosomes, smooth muscle cell contractility through the binding of actin, and protection of Notch1 from Fbwx7-facilitated protein degradation leading to a cancerous phenotype in breast carcinoma (Buggy et al., 2000; Chao et al., 2016; Hu et al., 2000; Van den Wyngaert et al., 2000). These data from confocal fluorescent microscopy of MCF-7 cells transfected with GFP-tagged HDAC8 showed HDAC8 localization in the nucleus and cytoplasm, specifically associated with vesicles dispersed throughout the cytoplasm. Other studies have shown evidence for HDAC8 in intracellular trafficking that corresponds to the results we have obtained. For example, HDAC8 involvement in intracellular trafficking is seen in histamine receptor positive neurons in recruitment of HDAC8 positive vesicles to peri-cellular localization during histamine activation (Takase et al., 2013). Yamauchi et al. demonstrated that HDAC8 associates with Rab7 positive vesicles and the Golgi. In addition they showed HDAC8 was required for influenza A viral entry into A549 lung carcinoma cells through endocytosis, promoting late endosome and lysosome motility, microtubule organization and centrosome cohesion (Yamauchi et al., 2011). Yamauchi also demonstrated that HDAC8 was responsible for peri-nuclear organization of late endosomes and lysosomes. Other work has demonstrated that when A549 cells were depleted

for HDAC8 the Golgi, late endosomes and lysosomes were dispersed throughout the cytoplasm. Disorganization of microtubules and centrosome separation was also observed after HDAC8 depletion (Yamauchi et al., 2011). These results correspond almost exactly to these findings and they provide strong evidence for HDAC8's role in vesicular trafficking and cytoskeletal organization. We found that vesicles positive for Rab6 and Rab7 were associated with HDAC8. H1.3 was also seen to be localized to vesicles with HDAC8 as determined by immunocytochemistry (figur18-22). Rab6 is found on exocytic vesicles and Golgi-related vesicles. Rab6 binds and recruits dynactin to membranes and microtubules (Figure 3) (Grigoriev et al., 2007). Rab7 is involved in lysosome transport, late endosomes and endocytic pathways (Jordens, 2001; Rojas, 2008; Via, 1997). Further data to support the model of HDAC8-H1.3 association with ER-Golgi vesicles was demonstrated by LC/MS/MS analysis of co-immunoprecipitated MCF-7 cell extracts, which showed that both HDAC8 and H1.3 are associated with vesicular proteins COPA, Sec22B, Sec23A, Sec23B, ERG1, and CLH1 (Table 5).

Another novel finding was that HDAC8 deacetylates H1.3 *in vitro*. Mass spectrometry has identified 3,600 acetylation sites in 1,750 human proteins and showed that lysine acetylation is implicated in the regulation of nearly all nuclear functions and many cytoplasmic processes (Chan et al., 2014; Chao et al., 2016; Lee et al., 2006; Li et al., 2014b; Qi et al., 2015; Waltregny et al., 2004;

Yan et al., 2013) . Linker histones are lysine rich and are known to be acetylated *in vivo*. EMSAs performed to determine the effect of acetylation on H1.3 nucleosome binding were inconclusive (data not shown). Theoretically, neutralizing the positive charge of lysine residues by adding an acetyl-group, would potentially lower the affinity of linker histones for negatively charged DNA, and thus alter its affinity for chromatin. Deacetylation of acetylated H1.3 could restore or enhance H1.3 affinity r binding strength to nucleosomes.

Proposed Cellular Function of the HDAC8-H1.3 Complex

HDAC8 and H1.3 possible interactions with clathrin coated vesicles (as seen in mass spec HDAC8 and H1.3 association with CLH1), late endosomes and ER-Golgi related vesicles are a significant insight into the possible functions of the HDAC8-H1.3 complex. Beyond cellular transport of these proteins, it is possible that H1.3 recruits HDAC8 to Sec and calterin proteins coating the outside of the vesicles to target H1.3 to specific cellular compartments. Cell cycle dependent microtubule reorganization in mitosis has also been shown to involve HDAC8s. Dispersed cytoplasmic distribution of HDAC8 and H1.3 during mitosis and vesicular distribution during interphase, could indicate that microtubules are deacetylated and properly assembled for interphase conformation. Vesicle formation is achieved and deacetylation of microtubules are maintained through HDAC8-H1.3-vesicle-mirotubule associations. During mitosis microtubules are disassembled and reassembled in their mitotic conformation, the Golgi and ER

are disassembled and merged with the nuclear membrane and HDAC8 and H1.3 are seen dispersed throughout the cytoplasm, which indicate that interphase HDAC8-H1.3-vesicle-mirotubule associations are no longer present. are not present. Another possibility is that H1's are known to leave the nucleus under conditions such as apoptosis or during DNA damage repair. This evacuation of H1's from chromatin could also cause HDAC8 binding to H1.3 in the cytoplasm causing HDAC8 to leave vesicles leading to microtubule destabilization and cell fragmentation during apoptosis. Future studies to verify possible microtubule stabilization by the HDAC8-H1.3 complex would include: microtubules assembly and stabilization assay *in vitro* by the HDAC8-H1.3 complex. HDAC8 knockdown studies in MCF-7 to determine the effect on microtubule dynamics apoptosis and vesicular organization, and clathrin H1.3 knockdown studies to determine altered HDAC8 cellular localization.

Proposed Model of Cellular Function of the HDAC8-H1.3 Complex

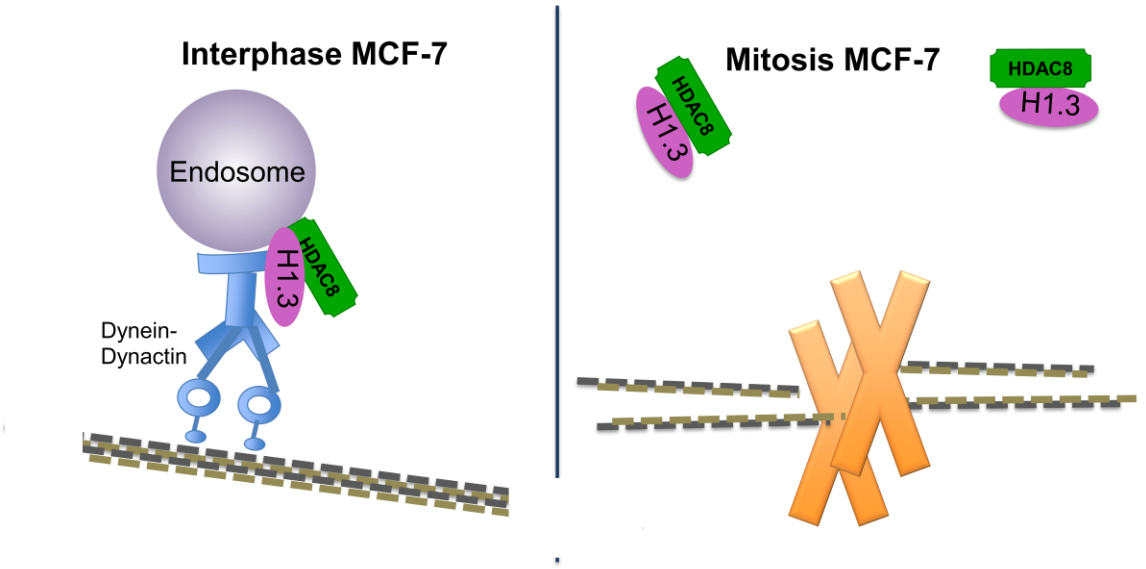

HDAC8 Substrate	Action	Possible Result
H1.3	Deacetylation	• Transport of H1.3 • De-Ac, increases H1.3 affinity for DNA. • Epigenetic regulation of H1.3 for cell signaling pathway such as apoptosis. • HDAC8 binds H1.3 in mitosis, keeping it away from chrmatin.
Tubulin	Deacetylation	• Stabilizes interphase conformation of microtubules, modulates endosome trafficking.

Figure 27. Proposed Model: Cellular Function of the HDAC8-H1.3 Complex. Deacetylation of H1.3 could increase its binding affinity for chromatin. Alternately, deacetylation of H1.3 by HDAC8 could lead to endosome targeting and cytoplasmic trafficking of H1.3. The cytoplasmic targeting of H1.3 could be a signal for cellular events such as apoptosis or mitosis.

REFERENCES

Ahn, H.J., Kim, Y.S., Kim, J.U., Han, S.M., Shin, J.W., and Yang, H.O. (2004). Mechanism of taxol-induced apoptosis in human SKOV3 ovarian carcinoma cells. Journal of Cellular Biochemistry *91*, 1043-1052.

Ascenzi, R., and Gantt, J.S. (1999). Molecular genetic analysis of the drought-inducible linker histone variant in *Arabidopsis thaliana*. Plant Molecular Biology *41*, 159-169.

Balasubramanian, S., Ramos, J., Luo, W., Sirisawad, M., Verner, E., and Buggy, J.J. (2008). A novel histone deacetylase 8 (HDAC8)-specific inhibitor PCI-34051 induces apoptosis in T-cell lymphomas. Leukemia *22*, 1026-1034.

Bellard, M., Dretzen, G., Giangrande, A., and Ramain, P. (1989). Nuclease digestion of transcriptionally active chromatin. In Methods in Enzymology, M.W. Paul, and D.K. Roger, eds. (Academic Press), pp. 317-346.

Bertin, A., Renouard, M., Pedersen, J.S., Livolant, F., and Durand, D. (2007). H3 and H4 histone tails play a central role in the interactions of recombinant NCPs. Biophysical Journal *92*, 2633-2645.

Bleher, R., and Martin, R. (1999). Nucleo-cytoplasmic translocation of histone H1 during the HeLa cell cycle. Chromosoma *108*, 308-316.

Buggy, J.J., Sideris, M.L., Mak, P., Lorimer, D.D., McIntosh, B., and Clark, J.M. (2000). Cloning and characterization of a novel human histone deacetylase, HDAC8. The Biochemical Journal *350 Pt 1*, 199-205.

Chakrabarti, A., Oehme, I., Witt, O., Oliveira, G., Sippl, W., Romier, C., Pierce, R.J., and Jung, M. (2015). HDAC8: a multifaceted target for therapeutic interventions. Trends in Pharmacological Sciences *36*, 481-492.

Chan, K.K., Leung, T.H., Chan, D.W., Wei, N., Lau, G.T., Liu, S.S., Siu, M.K., and Ngan, H.Y. (2014). Targeting estrogen receptor subtypes (ERalpha and ERbeta) with selective ER modulators in ovarian cancer. Journal of Endocrinology *221*, 325-336.

Chao, M.W., Chu, P.C., Chuang, H.C., Shen, F.H., Chou, C.C., Hsu, E.C., Himmel, L.E., Huang, H.L., Tu, H.J., Kulp, S.K.*, et al.* (2016). Non-epigenetic

function of HDAC8 in regulating breast cancer stem cells by maintaining Notch1 protein stability. Oncotarget *7*, 1796-1807.

Chatterjee, N., Wang, W.L., Conklin, T., Chittur, S., and Tenniswood, M. (2013). Histone deacetylase inhibitors modulate miRNA and mRNA expression, block metaphase, and induce apoptosis in inflammatory breast cancer cells. Cancer Biology & Therapy *14*, 658-671.

Chuang, M.J., Wu, S.T., Tang, S.H., Lai, X.M., Lai, H.C., Hsu, K.H., Sun, K.H., Sun, G.H., Chang, S.Y., Yu, D.S.*, et al.* (2013). The HDAC inhibitor LBH589 induces ERK-dependent prometaphase arrest in prostate cancer via HDAC6 inactivation and down-regulation. PloS One *8*, e73401.

Cirillo, L.A., and Zaret, K.S. (2003). Preparation of Defined Mononucleosomes, Dinucleosomes, and Nucleosome Arrays In Vitro and Analysis of Transcription Factor Binding. In Methods in Enzymology, C.D. Allis, and W. Carl, eds. (Academic Press), pp. 131-158.

Clark, M.D., Marcum, R., Graveline, R., Chan, C.W., Xie, T., Chen, Z., Ding, Y., Zhang, Y., Mondragon, A., David, G.*, et al.* (2015). Structural insights into the assembly of the histone deacetylase-associated Sin3L/Rpd3L corepressor complex. Proceedings of the National Academy of Sciences of the United States of America *112*, E3669-3678.

Clausell, J., Happel, N., Hale, T.K., Doenecke, D., and Beato, M. (2009). Histone H1 subtypes differentially modulate chromatin condensation without preventing ATP-dependent remodeling by SWI/SNF or NURF. PloS One *4*, e0007243.

Cooper G.M., Hausman R.E. (2004). The Cell a Molecular Approach, 3 edn (Washington DC: ASM Press).

Craig, J.M. (2005). Heterochromatin--many flavours, common themes. BioEssays : News and Reviews in Molecular, Cellular and Developmental Biology *27*, 17-28.

de Leval, L., Waltregny, D., Boniver, J., Young, R.H., Castronovo, V., and Oliva, E. (2006). Use of histone deacetylase 8 (HDAC8), a new marker of smooth muscle differentiation, in the classification of mesenchymal tumors of the uterus. The American Journal of Surgical Pathology *30*, 319-327.

de Ruijter, A.J., van Gennip, A.H., Caron, H.N., Kemp, S., and van Kuilenburg, A.B. (2003). Histone deacetylases (HDACs): characterization of the classical HDAC family. The Biochemical Journal *370*, 737-749.

Decroos, C., Bowman, C.M., Moser, J.A., Christianson, K.E., Deardorff, M.A., and Christianson, D.W. (2014). Compromised structure and function of HDAC8 mutants identified in Cornelia de Lange Syndrome spectrum disorders. ACS Chemical Biology *9*, 2157-2164.

Decroos, C., Christianson, N.H., Gullett, L.E., Bowman, C.M., Christianson, K.E., Deardorff, M.A., and Christianson, D.W. (2015a). Biochemical and structural characterization of HDAC8 mutants associated with Cornelia de Lange syndrome spectrum disorders. Biochemistry *54*, 6501-6513.

Decroos, C., Clausen, D.J., Haines, B.E., Wiest, O., Williams, R.M., and Christianson, D.W. (2015b). Variable active site loop conformations accommodate the binding of macrocyclic largazole analogues to HDAC8. Biochemistry *54*, 2126-2135.

Di Gennaro, E., Bruzzese, F., Caraglia, M., Abruzzese, A., and Budillon, A. (2004). Acetylation of proteins as novel target for antitumor therapy: review article. Amino Acids *26*, 435-441.

Dowling, M., Voong, K.R., Kim, M., Keutmann, M.K., Harris, E., and Kao, G.D. (2005). Mitotic spindle checkpoint inactivation by trichostatin a defines a mechanism for increasing cancer cell killing by microtubule-disrupting agents. Cancer biology & Therapy *4*, 197-206.

Fadri-Moskwik, M., Weiderhold, K.N., Deeraksa, A., Chuang, C., Pan, J., Lin, S.H., and Yu-Lee, L.Y. (2012). Aurora B is regulated by acetylation/deacetylation during mitosis in prostate cancer cells. FASEB journal : official publication of the Federation of American Societies for Experimental Biology *26*, 4057-4067.

Flanagan, T.W., Files, J.K., Casano, K.R., George, E.M., and Brown, D.T. (2016). Photobleaching studies reveal that a single amino acid polymorphism is responsible for the differential binding affinities of linker histone subtypes H1.1 and H1.5. Journal of Biology, open access, epub. http://www.ncbi.nlm.nih.gov/pubmed/?term=Flanagan%2C+T.W+2016+photobleaching. Biol Open. 2016 Feb 24;5(3):372-80. doi: 10.1242/bio.016733.

Galletti, P., Quintavalla, A., Ventrici, C., Giannini, G., Cabri, W., Penco, S., Gallo, G., Vincenti, S., and Giacomini, D. (2009). Azetidinones as zinc-binding groups to design selective HDAC8 inhibitors. Wiley online library: ChemMedChem *4*, 1991-2001.

Gao, J., Siddoway, B., Huang, Q., and Xia, H. (2009). Inactivation of CREB mediated gene transcription by HDAC8 bound protein phosphatase. Biochemical and Biophysical Research Communications *379*, 1-5.

Gao, Y.S., Hubbert, C.C., and Yao, T.P. (2010). The microtubule-associated histone deacetylase 6 (HDAC6) regulates epidermal growth factor receptor (EGFR) endocytic trafficking and degradation. The Journal of Biological Chemistry *285*, 11219-11226.

Garg, M., Perumalsamy, L.R., Shivashankar, G.V., and Sarin, A. (2014). The linker histone h1.2 is an intermediate in the apoptotic response to cytokine deprivation in T-effectors. International Journal of Cell Biology *2014*, 674-753.

Geeven, G., Zhu, Y., Kim, B.J., Bartholdy, B.A., Yang, S.M., Macfarlan, T.S., Gifford, W.D., Pfaff, S.L., Verstegen, M.J., Pinto, H.*, et al.* (2015). Local compartment changes and regulatory landscape alterations in histone H1-depleted cells. Genome Biology *16*, 289-296.

George, A.A., and Walworth, N.C. (2015). Escape from mitotic arrest: An unexpected connection between microtubule dynamics and epigenetic regulation of centromeric chromatin in *Schizosaccharomyces pombe*. Genetics *201*, 1467-1478.

Gine, E., Crespo, M., Muntanola, A., Calpe, E., Baptista, M.J., Villamor, N., Montserrat, E., and Bosch, F. (2008). Induction of histone H1.2 cytosolic release in chronic lymphocytic leukemia cells after genotoxic and non-genotoxic treatment. Haematologica *93*, 75-82.

GM, C. (2000). The Cell: A Molecular Approach, Vol 2nd (Sinauer Associates).

Gnanambal, K.M., and Lakshmipathy, S.V. (2016). Dictyoceratidan poisons: Defined mark on microtubule-tubulin dynamics. Life Sciences *148*, 229-240.

Green, A., Lonn, A., Peterson, K.H., Ollinger, K., and Rundquist, I. (2010). Translocation of histone H1 subtypes between chromatin and cytoplasm during mitosis in normal human fibroblasts. Cytometry Part A : the Journal of the International Society for Analytical Cytology *77*, 478-484.

Gregoire, S., Xiao, L., Nie, J., Zhang, X., Xu, M., Li, J., Wong, J., Seto, E., and Yang, X.J. (2007). Histone deacetylase 3 interacts with and deacetylates myocyte enhancer factor 2. Molecular and Cellular Biology *27*, 1280-1295.

Gregoretti, I.V., Lee, Y.M., and Goodson, H.V. (2004). Molecular evolution of the histone deacetylase family: functional implications of phylogenetic analysis. Journal of Molecular Biology *338*, 17-31.

Grigoriev, I., Splinter, D., Keijzer, N., Wulf, P.S., Demmers, J., Ohtsuka, T., Modesti, M., Maly, I.V., Grosveld, F., Hoogenraad, C.C.*, et al.* (2007). Rab6 regulates transport and targeting of exocytotic carriers. Developmental Cell *13*, 305-314.

Gurard-Levin, Z.A., Kilian, K.A., Kim, J., Bahr, K., and Mrksich, M. (2010). Peptide arrays identify isoform-selective substrates for profiling endogenous lysine deacetylase activity. ACS Chemical Biology *5*, 863-873.

Gurard-Levin, Z.A., and Mrksich, M. (2008). The activity of HDAC8 depends on local and distal sequences of its peptide substrates. Biochemistry *47*, 6242-6250.

Habold, C., Poehlmann, A., Bajbouj, K., Hartig, R., Korkmaz, K.S., Roessner, A., and Schneider-Stock, R. (2008). Trichostatin A causes p53 to switch oxidative-damaged colorectal cancer cells from cell cycle arrest into apoptosis. Journal of Cellular and Molecular Medicine *12*, 607-621.

Harshman, S.W., Chen, M.M., Branson, O.E., Jacob, N.K., Johnson, A.J., Byrd, J.C., and Freitas, M.A. (2013). Isolation and analysis of linker histones across cellular compartments. Journal of Proteomics *91*, 595-604.

Harshman, S.W., Hoover, M.E., Huang, C., Branson, O.E., Chaney, S.B., Cheney, C.M., Rosol, T.J., Shapiro, C.L., Wysocki, V.H., Huebner, K.*, et al.* (2014). Histone H1 phosphorylation in breast cancer. Journal of Proteome Research *13*, 2453-2467.

Hassig, C.A., and Schreiber, S.L. (1997). Nuclear histone acetylases and deacetylases and transcriptional regulation: HATs off to HDACs. Current Opinion in Chemical Biology *1*, 300-308.

He, S., Dong, G., Wang, Z., Chen, W., Huang, Y., Li, Z., Jiang, Y., Liu, N., Yao, J., Miao, Z.*, et al.* (2015). Discovery of novel multiacting topoisomerase I/II and histone deacetylase inhibitors. ACS Medicinal Chemistry Letters *6*, 239-243.

Hsieh, C.L., Ma, H.P., Su, C.M., Chang, Y.J., Hung, W.Y., Ho, Y.S., Huang, W.J., and Line, R.K. (2016). Alterations in histone deacetylase 8 lead to cell migration and poor prognosis in breast cancer. Life Sciences, epub http://www.ncbi.nlm.nih.gov/pubmed/26926079, Life Sci. 2016 Feb 26. pii: S0024-3205(16)30142-4. doi: 10.1016/j.lfs.2016.02.092.

Hu, E., Chen, Z., Fredrickson, T., Zhu, Y., Kirkpatrick, R., Zhang, G.F., Johanson, K., Sung, C.M., Liu, R., and Winkler, J. (2000). Cloning and characterization of a novel human class I histone deacetylase that functions as a transcription repressor. The Journal of Biological Chemistry *275*, 15254-15264.

Inoshita, T., and Imai, Y. (2015). Regulation of vesicular trafficking by Parkinson's disease-associated genes. AIMS Molecular Science *2*, 461-475.

Ishii, S., Kurasawa, Y., Wong, J., and Yu-Lee, L.Y. (2008). Histone deacetylase 3 localizes to the mitotic spindle and is required for kinetochore-microtubule attachment. Proceedings of the National Academy of Sciences of the United States of America *105*, 4179-4184.

Izzo, A., Kamieniarz-Gdula, K., Ramirez, F., Noureen, N., Kind, J., Manke, T., van Steensel, B., and Schneider, R. (2013). The genomic landscape of the somatic linker histone subtypes H1.1 to H1.5 in human cells. Cell Reports *3*, 2142-2154.

Izzo, A., and Schneider, R. (2016). The role of linker histone H1 modifications in the regulation of gene expression and chromatin dynamics. Biochimica et Biophysica Acta *1859*, 486-495.

Jordens, I. (2001). The Rab7 effector protein RILP controls lysosomal transport by inducing the recruitment of dynein-dynactin motors. Current Bioogyl *11*, 1680-1685.

Juan, L.J., Shia, W.J., Chen, M.H., Yang, W.M., Seto, E., Lin, Y.S., and Wu, C.W. (2000). Histone deacetylases specifically down-regulate p53-dependent gene activation. The Journal of Biological Chemistry *275*, 20436-20443.

Jullien, J., Astrand, C., Halley-Stott, R.P., Garrett, N., and Gurdon, J.B. (2010). Characterization of somatic cell nuclear reprogramming by oocytes in which a linker histone is required for pluripotency gene reactivation. Proceedings of the National Academy of Sciences of the United States of America *107*, 5483-5488.

Kachhap, S.K., Rosmus, N., Collis, S.J., Kortenhorst, M.S., Wissing, M.D., Hedayati, M., Shabbeer, S., Mendonca, J., Deangelis, J., Marchionni, L.*, et al.* (2010). Downregulation of homologous recombination DNA repair genes by HDAC inhibition in prostate cancer is mediated through the E2F1 transcription factor. PloS One *5*, e11208.

Kang, Y., Nian, H., Rajendran, P., Kim, E., Dashwood, W.M., Pinto, J.T., Boardman, L.A., Thibodeau, S.N., Limburg, P.J., Lohr, C.V.*, et al.* (2014).

HDAC8 and STAT3 repress BMF gene activity in colon cancer cells. Cell Death & Disease *5*, e1476.

Khan, D.H., He, S., Yu, J., Winter, S., Cao, W., Seiser, C., and Davie, J.R. (2013). Protein kinase CK2 regulates the dimerization of histone deacetylase 1 (HDAC1) and HDAC2 during mitosis. The Journal of Biological Chemistry *288*, 16518-16528.

Kim, G.S., Jung, H.E., Kim, J.S., and Lee, Y.C. (2015). Mutagenesis study reveals the rim of catalytic entry site of HDAC4 and -5 as the major binding surface of SMRT corepressor. PloS One *10*, e0132680.

Kim, K., Jeong, K.W., Kim, H., Choi, J., Lu, W., Stallcup, M.R., and An, W. (2012). Functional interplay between p53 acetylation and H1.2 phosphorylation in p53-regulated transcription. Oncogene *31*, 4290-4301.

Kim, K., Lee, B., Kim, J., Choi, J., Kim, J.M., Xiong, Y., Roeder, R.G., and An, W. (2013). Linker Histone H1.2 cooperates with Cul4A and PAF1 to drive H4K31 ubiquitylation-mediated transactivation. Cell Reports *5*, 1690-1703.

Kimata, Y., Matsuyama, A., Nagao, K., Furuya, K., Obuse, C., Yoshida, M., and Yanagida, M. (2008). Diminishing HDACs by drugs or mutations promotes normal or abnormal sister chromatid separation by affecting APC/C and adherin. Journal of Cell Science *121*, 1107-1118.

Kinoshita, T., and Seki, M. (2014). Epigenetic memory for stress response and adaptation in plants. Plant & Cell Physiology *55*, 1859-1863.

Kornberg, R.D., Lapointe, J.W., and Lorch, Y. (1989). Preparation of nucleosomes and chromatin. Methods in Enzymology, M.W. Paul, and D.K. Roger, eds. (Academic Press), pp. 3-14.

Kovacs, J.J., Hubbert, C., and Yao, T.P. (2004). The HDAC complex and cytoskeleton. Novartis Foundation Symposium *259*, 170-177; discussion 178-181, 223-175.

Krennhrubec, K., Marshall, B.L., Hedglin, M., Verdin, E., and Ulrich, S.M. (2007). Design and evaluation of 'linkerless' hydroxamic acids as selective HDAC8 inhibitors. Bioorganic & Medicinal Chemistry Letters *17*, 2874-2878.

Lattrich, C., Juhasz-Boess, I., Ortmann, O., and Treeck, O. (2008). Detection of an elevated HER2 expression in MCF-7 breast cancer cells overexpressing estrogen receptor beta1. Oncology Reports *19*, 811-817.

Lee, H., Rezai-Zadeh, N., and Seto, E. (2004). Negative regulation of histone deacetylase 8 activity by cyclic AMP-dependent protein kinase A. Molecular and Cellular Biology *24*, 765-773.

Lee, H., Sengupta, N., Villagra, A., Rezai-Zadeh, N., and Seto, E. (2006). Histone deacetylase 8 safeguards the human ever-shorter telomeres 1B (hEST1B) protein from ubiquitin-mediated degradation. Molecular and Cellular Biology *26*, 5259-5269.

Lee, S.J., Li, Z., Litan, A., Yoo, S., and Langhans, S.A. (2015). EGF-induced sodium influx regulates EGFR trafficking through HDAC6 and tubulin acetylation. BMC Cell Biology *16*, 24.

Li, H., Kaminski, M.S., Li, Y., Yildiz, M., Ouillette, P., Jones, S., Fox, H., Jacobi, K., Saiya-Cork, K., Bixby, D.*, et al.* (2014a). Mutations in linker histone genes HIST1H1 B, C, D, and E; OCT2 (POU2F2); IRF8; and ARID1A underlying the pathogenesis of follicular lymphoma. Blood *123*, 1487-1498.

Li, J., Chen, S., Cleary, R.A., Wang, R., Gannon, O.J., Seto, E., and Tang, D.D. (2014b). Histone deacetylase 8 regulates cortactin deacetylation and contraction in smooth muscle tissues. American Journal of Physiology Cell Physiology *307*, C288-295.

Li, Y., Kao, G.D., Garcia, B.A., Shabanowitz, J., Hunt, D.F., Qin, J., Phelan, C., and Lazar, M.A. (2006). A novel histone deacetylase pathway regulates mitosis by modulating Aurora B kinase activity. Genes & Development *20*, 2566-2579.

Li, Y., Peng, L., and Seto, E. (2015). Histone Deacetylase 10 Regulates the Cell Cycle G2/M Phase Transition via a Novel Let-7-HMGA2-Cyclin A2 Pathway. Molecular and Cellular Biology *35*, 3547-3565.

Lodish h, B.A., Matsudaira P, Krieger M, Scott MP, Zipursky SL, Darnell J (2003). Molecular Cell Biology, 5 edition (New York NY, USA: WH Freeman and Company).

Luger, K., Mader, A.W., Richmond, R.K., Sargent, D.F., and Richmond, T.J. (1997). Crystal structure of the nucleosome core particle at 2.8 A resolution. Nature *389*, 251-260.

Ma, Y., Cai, S., Lu, Q., Lu, X., Jiang, Q., Zhou, J., and Zhang, C. (2008). Inhibition of protein deacetylation by trichostatin A impairs microtubule-kinetochore attachment. Cellular and Molecular Life Sciences : CMLS *65*, 3100-3109.

Magnaghi-Jaulin, L., Eot-Houllier, G., Fulcrand, G., and Jaulin, C. (2007). Histone deacetylase inhibitors induce premature sister chromatid separation and override the mitotic spindle assembly checkpoint. Cancer Research *67*, 6360-6367.

Mannini, L., F, C.L., Cucco, F., Amato, C., Quarantotti, V., Rizzo, I.M., Krantz, I.D., Bilodeau, S., and Musio, A. (2015). Mutant cohesin affects RNA polymerase II regulation in Cornelia de Lange syndrome. Scientific Reports *5*, 16803.

Marino-Ramirez, L., Kann, M.G., Shoemaker, B.A., and Landsman, D. (2005). Histone structure and nucleosome stability. Expert Review of Proteomics *2*, 719-729.

Medrzycki, M., Zhang, Y., McDonald, J.F., and Fan, Y. (2012). Profiling of linker histone variants in ovarian cancer. Frontiers in Bioscience (Landmark edition) *17*, 396-406.

Medrzycki, M., Zhang, Y., Zhang, W., Cao, K., Pan, C., Lailler, N., McDonald, J.F., Bouhassira, E.E., and Fan, Y. (2014). Histone h1.3 suppresses h19 noncoding RNA expression and cell growth of ovarian cancer cells. Cancer Research *74*, 6463-6473.

Meier, K., and Brehm, A. (2014). Chromatin regulation: how complex does it get? Epigenetics : official journal of the DNA Methylation Society *9*, 1485-1495.

Millan-Arino, L., Islam, A.B., Izquierdo-Bouldstridge, A., Mayor, R., Terme, J.M., Luque, N., Sancho, M., Lopez-Bigas, N., and Jordan, A. (2014). Mapping of six somatic linker histone H1 variants in human breast cancer cells uncovers specific features of H1.2. Nucleic Acids Research *42*, 4474-4493.

Navarro, M.S., and Bachant, J. (2008). RanBP2: a tumor suppressor with a new twist on TopoII, SUMO, and centromeres. Cancer Cell *13*, 293-295.

Nguyen, G.D., Gokhan, S., Molero, A.E., Yang, S.M., Kim, B.J., Skoultchi, A.I., and Mehler, M.F. (2014a). The role of H1 linker histone subtypes in preserving the fidelity of elaboration of mesendodermal and neuroectodermal lineages during embryonic development. PloS One *9*.

Nguyen, G.D., Gokhan, S., Molero, A.E., Yang, S.M., Kim, B.J., Skoultchi, A.I., and Mehler, M.F. (2014b). The role of H1 linker histone subtypes in preserving the fidelity of elaboration of mesendodermal and neuroectodermal lineages during embryonic development. PloS One *9*, e96858.

Niegisch, G., Knievel, J., Koch, A., Hader, C., Fischer, U., Albers, P., and Schulz, W.A. (2013). Changes in histone deacetylase (HDAC) expression patterns and activity of HDAC inhibitors in urothelial cancers. Urologic Oncology *31*, 1770-1779.

Noll, H., and Noll, M. (1989). Sucrose gradient techniques and applications to nucleosome structure. In Methods in Enzymology, M.W. Paul, and D.K. Roger, eds. (Academic Press), pp. 55-116.

Okamura, H., Yoshida, K., Amorim, B.R., and Haneji, T. (2008). Histone H1.2 is translocated to mitochondria and associates with Bak in bleomycin-induced apoptotic cells. Journal of Cellular Biochemistry *103*, 1488-1496.

Olson, D.E., Wagner, F.F., Kaya, T., Gale, J.P., Aidoud, N., Davoine, E.L., Lazzaro, F., Weiwer, M., Zhang, Y.L., and Holson, E.B. (2013). Discovery of the first histone deacetylase 6/8 dual inhibitors. Journal of Medicinal Chemistry *56*, 4816-4820.

Pan, C., and Fan, Y. (2016). Role of H1 linker histones in mammalian development and stem cell differentiation. Biochimica et Biophysica Acta *1859*, 496-509.

Parenti, I., Gervasini, C., Pozojevic, J., Wendt, K.S., Watrin, E., Azzollini, J., Braunholz, D., Buiting, K., Cereda, A., Engels, H.*, et al.* (2015). Expanding the clinical spectrum of the "HDAC8-phenotype" - Implications for molecular diagnostics, counselling and risk prediction. Clinical Genetics.

Park, S.Y., Jun, J.A., Jeong, K.J., Heo, H.J., Sohn, J.S., Lee, H.Y., Park, C.G., and Kang, J. (2011). Histone deacetylases 1, 6 and 8 are critical for invasion in breast cancer. Oncology Reports *25*, 1677-1681.

Patil, H., Wilks, C., Gonzalez, R.W., Dhanireddy, S., Conrad-Webb, H., and Bergel, M. (2016). Mitotic activation of a novel histone deacetylase 3-linker histone H1.3 protein complex by protein kinase CK2. The Journal of Biological Chemistry *291*, 3158-3172.

Peng, H., Zhu, Q.S., Zhong, S., and Levy, D. (2015). Transcription of the Human Microsomal Epoxide Hydrolase Gene (EPHX1) Is Regulated by PARP-1 and Histone H1.2. Association with Sodium-Dependent Bile Acid Transport. PloS one *10*, e0125318.

Qi, J., Singh, S., Hua, W.K., Cai, Q., Chao, S.W., Li, L., Liu, H., Ho, Y., McDonald, T., Lin, A.*, et al.* (2015). HDAC8 Inhibition specifically targets Inv(16)

acute myeloid leukemic stem cells by restoring p53 acetylation. Cell: Stem Cell *17*, 597-610.

Rochefort, H., Platet, N., Hayashido, Y., Derocq, D., Lucas, A., Cunat, S., and Garcia, M. (1998). Estrogen receptor mediated inhibition of cancer cell invasion and motility: an overview. The Journal of Steroid Biochemistry and Molecular Biology *65*, 163-168.

Rojas, R. (2008). Regulation of retromer recruitment to endosomes by sequential action of Rab5 and Rab7. Journal of Cell Biology *183*, 513-526.

Ropero, S., and Esteller, M. (2007). The role of histone deacetylases (HDACs) in human cancer. Molecular Oncology *1*, 19-25.

Rountree, M.R., Bachman, K.E., and Baylin, S.B. (2000). DNMT1 binds HDAC2 and a new co-repressor, DMAP1, to form a complex at replication foci. Nature Genetics *25*, 269-277.

Ruiz-Vela, A., and Korsmeyer, S.J. (2007). Proapoptotic histone H1.2 induces CASP-3 and -7 activation by forming a protein complex with CYT c, APAF-1 and CASP-9. FEBS Letters *581*, 3422-3428.

Rutowicz, K., Puzio, M., Halibart-Puzio, J., Lirski, M., Kotlinski, M., Kroten, M.A., Knizewski, L., Lange, B., Muszewska, A., Sniegowska-Swierk, K.*, et al.* (2015a). A specialized histone H1 variant is required for adaptive responses to complex abiotic stress and related DNA methylation in *Arabidopsis*. Plant Physiology *169*, 2080-2101.

Saez, J.E., Gomez, A.V., Barrios, A.P., Parada, G.E., Galdames, L., Gonzalez, M., and Andres, M.E. (2015). Decreased expression of CoREST1 and CoREST2 together with LSD1 and HDAC1/2 during neuronal differentiation. PloS One *10*, e0131760.

Saleem, M., Abbas, K., Manan, M., Ijaz, H., Ahmed, B., Ali, M., Hanif, M., Farooqi, A.A., and Qadir, M.I. (2015). Review-epigenetic therapy for cancer. Pakistan Journal of Pharmaceutical Sciences *28*, 1023-1032.

Scaffidi, P. (2016). Histone H1 alterations in cancer. Biochimica et Biophysica Acta *1859*, 533-539.

Sekeri-Pataryas, K.E., and Sourlingas, T.G. (2007). The differentiation-associated linker histone, H1.0, during the in vitro aging and senescence of

human diploid fibroblasts. Annals of the New York Academy of Sciences *1100*, 361-367.

Siriaco, G., and Tamkun, J.W. (2013). A histone timer for zygotic genome activation. Developmental Cell *26*, 558-559.

Smith, B.C., and Denu, J.M. (2007). Acetyl-lysine analog peptides as mechanistic probes of protein deacetylases. The Journal of Biological Chemistry *282*, 37256-37265.

Smith, K.T., and Workman, J.L. (2012). Chromatin proteins: key responders to stress. PLoS Biology *10*, e1001371.

Song, S., Wang, Y., Xu, P., Yang, R., Ma, Z., Liang, S., and Zhang, G. (2015). The inhibition of histone deacetylase 8 suppresses proliferation and inhibits apoptosis in gastric adenocarcinoma. International Journal of Oncology *47*, 1819-1828.

Stenmark, H. (2009). Rab GTPases as coordinators of vesicle traffic. Nature Reviews, Molecular Cell Biology *10*, 513-525.

Takase, K., Oda, S., Kuroda, M., and Funato, H. (2013). Monoaminergic and neuropeptidergic neurons have distinct expression profiles of histone deacetylases. PloS One *8*, e58473.

Talasz, H., Sarg, B., and Lindner, H.H. (2009). Site-specifically phosphorylated forms of H1.5 and H1.2 localized at distinct regions of the nucleus are related to different processes during the cell cycle. Chromosoma *118*, 693-709.

Terme, J.M., Sese, B., Millan-Arino, L., Mayor, R., Izpisua Belmonte, J.C., Barrero, M.J., and Jordan, A. (2011). Histone H1 variants are differentially expressed and incorporated into chromatin during differentiation and reprogramming to pluripotency. The Journal of Biological Chemistry *286*, 35347-35357.

Terranova, R., Sauer, S., Merkenschlager, M., and Fisher, A.G. (2005). The reorganisation of constitutive heterochromatin in differentiating muscle requires HDAC activity. Experimental Cell Research *310*, 344-356.

Tomasi, T.B., Magner, W.J., and Khan, A.N. (2006). Epigenetic regulation of immune escape genes in cancer. Cancer Immunology, Immunotherapy : CII *55*, 1159-1184.

Trudgian, D.C., Ridlova, G., Fischer, R., Mackeen, M.M., Ternette, N., Acuto, O., Kessler, B.M., and Thomas, B. (2011). Comparative evaluation of label-free SINQ normalized spectral index quantitation in the central proteomics facilities pipeline. Proteomics *11*, 2790-2797.

Van den Wyngaert, I., de Vries, W., Kremer, A., Neefs, J., Verhasselt, P., Luyten, W.H., and Kass, S.U. (2000). Cloning and characterization of human histone deacetylase 8. FEBS Letters *478*, 77-83.

Verdin, E., and Ott, M. (2015). 50 years of protein acetylation: from gene regulation to epigenetics, metabolism and beyond. Nature Reviews, Moecular Cell Biology *16*, 258-264.

Ververis, K., Hiong, A., Karagiannis, T.C., and Licciardi, P.V. (2013). Histone deacetylase inhibitors (HDACIs): multitargeted anticancer agents. Biologics : Targets & Therapy *7*, 47-60.

Via, L.E. (1997). Arrest of mycobacterial phagosome maturation is caused by a block in vesicle fusion between stages controlled by rab5 and rab7. Journal of Biological Chemistry *272*, 13326-13331.

Vogelauer, M., Krall, A.S., McBrian, M.A., Li, J.Y., and Kurdistani, S.K. (2012). Stimulation of histone deacetylase activity by metabolites of intermediary metabolism. The Journal of Biological Chemistry *287*, 32006-32016.

Waltregny, D., De Leval, L., Glenisson, W., Ly Tran, S., North, B.J., Bellahcene, A., Weidle, U., Verdin, E., and Castronovo, V. (2004). Expression of histone deacetylase 8, a class I histone deacetylase, is restricted to cells showing smooth muscle differentiation in normal human tissues. The American Journal of Pathology *165*, 553-564.

Waltregny, D., Glenisson, W., Tran, S.L., North, B.J., Verdin, E., Colige, A., and Castronovo, V. (2005). Histone deacetylase HDAC8 associates with smooth muscle alpha-actin and is essential for smooth muscle cell contractility. FASEB journal : official publication of the Federation of American Societies for Experimental Biology *19*, 966-968.

Wang, C., Chen, J., Cao, W., Sun, L., Sun, H., and Liu, Y. (2015). Aurora-B and HDAC synergistically regulate survival and proliferation of lymphoma cell via AKT, mTOR and Notch pathways. European Journal of Pharmacology.

Watson JD, B.T., Bell SP, Gann A, Levine M, Losick R, (2004). Molecular Biology of the Cell, 5 edetion (San Francisco: Pearson Education Inc. Benjamin Cummings).

Wei, T., and O'Connell, M.A. (1996). Structure and characterization of a putative drought-inducible H1 histone gene. Plant Molecular Biology *30*, 255-268.

Weierich, C., Brero, A., Stein, S., von Hase, J., Cremer, C., Cremer, T., and Solovei, I. (2003). Three-dimensional arrangements of centromeres and telomeres in nuclei of human and murine lymphocytes. Chromosome research : an International Journal on the Molecular, Supramolecular and Evolutionary Aspects of Chromosome Biology *11*, 485-502.

Wilson, B.J., Tremblay, A.M., Deblois, G., Sylvain-Drolet, G., and Giguere, V. (2010). An acetylation switch modulates the transcriptional activity of estrogen-related receptor alpha. Molecular Endocrinology (Baltimore, Md) *24*, 1349-1358.

Wirth, M., and Jedrusik-Bode, M.A. (2009). Interplay between histone deacetylase SIR-2, linker histone H1 and histone methyltransferases in heterochromatin formation. Epigenetics : Official Journal of the DNA Methylation Society *4*, 353-356.

Yamauchi, Y., Boukari, H., Banerjee, I., Sbalzarini, I.F., Horvath, P., and Helenius, A. (2011). Histone deacetylase 8 is required for centrosome cohesion and influenza A virus entry. PLoS Pathogens *7*, e1002316.

Yan, W., Liu, S., Xu, E., Zhang, J., Zhang, Y., Chen, X., and Chen, X. (2013). Histone deacetylase inhibitors suppress mutant p53 transcription via histone deacetylase 8. Oncogene *32*, 599-609.

Zhang, X., Bao, B., Yu, X., Tong, L., Luo, Y., Huang, Q., Su, M., Sheng, L., Li, J., Zhu, H.*, et al.* (2013). The discovery and optimization of novel dual inhibitors of topoisomerase II and histone deacetylase. Bioorganic & Medicinal Chemistry *21*, 6981-6995.

Zhang, Y., Cooke, M., Panjwani, S., Cao, K., Krauth, B., Ho, P.-Y., Medrzycki, M., Berhe, D.T., Pan, C., McDevitt, T.C.*, et al.* (2012). Histone H1 Depletion Impairs Embryonic Stem Cell Differentiation. PLoS Genetics *8*, e1002691.

Zullo, K.M., Guo, Y., Cooke, L., Jirau-Serrano, X., Mangone, M., Scotto, L., Amengual, J.E., Mao, Y., Nandakumar, R., Cremers, S.*, et al.* (2015). Aurora A Kinase Inhibition Selectively Synergizes with Histone Deacetylase Inhibitor

through Cytokinesis Failure in T-cell Lymphoma. Clinical cancer research : an official journal of the American Association for Cancer Research *21*, 4097-4109.

APPENDIX

LIST OF ABBREVIATIONS

LIST OF ABBREVIATIONS

ABA	Abscisic Acid
Ac-Mono	Acetylated mononucleosome
ADP	Adenosine diphosphate
AKAP95	Aurora B kinase associated protein 95
APC	Anaphase promoting complex
APL	Acute promyelocytic leukemia
Arg	Amino acid Arginine
ATP	Adenosine tri-phosphate
Bak	Localizes to mitochondria, and functions to induce apoptosis
Bicaudal-D	Cargo-binding region of the dynein adaptor
bp	Base pair
CAF-1	Chromatin assembly factor 1
Cdc2	Cyclin dependent kinase 2
Cdc20	Cyclin dependent kinase 20
CdLS	Cornelia de Lange Syndrome
CK2	Protein kinase, casein kinase 2,
Co-IP	Co-immunoprecipitation
Co-REST	Corepressor to REST
CREB	cAMP response element-binding protein
DMAP1	DNA Methyltransferase 1
DNA	Deoxyribonucleic acid
DNMT	DNA Methyltransferase
E2F	Cell cycle transcription factor
E2F	Group of genes that codifies a family of transcription factors
EGFR	Epidermal Growth Factor Receptor
EGR	Early growth response protein
ER	Estrogen receptor
ERRα	Estrogen Related Receptor Alpha
G1	G1-phase of the cell cycle
G2/M	Transition between the G2-phase and M-phase of the cell cycle
H1	Linker histone 1
H2A	Core histone 2A
H2B	Core histone 2B
H3	Core histone 3
H4	Core histone 4

HA95	*HA95* is a protein of the chromatin and nuclear matrix regulating nuclear envelope dynamics
HAT	Histone acetyltransferases
HDA1	Yeast Histone deacetylase 1Class II
HDAC	Histone deacetylase
HDAC1	Histone deacetylase 1
HDAC2	Histone deacetylase 2
HDAC3	Histone deacetylase 3
HDAC8	Histone deacetylase 8
HDACi	Histone deacetylase inhibitors
hEST1B	human Ever Shorter Telomeres 1B
HMG	High Mobility Group protein
HMG	High mobility group protein
HP1	Heterochromatin binding protein 1
hTERT	human Telomerase Reverse Transcriptase
kb	kilo base
Lys	Amino acid Lysine
Mi-2	Nucleosome-remodeling protein
Mono	Mononucleosome
MOTC	Microtubule organizing center
mSin3	Corepressor complex containing HDAC1 & 2
MyoD	Protein involved in muscle differentiation
N-CoR	Nuclear receptor corepressor
NAD+	Nicotinamide adenine dinucleotide
NAP-1	Nucleosome assembly protein 1
NCP	Nucleosome core particle
nm	nanometer
NuMA	Nuclear mitotic apparatus protein
NuRD	Nucleosomal remodeling and deacetylase complex
p32	Transcription Factor
p53	Transcription factor, tumor suppressor protein
PCNA	Proliferating cell nuclear antigen, is a DNA clamp
PKA	Protein kinase A
PKG	Protein kinase G
Pol	Polymerase
Rab11	Member of the Ras superfamily of monomeric G proteins
Rab5	Member of the Ras superfamily of monomeric G proteins
Rab6	Member of the Ras superfamily of monomeric G proteins

Rab7	Member of the Ras superfamily of monomeric G proteins
REST	RE1 silencing transcription factor
RNA	Ribonucleic acid
RPD3	Yeast Class I HDAC
S-phase	Replication phase of the cell cycle
Ser	Amino acid serine
siRNA	Small interfering RNA
SirT1-7	Sirtuins 1 through 7
SMC3	Structural maintenance of chromosomes family of proteins
SMRT	Silencing mediator for retinoic acid and thyroid hormone receptors
SNF2H	**SNF2h** is the catalytic subunit of several chromatin remodeling complexes, such as CHRAC, RSF, ACF, NuRD and NoRC. **SNF2H** is a member of the **SWI/SNF** superfamily
Suv39H1	Suppressor of variegation 3-9 homolog 1
TF	Transcription Factor
Topo II	Topoisomerase II
TRAIL	Tumor necrosis factor-related apoptosis inducing ligand
TRAP	Transcription activator-HAT complex
TSA	Trichostatin A